UNIVERSITÉ DE MONTRÉAL

OPTIMIZATION OF CUTTING PARAMETERS FOR POCKET MILLING ON THE SKIN PLATE IN AL AND AL-LI MATERIALS

HADI MORADI

DÉPARTEMENT DE GÉNIE MÉCANIQUE

ÉCOLE POLYTECHNIQUE DE MONTRÉAL

MÉMOIRE PRÉSENTÉ EN VUE DE L'OBTENTION

DU DIPLÔME DE MAÎTRISE ÈS SCIENCES APPLIQUÉES

(GÉNIE MÉCANIQUE)

AVRIL 2014

UNIVERSITÉ DE MONTRÉAL

ÉCOLE POLYTECHNIQUE DE MONTRÉAL

Ce mémoire intitulé:

OPTIMIZATION OF CUTTING PARAMETERS FOR POCKET MILLING ON THE SKIN PLATE IN AL AND AL-LI MATERIALS

présenté par : MORADI Hadi

en vue de l'obtention du diplôme de : Maîtrise ès sciences appliquées

a été dûment accepté par le jury d'examen constitué de :

M. MAYER René, Ph.D., président

M. BALAZINSKI Marek, Docteur ès Sciences, membre et directeur de recherche

M. BIRGLEN Lionel, Ph.D., membre

DEDICATION

Dedicated to my wife and my son

ACKNOWLEDGMENTS

I would like to take this opportunity to express my sincere gratitude to my advisor, Professor Marek Balazinski. Without his thrust, guidance, patience and supports, my research would not have been successful. Undoubtedly, he was the most influential person during my Master of Science program and I hope the bond that we established will continue for many years to come.

My immense appreciation extends to the technicians of the laboratory of machining and metrology. They have been very much helpful in the course of this research project.

RÉSUMÉ

L'objectif de cette étude est d'optimiser des paramètres de coupes pour l'usinage de poche sur une plaque mince en alliage d'aluminium et en alliage d'aluminium-lithium. Ces plaques minces sont utilisées dans l'industrie aéronautique pour fabriquer le fuselage d'un avion. Présentement, ces poches sur les plaques minces sont fabriquées par usinage chimique. Cette méthode chimique est dite nocive pour l'environnement. La méthode chimique pourrait être remplacée par une méthode mécanique comme l'usinage. En plus, les paramètres de coupes seront optimisés pour l'alliage d'aluminium-lithium.

L'effet des paramètres de coupes a été étudié par des expériences utilisant la méthode de Taguchi. L'analyse de rapport signal sur bruit (Signal to Noise ratio) a été menée sur les données recueillies pour illustrer la significativité des facteurs des plans d'expériences et de leur contribution. La rugosité de la surface sur les pièces a été aussi étudiée et des paramètres optimaux ont été définis. Des vérifications ont été accomplies et la poche sur la plaque a été usinée à la satisfaction des exigences de l'ingénierie de l'industrie.

ABSTRACT

In the present work the pocket machining (milling) of the thin skin components made of aluminium and aluminium-lithium (Al-Li) alloys is studied. These milled components are known as principle parts of commercial airplanes. They have significant impacts on the airplane body weight and fuel consumption. Chemical milling is the main method used for pockets machining on these components. However, this method is not considered as an environmentally friendly operation due to severe contamination problems. To remedy these difficulties, this study intends to replace the chemical milling by an alternative machining method capable to do pocket machining. To that end, pocket milling was selected as machining method. Furthermore, in order to reduce the weight of airplane, an alternative material such as Al-Li alloys is proposed to replace the aluminum alloys.

In the first phase of this study, a comprehensive literature review was conducted on milling and pocket milling of aluminum and aluminum-lithium alloys. The sample parts required for cutting operations were prepared in accordance with in specified dimensional geometries of the real parts used in industry. A milling fixture was then designed and manufactured in order to perform machining operations on the sample parts. The experimental tests were planned according to the Taguchi method design of experiment. The cutting parameters studied included: RPM, chip thickness (feed rate), depth of cut and lubricant. The one way and profile contouring milling operations were selected as machining strategies. A process failure mode and effect analysis (FMEA) was executed to determine the main failure modes during pocket milling operations and the surface roughness was used as performance criteria.

The experimental results were analyzed using Signal to Noise ratio (S/N) strategy though Taguchi method. According to the experimental results, the optimal setting levels of cutting parameters are RPM (10000 rev/min), chip thickness (0.0508 mm), depth of cut (0.45 mm) and lubricant (MQL, 40 ml/min). Finally, the experimental verification tests were performed.

According to the literature, a similar machining specification can be applied for conventional aluminium alloys and the Al-Li alloys. Consequently, in order to reduce the experimental cost and time, the optimum setting levels of process parameters proposed in this work could be applied in the machining of Al-Li work pieces.

TABLE OF CONTENT

LIST OF TABLES

LIST OF FIGURES

LIST OF ABREVIATIONS

Al-Li	Aluminum-Lithium
PM	Powder Metallurgy
MQL	Minimal Quantity of Lubricant
HSM	High Speed Machining
CAM	Computer Aided Manufacturing
FEA	Finite Element Analysis
FMEA	Failure Mode and Effect Analysis
CMM	Coordinate Measurement Machine
RPN	Risk Priority Number
DOE	Design of Experiment
S/N	Signal to Nose ratio
CMM	Coordinate Measurement Machine

INTRODUCTION

As similar as many machines, an airplane consists of many metallic and non-metallic components with various shapes and dimensional geometries (see figure (1.1)).

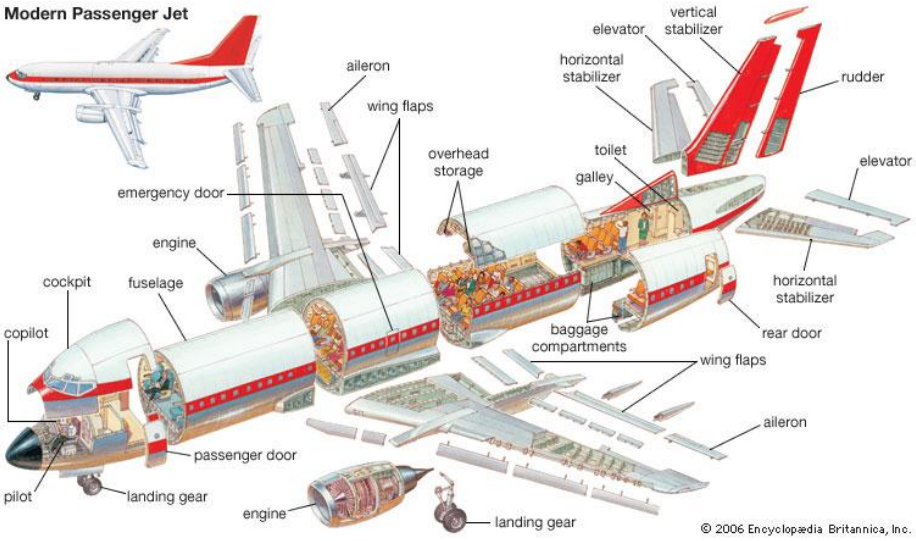

Figure 1.1 A common passenger airplane [1]

Due to its excellent mechanical properties, aluminum alloys are widely used for the frame of commercial airplanes [2]. To that end, they are usually available as large formed thin sheets. The surfaces of these sheets are also precisely machined with pocket milling operation. Chemical milling is the most common method used for pocket milling. This method is considered non-environmentally friendly as it poses severe difficulties to environment and operators health.

The main purpose of this project is to present a strategy to replace the chemical milling by a mechanical milling operation. Furthermore, in order to reduce the weight of airplane and fuel consumption, it is planned to propose new materials instead of commercial aluminium alloys that are currently used in aerospace industry. To that end, this work intends to use Aluminum-Lithium (Al-Li) alloys instead of the common aluminum alloys. In fact, since Al-Li alloys consist of lithium, it has less weight compared to common commercially used aluminum alloys.

In this project, the optimal cutting conditions for pocket milling of aluminum alloys will be defined and accordingly will be applied on Al-Li alloys. This will help the reduction the experimental time and cost. A brief overview of aluminum alloys and Al-Li alloys will be presented in the next sections.

CHAPTER 1 ALUMINUM ALLOYS SPECIFICATION

In this chapter, a general overview of aluminum alloys and Al-Li alloys are presented. The nomenclature of aluminum alloys with mechanical and physical properties of Al-Li alloys are discussed. The main applications and production methods of Al-Li alloys are described. Furthermore, various commercially used Al-Li alloys are introduced.

Two real pocket milled part, currently used in Bombardier products will be presented. Finally, the chemical milling operation that is currently used to generate pockets on thin-skin metal parts are introduced.

1.1 Aluminum Alloys Nomenclature

The Aluminum alloys are classified in the two major categories: cast alloys and wrought alloys. Each category affected by the phase solubility that itself is directionally influenced by the thermal treatment methods. The typical treatment methods are solution heat treatment, quenching, and aging hardening. The nomenclature of wrought alloys nomenclatures are presented with four digit numbers as follows[3] :

- 1xxx Controlled unalloyed (pure) compositions.
- 2xxx Alloys in which copper is the principal alloying element, though other elements, notably magnesium, may be specified.
- 3xxx Alloys in which manganese is the principal alloying element.
- 4xxx Alloys in which silicon is the principal alloying element.
- 5xxx Alloys in which magnesium is the principal alloying element.
- 6xxx Alloys in which magnesium and silicon are principal alloying elements.
- 7xxx Alloys in which zinc is the principal alloying element, but other elements such as copper, magnesium, chromium, and zirconium may be specified.
- 8xxx Alloys Consists of tin and some lithium
- 9xxx Reserved for future use.

The Al-Li alloys can be categorized in group 8xxx. There are three digit numbers and a decimal value (casting alloys limit) for cast alloys nomenclatures as follows [3]:

- 1xx.x Controlled unalloyed (pure) compositions, especially for rotor manufacture.
- 2xx.x Alloys in which copper is the principal element, but other elements may be specified.

- 3xx.x Alloys in which silicon is the principal element, but other elements such as copper and magnesium are specified.
- 4xx.x Alloys in which silicon is the principal element.
- 5xx.x Alloys in which magnesium is the principal alloying element.
- 6xx.x Unused.
- 7xx.x Alloys in which zinc is the principal element, but other elements such as copper and magnesium may be specified.
- 8xx.x Alloys in which tin is the principal element.
- 9xx.x Unused.

The mechanical and heat treatment methods can be applied on aluminum alloys. The correct type of heat treatment method could be identified from specific alphabetic letters and digits added to each aluminium alloy. This system was established by aluminum association and was shown in tables 1.1 and 1.2 [4].

Table 1.1 Destination system for basic treatment of aluminum alloys [4]

F	As fabricated
O	Annealed wrought products only
H	Strain- hardened
W	Solution heat-treated
T	Thermally treated to produce tempers other than F, O, or H

Table 1.2 Subdivisions of the treatments H and T [4]

H1	Strain- hardened only
H2	Strain- hardened and partially annealed
H3	Strain- hardened and stabilized
T1	Cooled from an elevated temperature shaping process and naturally aged
T2	Cooled from an elevated temperature shaping process, cold worked, and naturally aged
T3	Solution heat-treated, cold worked, and naturally aged
T4	Solution heat-treated, and naturally aged
T5	Cooled from an elevated temperature shaping process and artificially aged
T6	Solution heat-treated, and artificially aged
T7	Solution heat-treated, and overaged/ stabilized

T8	Solution heat-treated, cold worked, and artificially aged
T9	Solution heat-treated, artificially aged, and cold worked
T10	Cooled from an elevated temperature shaping process, cold worked, and artificially aged

1.2 Mechanical and Physical Properties of Al-Li Alloys

Lithium is known as the lightest metal with much lower density (540 (kg/m^3)) compared aluminum (2700 (kg/m^3)) [5, 6]. Due to unique properties such as high strength and low density, Al-Li alloys are distinguished from aluminum alloys [5, 7]. Higher modulus, excellent cryogenic toughness, and higher stiffness result when more lithium is added to aluminum alloys composition. However this may also reduce the ductility and fracture toughness of the new alloy. Adding 1% of lithium in the aluminum alloy composition may lead to 3% reduction in the density and 5-6% increase in the modulus of the new alloy. It is to underline that the Al-Li alloys have explosion potential when they are melted with water and salt bath, and with fire when they appear as dust [6, 8].

1.3 Application of Al-Li Alloys

The Al-Li alloys are widely used in aerospace industry (military and space applications), where their low weight has significant impacts on efficiency, fuel consumption and aircraft payload [3, 6, 8]. Considering that Al-Li Alloys have significant fatigue resistance, they are used in lower wing surfaces, leading and trailing edges, access covers and seat skins of the commercial airplanes. Furthermore, they are widely used in center fuselage, control surfaces and main wing box of military aircrafts. These alloys are among the best materials for cryogenic applications such as liquid oxygen, hydrogen fuel tanks and tankage of booster systems. Moreover, they are known as a good alternative to aluminum alloys for specific applications in helicopters, rockets and satellite systems [6, 8]. Alloy 1420 was primarily used in MIG-29 aircraft fuselage in the form of welded structure in 1980 [6]. Al-Li alloy applications in commercial and fighter aircraft is shown in figures (1.2, and 1.3).

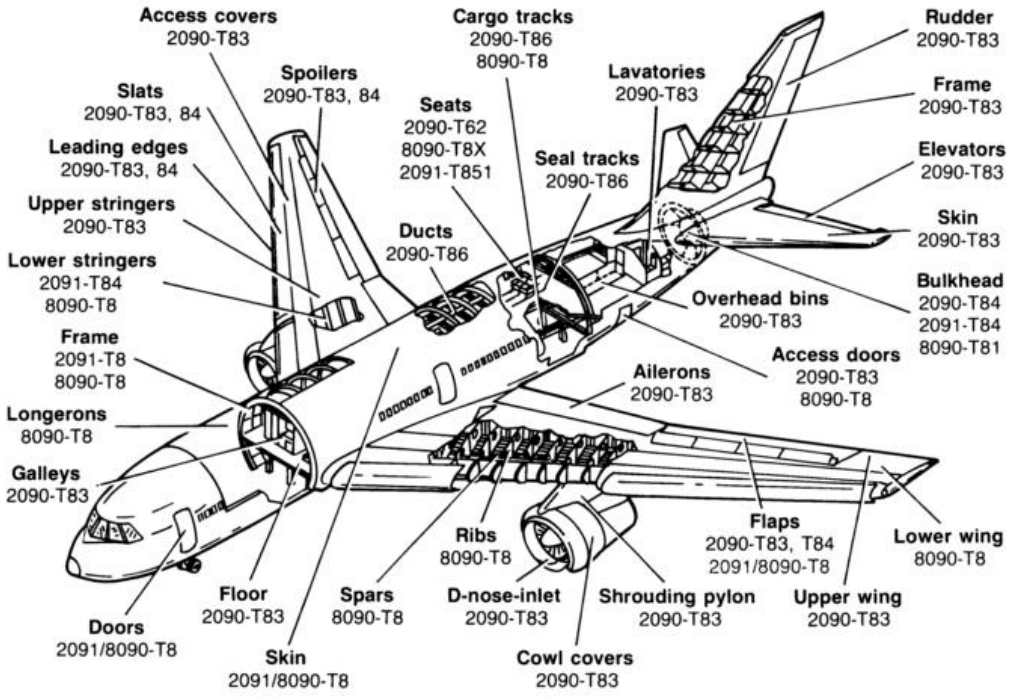

Figure 1.2 Al-Li alloy applications in a commercial aircraft [3]

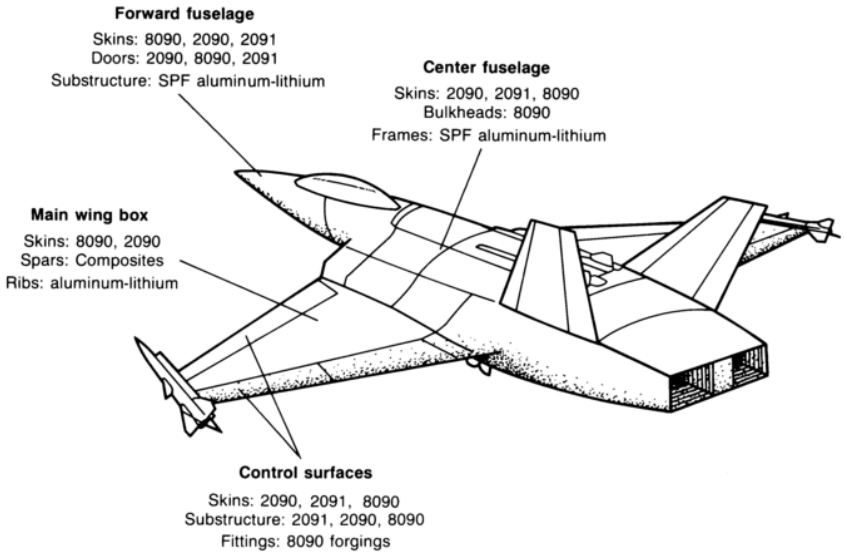

Figure 1.3 Al-Li alloy applications in a fighter aircraft [3]

1.4 Production Methods of Al-Li Alloys

Al-Li alloy can be produced by the ingot metallurgy process (IM-process) that is considered as a low-cost process. Another process used to produce this material is powder metallurgy (PM-process). Using this process, different composition and microstructure can be achieved. The

Alcoa Company currently uses these two methods for Al-Li alloy productions. A third method to produced Al-Li alloy is the melt-spinning or splat-cooling process that this process is kind of PM-process [5].

1.5 Commercial Al-Li Alloys

The commercial Al-Li alloys in the market are listed as below:

1- Weldalite 049 (composition(wt%):Cu5.4,Li1.3, Ag0.4, Mg0.4, Zr0.14, bal.Al)
2- Alloy 2090 (composition(wt%):Cu2.7, Li2.2, Zr0.12, bal.Al)
3- Alloy 2091 (composition(wt%):Cu2.1, Li2.0, Zr0.10, bal.Al)
4- Alloy 8090 (composition(wt%):Cu1.3, Li2.54, Mg0.95, Zr0.12, bal.Al)[8]
5- Alloy 1420 (composition (wt%):Li2.0, Mg5.0, Zr0.1, Si0.15, Fe0.15, bal.Al)
6- Alloy 1421 (composition(wt%):Li2.1, Mg5.2, Si0.1, Fe0.15, bal.Al)
7- Alloy 1460 (composition (wt%):Cu3.0, Li2.0, Si0.15, Fe0.1, bal.Al)
8- Alloy1441(composition(wt%):Cu1.75,Li2.0,Mg0.9,Zr0.1,Si0.1,Fe0.1,bal.Al) [6]

The mechanical properties of few Al-Li alloys are shown in the table 1.3.

Table 1.3 Al-Li physical properties [8]

Property	2090	2091	8090
Density, g/cm^3	2.59	2.58	2.55
Melting range, C^o	560-650	560-670	600-655
Elastic modulus, GPa	76	75	77
Thermal conductivity at 25 C^o, W/m-k	84-92.3	84	93.5
Specific heat at 1000C, J/kg-k	1203	860	930

Table 1.4 presents the production methods used to make Al-Li alloys, as well as the producer.

Table 1.4 Major producers of Al-Li alloys [3]

Producer	Alloys	Products
Producers with casting facilities		
British Alcan	8090	Sheet, plate, extrusions, forgings
Alcoa	2090, 2091, 8090	Sheet, plate, extrusions, forgings
Pechiney	2091, 8090, CP276	Sheet, plate, extrusions, forgings
Reynolds	Weldalite	Sheet, plate, extrusions, forgings
Producers without casting facilities		
ILM	8090, 2090	Extrusions
Otto Fuchs	8090	Extrusions, forgings
Menziken	8090	Extrusions
VAW	8090	Extrusions
HyDuty	8090	Forgings
Hoogevens	8090	Sheet, plate

As reported by the European Cooperation for Space Standardization (ECSS), the price of wrought 8090 Al/Li alloy is around 15-18 € per kg [9].

1.6 Two Industrial Sample Parts in Skin Aluminum Shape

The aluminum frame monolithic, ribs and skins are known as large and weak-rigidity structural parts used in the aircraft manufacturing industries [10]. A few of these components have several pockets on their surface. Two types of typical aluminium skin parts were presented by Bombardier as example parts for this study (see Figures1.4 and 1.5).

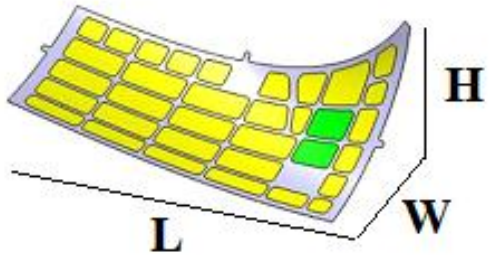

Figure 1.4 Lateral skin of the CRJ 700

The presented components have the following geometrical and surface characteristics: dimension: 2.420 x 1.050 x 0.650 m; thickness: 1.6 mm; global reduction: 1.47 mm; number of pockets: 33.

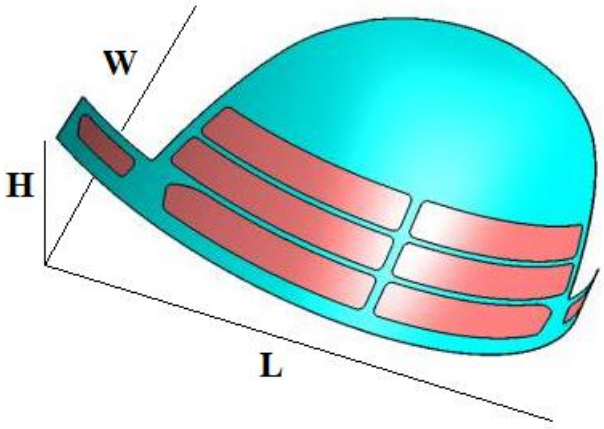

Figure 1.5 Canopy of Challenger 300 (BD100)

The skin parts are available in the dimensions of 2.150 m x 1.160 m x 0.720 m, 2.54 mm in the thickness with eight pockets in the surface. These parts are extremely large and thin. Chemical milling is generally used to generate the pockets.

1.7 Classic Manufacturing Method for Pocket on Aluminum Sheet

Chemical milling is widely used in aerospace, electronics, medical and automotive industries. It is basically considered as a corrosion controlled process that is widely used to produce high precision complex shaped components such as a deep interval cavities and miniaturized microelectronics (micro electro mechanical systems (MEMS), semiconductor industries) [11-13]. Other applications of chemical milling include material removal and consequently weight reduction in sheet shaped components and many engineering materials such as steel and silicon [12].

Chemical milling is a material removal process which uses the microscope electrochemical cell action when the workpiece is immersed in a chemical agent [14, 15]. The material removal is conducted by chemical dissolution, strong acidic or alkaline chemical contacts with surface of work-piece [11].

Chemical milling can be used to create and manufacture forms such as pockets, contours, overal metal removal and chemical blanking (thin sheet). Other applications include photochemical (microelectronic parts), chemical or electrochemical polishing (polishing and deburring edge) and chemical jet machining [11, 14].

The main reasons for the increasing demands for chemical milling are [11, 12, 16]:

1- The process is very cheap compared to other manufacturing processes.

2- No special tool and skilled operators are required.

3- The method can be operated relatively fast and simple.

4- There is a lot of information about this process,

5- Generally, no finishing operations are demanded.

6- High precision for complex geometry is possible.

A typical immersed etching machine is presented in figure (1.6).

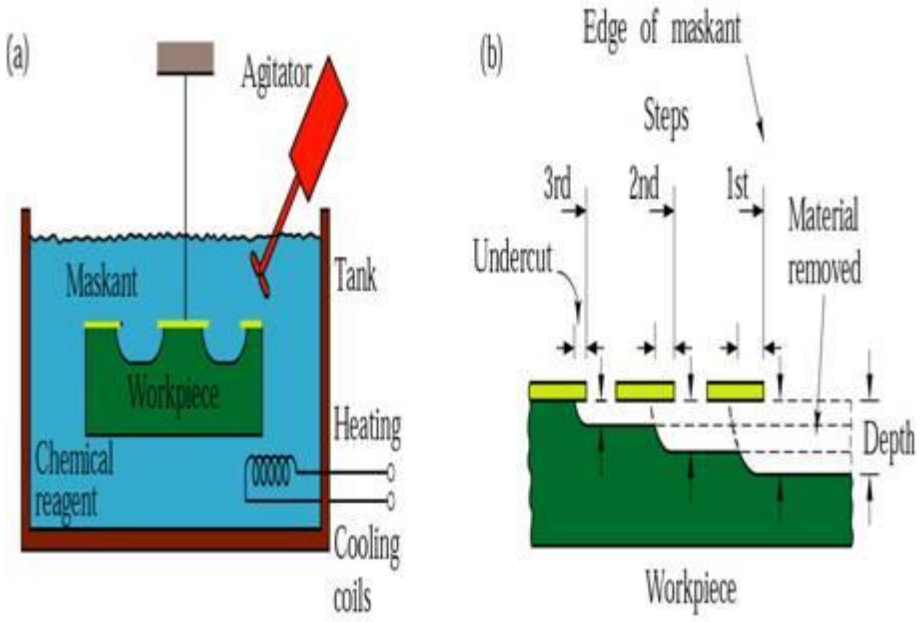

Figure 1.6 Typical chemical milling set-up [17]

However chemical is not considered as an environmentally friendly machining operation, owing to the use of strong acidic or alkaline chemicals for material removal. Therefore, an alternative material removal process is used in this research work.

CHAPTER 2 MACHINING OF ALUMINUM AND AL-LI ALLOYS

Very limited information is available on the machining of Al-Li alloys; it is believed that conventional aluminum alloys and Al-Li alloys have similar machining specifications. Fortunately, since extensive investigations are reported on machining of aluminum alloys, the following passage present the literature review on the milling of aluminum alloys and Al-Li alloys.

2.1 Machining of Aluminum Alloys

The literature review covers factors governing the machining of aluminum alloys such as cutting factors used and the machining responses obtained. The main cutting factors are feed rate and depth of cut), coolant, lubrication mode (MQL, dry), pocket milling strategy, and cutting tools. The main machining responses are surface roughness, cutting forces, deformation, and residual stresses.

2.1.1 Cutting parameters

A relative motion between the workpiece and the cutting tool generates the material removal process in the milling operation. The main cutting parameters involved in milling operation are cutting speed, feed rate and depth of cut. Cutting speed indicates the surface speed at which the workpiece pass the cutting tool, irrespective of the machining operations used. Feed rate is known as the relative velocity as which the cutting tool is advanced against the work part. Depth of cut denotes the volume of the material could be removed in a unit of time. The material removal rate is determined upon appropriate selection of the depth of cut, feed rate and cutting speed [18].

2.1.1.1 Cutting Speed

Cutting speed is calculated by using Eqn 2.1 [19]:

$$V_C = \frac{\pi D N}{1000} \qquad (2.1)$$

where, V_c is the cutting speed (m/min), D is the diameter of cutting tool (mm) and N is the spindle speed (rpm). According to Eqn. 2.1, the cutting speed is directly proportional to the

cutting tool diameter and spindle speed. Maximum spindle speed is a specification of the machine tool and of the maximum diameter according to the dimension of the pocket.

The maximum allowable cutting speeds for cast and wrought aluminum alloys are 2000 m/min and 4000 m/min, respectively [18, 20, 21].

The cutting tool material is another factor that could limit the cutting speed. Y. Wang et al. studied the wear mechanism of polycrystalline diamond (PCD) tool in high speed milling of Al-Si alloy at cutting speed of 5000 m/min. It should be mentioned that the cutter diameter was 125 mm with 8 inserts and revolution was 12732 (rpm) [22].

Cutting speed has a direct influence in surface roughness of aluminum parts. When cutting speed increases, four main regions appear in the cutting operation as shown in figure (2.1). Region I is affected by build-up edge formation and a deteriorated surface roughness results. The surface quality is improved in Region II when cutting speed is increased. Chatter vibration may occur in region III when cutting speed increases. However, at this cutting condition, acceptable surface quality can be achieved in aluminium alloy. Due to virtual chips, a poor surface finish is observed in region IV [20].

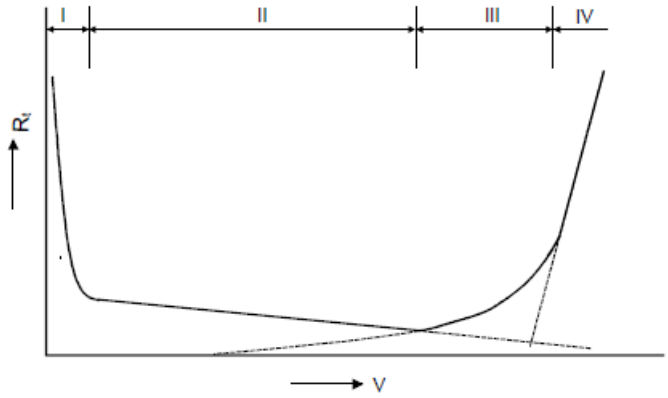

Figure 2.1 Surface roughness of aluminum parts vs the cutting speed [20]

2.1.1.2 Feed Rate

Commanded feed rate could be different along the tool path according to the actual feed rate. The machine tool properties such as acceleration/deceleration and jerk affect the feed rate. The unsmooth acceleration/deceleration control in feed movement is the main reason of tool vibration

in machining operations. Figure (2.2) illustrates the feed rate changing along a pass as cutting tool moves to the end of tool path [23-25].

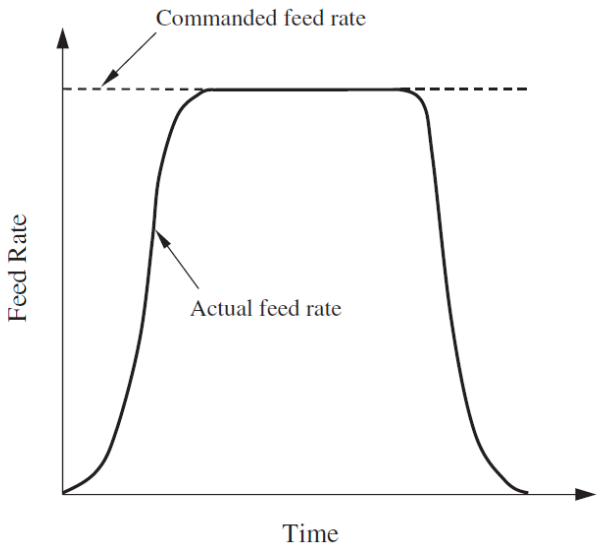

Figure 2.2 Commanded and actual feed rate

The cutting tool direction in pocket machining changes when the cutting tool reaches the workpiece side. When tool direction changes, the feed rate must stop completely and the cutting tool moves to the next point.

Figure (2.3) presents a common tool path at the boundary of the pocket.

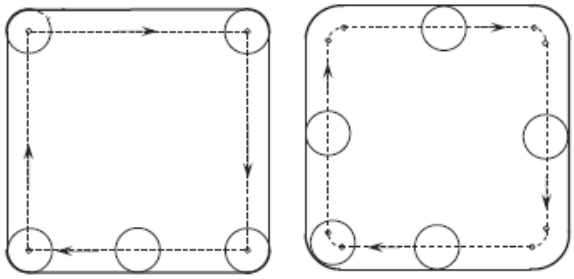

Figure 2.3 Typical tool path at the pocket sides

The feed rate of an end mill along a circular tool path with radius R and the maximum machine acceleration A can be calculated from Eqn. 2.2 [23]:

$$V_f = \sqrt{AR} \qquad (2.2)$$

Another important machining factor is the chip thickness that is directly affected by feed rate and spindle speed. The chip thickness influences the quality of the machined parts. The chip thickness can be calculated from Eqn. 2.3:

$$h(\emptyset_j) = f_t \sin(\emptyset_j) \qquad (2.3)$$

where, $h(\emptyset_j)$ is the chip thickness, f_t is feed rate per tooth and $\emptyset_j$ is the instantaneous immersion angle. The variation of chip thickness in a milling operation varies the cutting forces. The geometry of a milling process as well as chip load and cutting forces are shown in figure (2.4) [26, 27]. The machining time and surface roughness could be changed when feed rate changes.

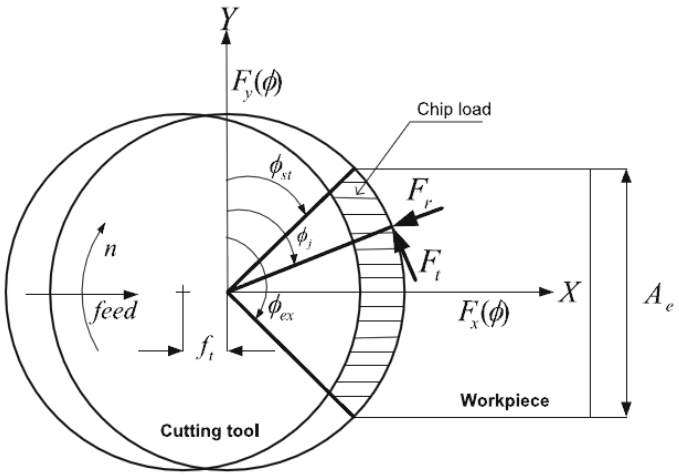

Figure 2.4 Geometry of a milling process

2.1.2 Cutting Fluid or Coolant

The main benefits of lubrication in machining are:

1- Lubrication of tool/chip/workpiece interfaces.
2- Cooling the workpiece and the tool.
3- Prevent or delay formation of a build-up edge (BUE) on the tool.
4- Prevention of corrosion of the workpiece and/or the machine tool.
5- Help to evacuate the chips out of the cutting area.

Four main types of cutting fluids are straight petroleum-based oils, emulsifiable oils, synthetic fluids, and semisynthetic fluids. The property of straight oil can be improved by adding few materials such as oleic acid, neatsfoot oil, and lard oil to it. There are a few cutting fluids that can be used in harsh cutting conditions such as broaching, tapping, and threading. Adequate rust

preventives, antibacterial agents, and extreme pressure additives could be achieved by using the emulsifiable oils (mixtures of oil and water).Synthetic fluids can be used in milling and turning processes for lubrication and cooling purposes.

The appropriate selection of cutting fluids in high speed machining process depends on many factors such as workpiece material, cutting tool, machining process and cutting speed used.

Under dry cutting of the cast iron or Inconel 718, the tool failure may occur due to thermal shock when cubic boron nitride (CBN) tool is used. To avoid tool failure, the cutting zone must be cooled down.

Generally the higher cutting speed increases the cutting temperature. In high speed machining, the cutting temperature mostly transfer out by chips. This allows smooth cutting operations. The lower coefficient of thermal expansion of aluminum alloys than other metals as well as lower cutting forces in aluminium alloys may affect the machined part tolerance in high speed machining operations. The build-up edge (BUE) formation during low speed machining of aluminium alloys may reduce when cutting fluid is used. Chip removal can be done quicker when using cutting fluid. However the cutting fluid does not significantly improve the tool wear rate in high speed machining.

Semisynthetic fluids can be used for machinable aluminium alloys. The main advantages of lubricated machining of aluminum alloys are rapid chip evacuation; adequate cooling of the tool/work surfaces and relatively lower machining cost. It is more necessary to use the cutting fluid for machining of the silicon-containing aluminum alloys than the conventional aluminum alloys. The oils or emulsions are more preferred than the synthetics and semi synthetics.

The cutting fluids should be injected into the cutting surface at an appropriate time. The injection methods are mist cooling, high pressure jets, and shop air [28].The main lubrication strategies applied in machining processes are wet, mist and minimum quantity of lubrication (MQL).

When machining high resistance aerospace alloys (e.g. AlZnMgCu or AlCuMg), the pressure of lubricant is not sufficient for chip evacuation. The MQL seems to be the best solution to overcome this difficulty. The behavior of the cutting tools for high speed milling of Al-Si alloys, as well as the possibility of using MQL were investigated by Lopez et al. [29].

As shown in [29], during milling of a near-eutectic Al-Si alloy (AlSi12CuNi1) under MQL condition, rapid tool wear was observed in uncoated carbide tool than that observed in TiAlN coated carbide tool.

Kishawy et al. investigated the adequacy of different lubrication modes during high speed milling of aluminum alloy A356. Wet (CM2 coolant), dry and MQL (synthetic phosphate ester BM2000 with pressure) conditions were used and the tool wear, surface roughness and cutting forces were measured. It was observed that the better results were obtained under MQL condition [30].

Tsao [31] investigated the end milling of A6061P-T651 aluminum alloy using coated tungsten carbide end mill tool under dry and lubricated conditions. The sulfurous boric acid ester was used as a cutting fluid and lower tool wear was resulted.

Lopez de Lacalle et al. [32] studied the built up edge formation during high speed milling of wrought aluminum alloy (5083-H112). Two cutting fluids techniques such as emulsion of oil in water and spray of oil micro-drops in air were used. As shown in [33], the MQL had better performance than wet condition. As concluded in [32], the nozzle position has a significant effect on the tool life and tool wear.

Zaghbani et al. [34] investigated the fine and ultrafine dust emission during high speed milling of 6061-T6 aluminum alloy in wet and dry conditions. It was observed that the generated energy in the chip formation zone had a direct effect on the dust generation. The particles size is highly affected by the lubrication mode. The submicron size range was produced more in the wet milling than dry milling.

Hwang et al. evaluated the machinability of aluminum alloy (6061) under MQL and wet flood conditions. Higher cutting forces were recorded in MQL compared to wet machining. It was found that the lubrication mode has a significantly affect in the surface roughness [35].

According to Tosun and Huseyinoglu [36], during milling of 7075-T6 aluminum alloy under MQL and wet lubrication conditions, better surface roughness was obtained in MQL condition.

The machinability of ball-end milling of aluminum (Al 6063) was investigated under dry, wet and mist cutting conditions [37]. The flow rates 16 (l/min) and 90 (ml/min) were used in wet and mist conditions, respectively. Lower cutting forces and better surface quality were observed in the mist condition than that observed in dry and wet conditions [37].

The lower application of cutting fluids is the primary objective for industries to better protect the environment against contamination and hazardous materials. Boswell and Islam [38] identified the enough environmental cutting fluid for machining of aluminum alloy. No significant results were reported in their previous study on machining of aluminum with minimal quantities of lubrication (MQL) did not show. In their new study, end milling of a hypo-euthectic grade of Al-Si alloy (6061) was conducted and it was found that suitable MQL technique has the most significant impact on tool life compared to other cooling methods. To that end, five cooling conditions were tested such as dry, flood, cooled air, MQL and combined cooled air with MQL. The lowest cutting forces were observed in MQL, combined cooled air with MQL, flood, dry and cooled air. The surface quality when using MQL and combined cooled air with MQL were relatively similar as that observed when using milling with flood coolant. The lower cutting forces were resulted at higher levels of cutting speed when using the MQL and combined cooled air with MQL.

According to reported works in the literature, better surface quality, lower cutting forces, better tool life and chip formation can be achieved under MQL condition. Furthermore, the environment and operators can be protected against hazardous particles as a result of wet machining. Conducting an environmentally friendly machining is also considered as one of the main goals of this research work.

2.1.3 Cutting Tool Materials

The main cutting tool materials used to machine aluminum alloys are tool steel, high-speed steel (HSS), cemented carbide and diamond. The ceramic tools have a chemical interaction with the aluminum matrix and rapid tool failure may occur. The similar problem may occur when the coated carbide integrated with titanium alloy is used. The cubic crystalline boron nitride (CBN) tool is not recommended for machining aluminium alloys [20].

Lopez et al. [29] used the TiAlN coated carbide tool and PCD tool during milling of Al-Si alloys. A rapid tool wear was observed in coated carbide tool. This exhibited that coated carbide tools are not suitable candidates for high speed milling of Al-Si alloys.

Different cutting tools were investigated according to the surface roughness in milling of 7075-T6 aluminum alloy by Tosun and Huseyinoglu. Better surface roughness was achieved by the WC-Co tool [36].

Wang et al. investigated the tool wear mechanism of a polycrystalline diamond (PCD) tool during milling of Al-Si alloy. The diffusion on the flank face and adhesive on the rake face were identified as the main reasons of the tool wear. The high heat generation due to friction at tool-work interface reduced the tool hardness and caused the abrasive wear. The adhesive wear was also resulted by chip pressure [22].

Xu et al. [39] studied the high and low speed milling on 2024-T351 aluminum alloy using TiAlN coated carbide cutting tool. The surface roughness and residual stresses were recorded. According to experimental results, excellent surface quality was obtained under high speed than that observed in low speed.

According to literature, the PCD is considered as the best cutting tool material used in milling of aluminum alloys. The next appropriate tool material is carbide. However as requested by industrial partner, the carbide tools were used in this research study.

2.1.4 Pocket Milling Strategy

Machining time is a considerable machining parameter that can be improved by adequate selection of machining strategy. Machining program generated by CAM soft-ware should be integrated to numerical control unit (NCU) using certain constraints such as speed, accelerations, jerks and tool path. Discontinuity in the tool path resolved by a circular arc in the NCU and there is an equation to identify the radius of the arc. According to Master CAM software, the main pocket machining strategies are zig-zag, parallel spiral, true spiral, morph spiral and one way.

The main effective factor on the tool path cycle time is the length of path. The parallel spiral strategy is the most rapid strategy in the Master CAM which does not consider the cinematic behaviors of the machining operation. With respect to the feed rate used, the true spiral strategy is the most rapid method. Another effective parameter on the cycle time is length of segment. This parameter can be calculated by using the interpolation cycle time and the feed rate. If the block length is smaller than the length of segment, the feed rate would be restricted and needs to be

recalculated. The morph spiral strategy has more small size segment and true spiral has bigger segments.

Another criterion of a good strategy is the change of direction in the tool path that can be defined by an angle between two directions. The angles could be divided to following 3 sectors. 0^o to 45^o is most favorable, 45^o to 90^o is costly and 90^o to 180^o is very costly. Morph spiral strategy has shown the best results by means of change in the direction. However this strategy has the greatest number of small segments. In addition, the one strategy is costly when change of direction is required. It could be inferred that the appropriate strategy is divergent parallel spiral strategy [40].

In the machining program, the pockets are two and a half dimensional that these features are the large part of 3axis milling process. Productivity and surface quality are affected by machining strategy generated by CAM system. The stability analysis (uniform cutting load and chatter-vibration), and machining parameters (tool selection, tool path pattern, machining order, etc.) are important elements of machining strategy. Uniform cutting load, as well chatter free condition are the main requirements of high speed pocket milling, that could be achieved by using sub machining region. With respect to type of shape or wall used, the pocket can be classified as simple or complex. If the wall is perpendicular to the base plan, this is a simple pocket while if there is a slant in the wall this can be a complex pocket. The simple pocket can be machined layer by layer in rough and finish machining operations. However, a complex pocket between roughing and finishing a semi-finishing is needed [41].

The tool path of spiral strategy for pocket machining (roughing) could be generated by offsetting the pocket profile. The calculation of the offset's geometry can be affected by tool's diameter and the stock allowance. It means that if the tool radius is bigger than the pocket corners radius, it appears that some sections would be removed. In order to avoid overlap in the last path, it is advised to use the lower value of the offset compared to corner radius.

Chatelain et al. [42] proposed new trajectory for spiral strategy that starts in the center of pocket in the circular shape and it was gradually changed to the profile of pocket when the tool comes near the boundary of pocket. This new strategy indicated that the machining time was reduced when larger feed rate was used.

Stability of machining operation is the main concern during high speed machining of the thin component. The chatter vibration may damage the thin webs and results into a poor surface quality. Smith and Dvorak developed a strategy to support the uncut sections of the thin webs parts during high speed milling operations. The cutting tools with no corner radius minimize the normal force to the thin web [43].

In order to improve the surface quality during milling of curved surfaces, Balazinski et al. [44] presented an adequate orientation and direction of cutting tool displacement. A defined scallop height could be achieved in milling by using a method to calculate the step over of a Toroidal cutting tool. The machining error with a shorter and cheaper cutting tool path could be evaluated by this method.

Lee et al. evaluated the effects of tool path and tool angle on deflection and surface integrity of the thin cantilever- shaped aluminum plate during high speed ball end milling operation. The maximum deflection was observed when the 45° tilt angle was used [45].

Vakondios et al. examined the effects of various milling strategies (vertical, push, pull, oblique, oblique push and oblique pull) and cutting parameters (axial and radial depth of cut, feed rate, inclination tilt and lead angles) on surface roughness of ball end milled Al7075-T6 parts. The best surface quality was observed when using inclination angles ±5° [46].

According to the literature, the main pocket milling strategies are internal and external spiral, zigzag, and one way strategies. The lower machining time, higher stability and better surface quality are the quality characteristics proposed for better selection of milling strategies. In this project, one way strategy was selected as a desirable strategy which allows pocket milling on the double curved surfaced of the thin-skin parts.

2.1.5 Deformation and deflection

There are six orders of deviation from the nominal form of the surface. The first order deviation is resulted by machine tool errors, work piece deformation, and unsuitable clamping. The second order deviation arises from geometry tolerances such as flatness, circularity, and waviness. The shape and condition of the cutting edge, chip formation and the process kinematics affect the

third and fourth orders of deviation. The structure of the workpiece material such as physical and chemical mechanisms (e.g. slip, diffusion, and residual stress) have the crucial effects on the fifth and sixth order deviations [46]. Distortion and deformation are resulted from residual stress. The thermal strain, elastic-plastic strain and micro structural changes are the main governing factors on the residual stresses, which themselves are strongly affected by tool geometries, cutting conditions used and work materials [47].

Guo et al. [48] established a 3D finite element model (FEM) to predict the machining deformation of the thin-walled frames. The cutting forces, clamping forces and initial residual stresses were studied.

The deformation of the thin plate of aluminum alloy during milling operation was reported in [49]. The work part used was a cantilever plate of 7075 aluminum alloy. It was found that the heat generation is not the main reason of deflections, while they are generated by residual stress after milling operations. The recorded residual stresses were 400 MPa on the surface and zero at the 0.05mm depth.

Aijun and Zhanqiang [50] proposed a new analytical model to predict the static deformation of thin-wall plate with low rigidity. A theoretical deformation model was developed by finite element method (FEM) to predict the part deformation. In regard to milling forces, location of cutter and the thickness of part, the geometrical accuracy of the thin-wall plate could be increased using this method.

Cao el al. [51] analyzed errors of the side walls of aluminum LY12CZ in milling operation, when different cutting condition were used. The lower deformation is resulted when the rigidity of machining area is increased.

According to Wang et al. [52], the milling cutting forces are the main governing factors on the work part deformation.

S. Lin et al. [53] studied the effects of fixturing on the deformation of the thin-walled milled part. As reported in [53], the main governing factors on the milled work part deformation are cutting forces, fixtures, fiber direction of material, plastic deformation and cutting strategy.

Huzeng et al. [19] introduced a method and instrument to measure the cutting force in high speed milling of wrought aluminum alloy in 2012. It was reported that the lower cutting forces and

work part deformation are resulted when using down milling with lower levels of depth of cut and feed rate.

The deflection of the thin-wall work parts are strongly affected by the work part thickness and properties. The deflection of different milled aluminum alloys were studied by Han et al. it was found that the material strength has no significant effect on the deflection. Lower defection is resulted when suing thicker material. This in fact increases the structural stiffness [2].

Lower cutting forces and deflection were resulted when high speed machining was used.

2.1.6 Residual Stress

Aluminum alloys can be machined at high levels of feed rate and cutting speed. The subsurface of machined work part is affected by thermal and mechanical loads. These loads could be changed by cutting conditions. The scrape rate can be reduced when residual stress reduces. It is important to identify the effects of residual stresses in machining of aluminium alloys.

Special attention has been paid to material removal in the past few years, since it is observed that several parts need to be machined up to 95% of their weights. The thin plates were developed in the aerospace industries to better reduce the fuel consumption. One main difficulty is to understand the effect of cutting parameters on machining responses when the shape and size of machined part is changed. For instance, the relationship between the residual stress and variation of cutting parameters, cooling strategy and tool geometry are yet to be understood.

The high performance cutting (HPC) is recently developed to improve the performance of the machine tools and cutting tools and increase the material removal rate. In HPC, higher levels of feed rate and cutting speeds are used to decrease the machining time. Decreased residual stress may increase the work part life time, especially in thin plates.

The residual stress appears in the raw material, even if no mechanical stresses, such as axial load, force, torques or thermal gradient are applied. These stresses could be affected by mechanical and thermal loads.

The residual stress can be grouped into tensile and compressive residual stresses, which are both widely affected by thermal and mechanical loads. The final residual stress would be the superposition of the residual stresses in the raw material and machining processes.

The residual stresses could be controlled by modification of the machining process parameters and consequently the mechanical and thermal loads. The mechanical loads cause the compressive residual stresses and the thermal loads cause the tensile residual stresses. It is strongly suggested to define the relationship between the machining parameters and tool geometries with mentioned loads.

Few studies reported the effects of machining parameters on the residual stresses aluminum alloys. The effect of high speed cutting on the residual stresses in turning and milling was investigated by Ploger and Gey [21].

The residual stresses in milling of forged aluminum alloys were studied by Denkena et al. Various levels of cutting speed and feed per tooth were used and the initial residual stress of ±25MPa was recorded. Moreover, the maximum compressive residual stresses were observed around the thickness of 50 μm. It was discovered that when feed rate increases from 0.2mm to 0.3mm, an increased compressive residual stress is observed in the deeper layer of surface.

It is to note that at higher levels of cutting speed and feed rate, the lower compressive residual stress was observed in dry machining compared to that observed in wet machining. The residual stress generally varies when milling tools with various corner radiuses are used.

At lower corner radius, the compressive residual stresses tend to decrease. When the biggest radius r_ε=1.5mm is used, a machined surface free of residual stresses would appear [21].

Residual stresses are the marked effects on the surface integrity that may affect fatigue life of the machined part as well as the assembly operations. Shot-peening process is generally used to adjust the level of compressive residual stress. Although the mechanisms of residual stresses are yet to be found, but it is thought that the plastic deformation and thermal loads are the main reasons of the residual stress [54].

Yuanwei [55] developed a FEM model of high speed milling of 7075-T7351 aluminium alloy and studied the effects of the residual stress on component life. The simulation results fitted well with those recorded experimentally. It was found that the main reason of distortion is the original residual stresses.

C. Fu et al. [10] used finite element model (FEM) to predict the machining cutting forces and stresses in high speed end milling 7075 aluminium alloy.

As shown in [39], et al. in 2012, the original compressive residual stresses could be increased when using high speed. However, low level of speed, they might change to tensile residual stress. The results show that machining feed in perpendicular to the pre-stretch direction of the part increases the compressive stresses, especially in high speed machining.

Cai et al. [56] studied the surface topography, surface roughness and residual stress profile in high speed milling operation. Blank residual stresses as constant bias were observed. The residual stress had a variation range of ±60 MPa from superficial surface to depth 90μm. The residual stress at depth of 0μm was changed from tensile to compressive modes, when cutting speed was increased. At cutting speed 1000 (m/min) the compressive residual stress was changed to tensile when higher levels of depth of cut were used. By moving into the work part and changing the cutting speed from 600 to 800 (m/min), residual stresses changed from tensile to the compressive. Vice versa, at cutting speed 400 m/min, the compressive residual stress was changed to tensile residual stress.

The effects of cutting parameters and cutting temperature on the surface roughness and residual stresses in high speed milling of aluminum alloys were reported in [57]. Higher tensile stresses were recorded at cutting speed interval 250- 1250 (m/min). An increased feed per tooth led to higher cutting forces, residual stress and cutting temperature.

Li et al. [58] studied the effect of cutting speed and feed rate on residual stresses during milling of 7075T7451 aluminum alloy. It could be stated that the cutting speed and the feed rate had the same impact on the recorded residual stresses in the feed and orthogonal machining directions. The mechanical load was found as the main effective factor on the compressive residual stresses. It was observed that the residual stress is not affected at higher cutting speed. The normal direction of cutting according to the feed had a compressive residual stresses. The optimal compressive residual stress was achieved at feed rate 2500-2600 (mm/min).

A mathematical model to predict the surface residual stress in end milling operation was proposed in [47]. The Taguchi's L_{16} orthogonal array was used as design of experiment. The investigated cutting factors were cutting speed; feed rate, radial and axial depth of cut. The maximum compressive stress was recorded at cutting speed 376.8 m/min, feed rate 0.13 mm/z, radial and axial depth of cut 3 and1mm.

2.1.7 Surface Roughness

Higher friction coefficients appear between the rough surfaces than smooth surfaces. The mechanical performance of the parts could be predicted by surface roughness, because the cracks and corrosion could occur quicker on the rough surfaces. Controlling the surface roughness is difficult and expensive task [59].

Machined surfaces, especially milled surfaces are widely used in the assembly. The better surface quality may improve the fatigue strength and creep. The surface roughness could affect several functional attributes such as heat transmission, ability to keep the lubricant, surface friction, wearing etc. The main factors that affect the quality of machined surfaces are material properties, cutting parameters, tool geometry, and machining strategy [60]. This exhibits that the simultaneous control and improvement of the surface quality is considered as a difficult task. An excellent surface quality can be achieved when appropriate cutting parameters and control strategies are used [61].

2.2 Machining of Al-Li Alloys

As literature review of Al-Li alloys machining, it should be mentioned that there are a few studies and researches in this area. In the other hand, there are a lot of studies and researches about the mechanical properties of Al-Li alloys in comparison of the conventional aluminum alloys [6].

As reported by European Cooperation for Space Standardization (ECSS) [9], similar characteristics were observed during machining of Al-Li alloys and other commercial aluminum alloys.

The research work done by Mould and Frod [62], in corporation with British Aerospace PLC is considered as the primary source of information on machinability of Al-Li alloy 8090. No significant difference was observed in terms of machine tools, cutting tools, and equipment for machining. It was a user experience during a production process and the response of experimental test.

Distortion and close up of the flange and behavior of slot in an enclosed pocket were examined during machining of two pieces with material FHD 8090 and FHD alloy L93 components as illustrated in the figure (2.5).

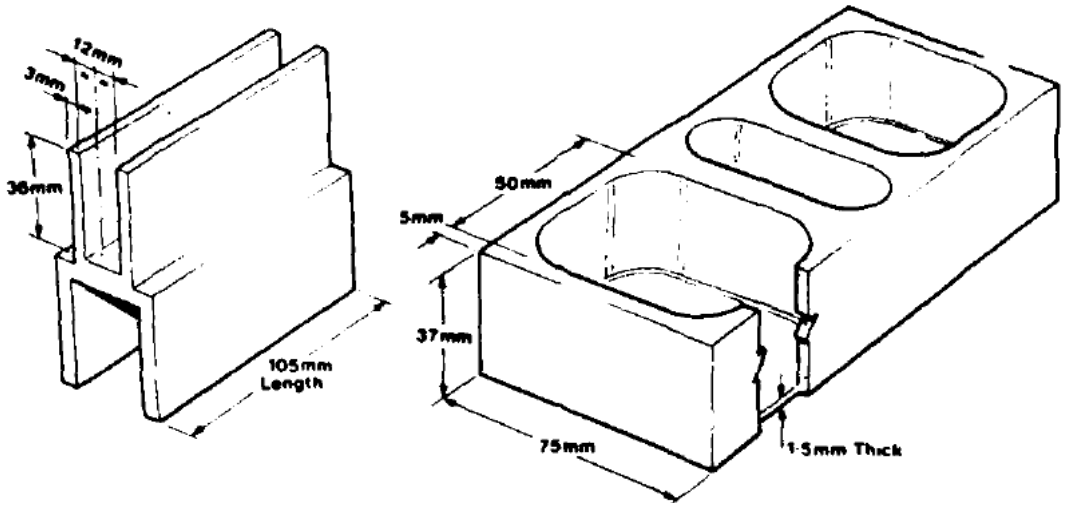

Figure 2.5 The examined pieces 8090 and alloy L93 components [62]

Standard aerospace M42 (HSS) with two tooth and four tooth milling cutters were used. The results were compared with machining results of a L93. The K20 carbide was used to clean up the surfaces of the materials 8090 and L93. It seems that behavior of material Al-Li (8090) is like a pure aluminum [62].

The distortion of flange (Fig 1.6) was less than 120μm, when a machining length of 105 mm was used. The experimental results can be confirmed by experimental verifications in the production line. Further cutting operation were conducted on these materials to investigate the distortion characteristics, surface texture and high flanges when tungsten carbide cutting tools were used.The work pieces for this test are shown in figure (2.6) [62].

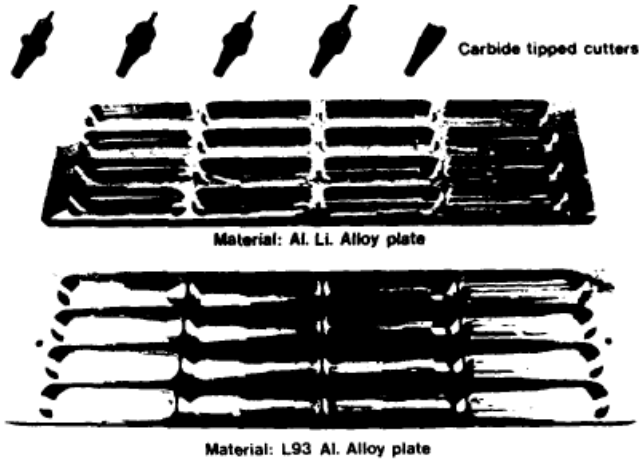

Figure 2.6 Work parts and tungsten carbide tools [62]

A conventional water soluble mineral oil at 40:1 ratio was used as coolant in this work. Proof, tensile and elongation result were fitted with tolerance when the material arrived in solutionised condition normal. The rough machining was conducted at speed 1200 mm/min at 6000 r.p.m while finishing operations was performed at feed rate 500 mm/min and speed 6000 r.p.m. These cutting parameters were selected to reduce the stress in the machined part [62].

One more cutting test was performed to investigate the dimension results for drawn work part tolerances. The corrected tolerances were obtained for two materials. The work piece for this test was the BAe 146 aircraft as shown in figure (2.7) [62].

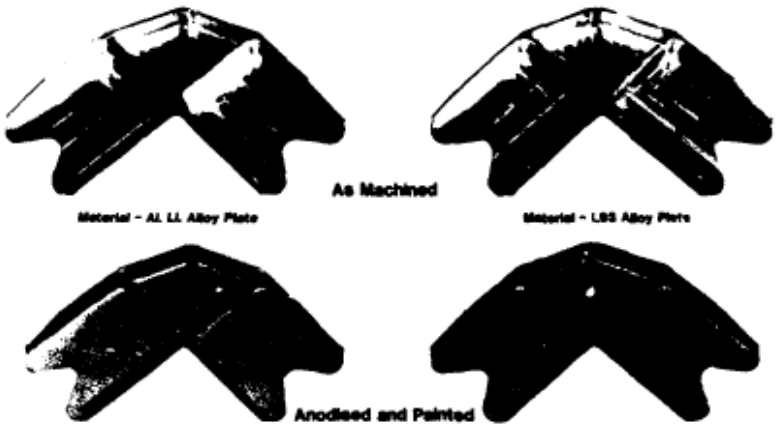

Figure 2.7 Bracket used for dimensional test [62]

Another machining test was performed to define the distortion and cutter burn according to overheating of the material [62].

As reported in [62], the Al-Li 8090 has the similar machinability as those observed for conventional aluminum alloys.

Finally the last machining test was conducted on the work part shown in the figure (2.8). The cutting parameters used were feed /surface speed ratios excessive to normal practice, tool materials and geometries known to burn L93 and worn tools to machining the material Al-Li 8090. The following observations were made:

1- The work part 8090 Al-Li alloy was machined better under the FHT condition.

2- There is no need to change the cutting tool material (HSS or tungsten carbide).

3- There is no need to change the metal removal machine tool [62].

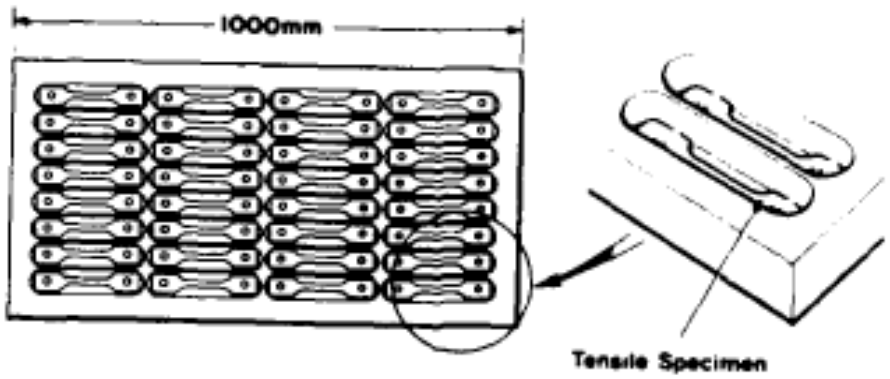

Figure 2.8 Work part used in severe machining condition [62]

Lequeu et al. designed a new copper-lithium alloy (2050) to produce medium and thick plates. The new product was tested in barrel machining method and the distortion and residual stress were recorded. Two test bars L & LT are used in this method and the full thickness will be controlled in machining. A stiff structure was made and the machining behavior of this material was evaluated from unsymmetrical machining operation. the diagram of distortion of the tests bar are shown in figure (2.9) [63].

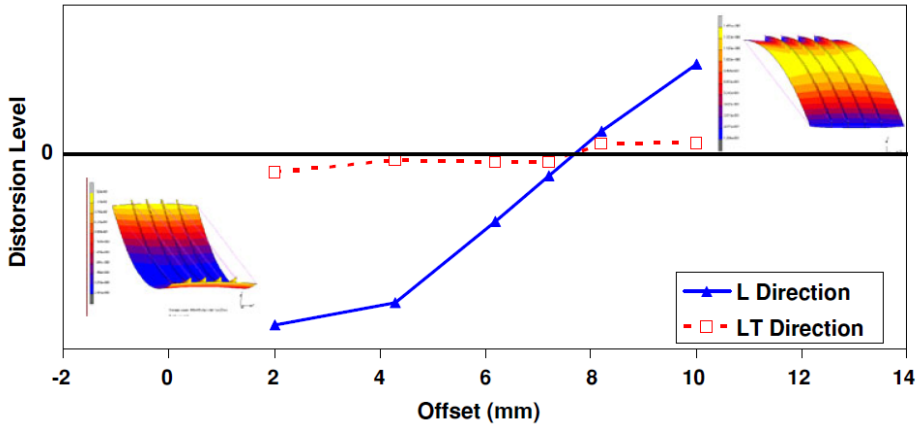

Figure 2.9 The distortion diagram test bars [63]

As presented in the in the figure (1.9), the Al-Li alloy 2050 work parts has negligible deflection in the LT. According to reported results in [63], the machining strategy and off-set can be kept constant.

Wilson et al. in corporation with Alcan international Ltd. investigated the recycling of the Al-Li chips and scraps in 1987 and 1993. Various parameters such as cost of scrap, strategy, storage, drying and de-oiling and recovery of Al-Li scraps were investigated. The aircraft machining chips and scraps are shown in the figure (2.10) [64, 65].

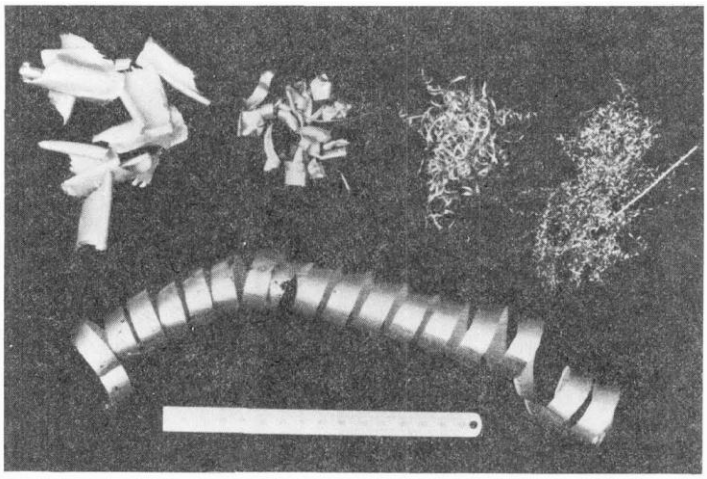

Figure 2.10 Aircraft machining chips and scraps of Al-Li material [64]

The generated chips when machining Al-Li materials were compared with those observed when machining other aluminum alloys such as 7075, 2014, 2024. Al-Li materials have better corrosion resistance than conventional aluminum alloys. The processes to define this advantage of Al-Li material are shown in the figures (2.11, 12, and 13) [65].

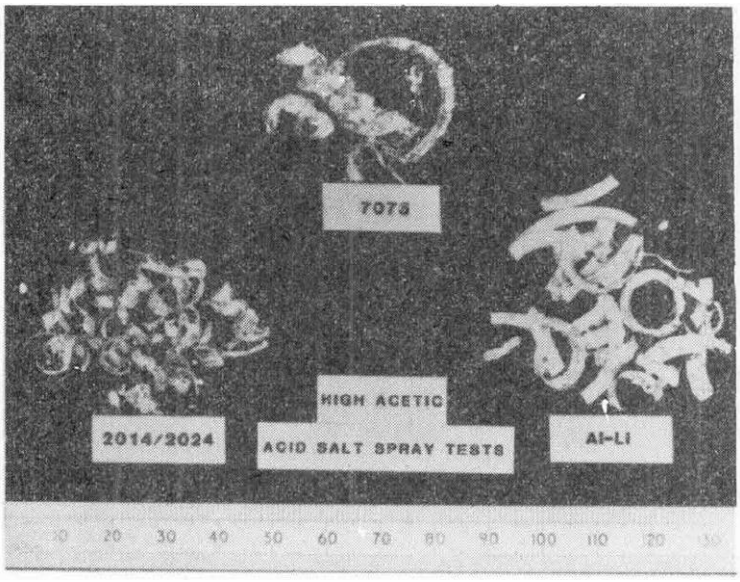

Figure 2.11 Chips in the acid salt spary test [65]

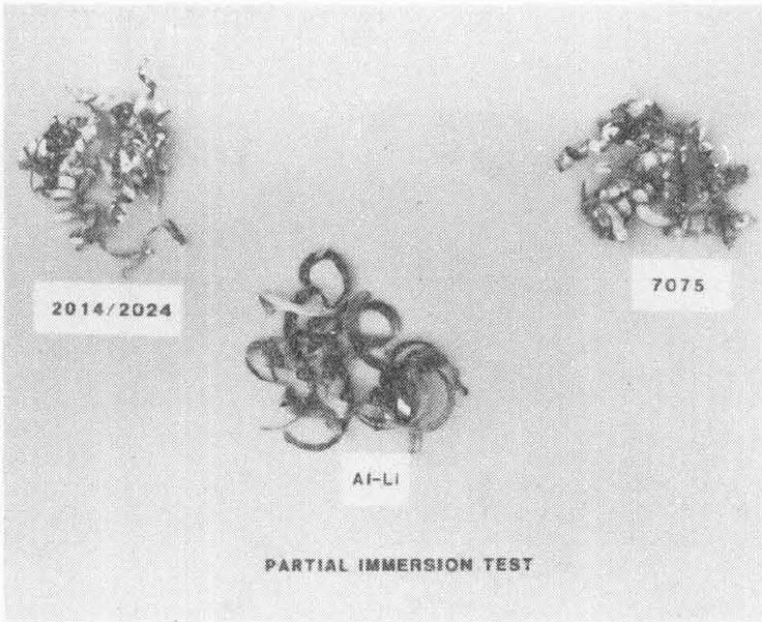

Figure 2.12 Chips in the partial immersion test [65]

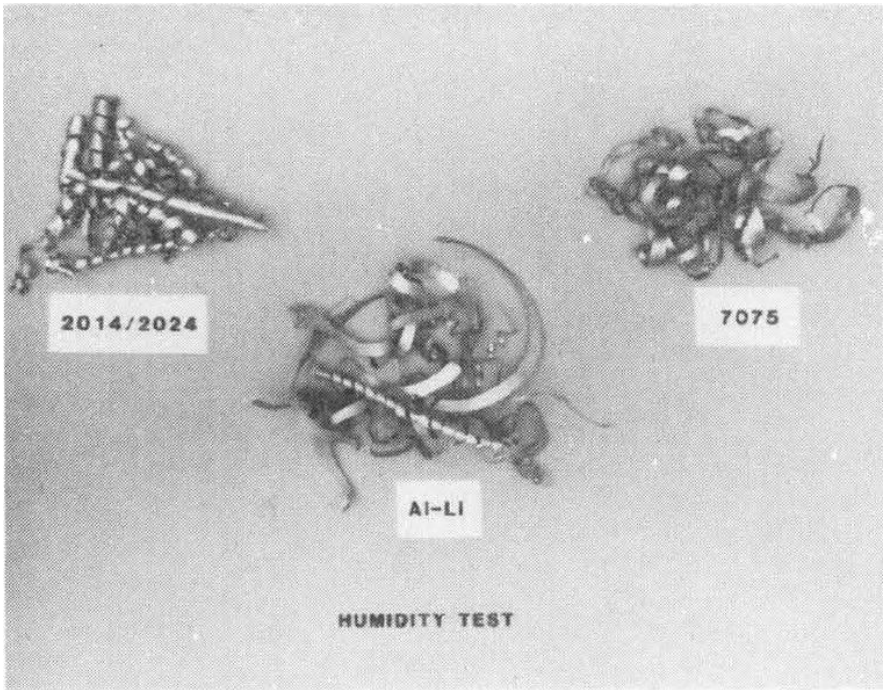

Figure 2.13 Chips in the humidity test [65]

Astronautics Laboratory (AFSC) by National Institute of Standards and technology presented the compatibility of aluminum alloys (8090-T3 and 2090-T81, WL049-T351 and Al alloy 2219) for Cryogenic Tanks. The machining results of impact specimens showed that they were highly variable. The surface roughness of alloy 8090-T3 and alloy 2090-T81 were in the ranges of 40-60µin and 16-20µin respectively. The specimens thickness tolerances were also ±0.005 in [66].

Machinability of alloy 2090 was compared with the B-rated aerospace alloys, 2024-T351 and 7075-T65 [3]. The machining chips in B-rated aerospace alloys can be easily broken and a good surface finish can be achieved. Strong supporting and fixture techniques must be performed when machining material 2090. It is proposed to use sharp positive-rake angled tools and coolant during the machining of alloy 2090.

The manufacturing of Al-Li alloys (2090, 2096, 2098, 2195, L277, C458, 2297, and 2397) were compared by the non-Li aluminum alloys (2219, 2024, 7075, 7050, 6061) [67].

2.3 High Speed Machining (HSM)

High speed machining is considered as an economical, technical, and social evaluation in the manufacturing science. With respect to economical evolution, increased quantity of products require more advanced cost management approach [68].

According to predefined tool life, different cutting speeds can be used in each material. The higher speed can be used in high-speed machining when the shear localization could be developed completely in the primary shear zone [69]. However, this definition is not applicable in practice [70].

Salomon conducted several machining tests in the late 1920's on nonferrous metals such as aluminum, copper and bronze at wide range of speeds up to 16,500 m/min (550 m/s). According to Salomon, there is a maximum increasing temperature in the machining at a given cutting speed and by increasing the cutting speed the temperature decreased. And by using this rule the high speeds could be executed to have better cutting conditions. At the late 1950's, more advanced research studies in high speed machining were proposed. Up until to the mid-80's, the major industrial demands from high speed machining were prosing strategies to reduce forces, stresses and tool wear. However, segmented chip formation was also observed in, which is not however favorable in high speed machining [69, 71].

Many industrial sectors such as defense, aerospace and automotive use the high speed machining technology. Many aerospace manufacturing companies use the carbide tool in high speed micro and macro cutting operations [70]. High-speed machining of thin walled aluminum components is considered as a cost effective machining process that require high removal from the bulk material [69].

Other industries such as tool and die industries use high speed machining. Since high speed machining of hard metal is a complicated task, the heat treatment and annealing condition are generally used to decrease the hardness of the hard metals. The grinding and nontraditional machining processes such as electro discharge machining (EDM) could be used to machine hard materials. These processes are expensive, but since high speed machining tools can be directly applied in these systems, higher production rate and less manufacturing cost are anticipated [72].

Other main benefits of the high speed machining are good surface quality, improved process efficiency, reduced cutting forces, reduced temperature between the tool and the work part and increases material removal rate [73].

The high speed machining of hard materials is related to tool material properties. The tools need to have an appropriate hardness and wear resistance in high temperature. When HSM is used, 90% of the cutting zone temperature is transferred out by the chips and the rest would be remained in the work part and cutting tool. This phenomenon may lead to reduced tool wear and longer tool life [72].

Furthermore, since better surface quality is expected in HSM, generally no more additional finishing process is required, which effectively reduce the non-desirable expenses [74, 75]. The following lines list the main advantages and disadvantages of HSM.

2.3.1Advantages of HSM

- Reducing the time of machining.
- Quality of surface increase.
- With partially vibration and chatter free the surface quality increase.
- The cutting forces in high speed machining will be lower because of increasing the temperature in the interface of tool- work piece and the formation of chips are easier.
- Dimension accuracy improves because of better thermal stability of work piece in high speed machining.

2.3.2 Disadvantages of HSM

- The high speed machining process is expensive process.
- Repair and maintenance are expensive.
- If the time is the reason of using HSM by break down the machine there would be a delay in production.
- Higher energy consuming.
- Automatic safety devices are necessary.

According to spindle speed used, it can be stated that whether or not the process is high speed machining. If the spindle runs more than 8000 revolutions per minute, the corresponding cutting process is called high speed machining [76]. Another way to define a high speed machining is to check if the cutting speed exceeds 500 m/min or more [72]. Furthermore, If DN number

(diameter of spindle (mm) × spindle speed (rpm)) is within the range between 500000 to 1500000 the spindle is a high speed [76]. The last definition method is to use the horse power of the spindle [72].

Nowadays, the aerospace and automotive industries widely use the high speed cutting. The thin-wall structures of electronic equipment could be manufactured by high speed cutting and low cutting force, high productivity and part quality and accuracy could be resulted. Xu et al. [77] presented that machining parameters in high speed milling can be rapidly optimized based on chatter stability theory. Sheet metal assembly could be simply completed, when their thin parts are machined using the HSM. The HSM could be applied for light metal alloys, non-ferrous metals, plastics, steel, cast iron and hard material alloys [71].

In this project, the high speed pocket milling is performed on the Al-Li thin-sheet skin. It is expected that lower cutting force, lower thermal shock and better surface quality will be achieved using the proposed method.

CHAPTER 3 FAILURE MODE AND EFFECT ANALYSIS (FMEA)

The failure mode and effect analysis (FMEA) is a systematic proactive method for qualitative failure analysis. It was developed by reliability engineers in the 1950s to study problems that might arise from malfunctions of military systems. A FMEA is often the first step in the study of a system's reliability. It involves reviewing as many components, assemblies, and subsystems as possible to identify failure modes, and their causes and effects. For each component, the failure modes and their resulting effects on the rest of the system are recorded in a specific FMEA worksheet. FMEA is used to evaluate processes for possible failure and to prevent them by correcting the process rather than reacting to adverse events after failures have been occurred. [78].

The FMEA is a systematic action to:

1- Identify the potential failures in the system's design, product and process, followed by investigating the effects of each failure when it occurs.
2- Identify the actions that can reduce the probability of occurrence of these failures.
3- Identify and execute the actions to reduce the possible severity and deterioration of errors.
4- Identify and execute appropriate activities to increase the detection ability of error in final assembly.
5- Documentation of the design and production process.

FMEA must be performed by qualified experts in design, manufacturing and production, assembly, support services, repair and maintenance, and quality control.

The main applications of FMEA are grouped into four categories:

1- When there is a new system, product designing or production processing.
2- When there is a change in the existed product design or production process.
3- When there is a new application of the existed product design or production process.
4- When it is required to improve the existing product design or production process.

As noted earlier, the FMEA is used to prevent the failure before it happens. The error detection and repair are costly, especially when they are detected in the design stage. Changing the design will cause changes in the production tooling, dies, and fixtures.

Furthermore, the FMEA increases the efficiency of a process, before the final products are affected by errors observed in the design and production steps. The correction could be easily applied of low cost when using FMEA. Other benefits of FMEA are reduced reworks, corrective actions, quality and reliability improvement, increased product safety and decrease the marketing time.

Analysis of failure can be conducted from analysis forms and assessment guidelines that are used to evaluate the severity, occurrence and detection of potential failures.

The necessary information for FMEA is presented as follow:

3.1 Functions

In this section FMEA designer, intents to analyze the failures factors of the operating system. One of the FMEA methods currently applied in the operation process is PFMEA (Process Failure Mode and Effect Analysis). The failures and effects of production and manufacturing processes could be analyzed in stage. In the current project, the process is pocket milling and the result is the machined parts with certain demands by the industrial partner Bombardier as listed below:

- Tolerance on the thickness, periphery and position of the pocket
- Surface roughness of the pocket milled surface
- Conductivity
- Micro cracks
- Visual effects
- Residual stress
- Distortion

The PFMEA defines which of the presented factors have the most crucial effects on the failure of the thin skin machined parts. In addition, the effects of milling parameters on these factors can be evaluated. These failure factors, as listed in the first column of the PFMEA form, can affect the machined part.

3.2 Potential failure mode

A potential failure mode is present when system and production process cannot satisfy the request of design or client. These failures could also be defined by using the brain storming technique. The expected potential failures in this project are:

- Thinning of the thickness
- Stretching the pocket
- Roughing the surface of pocket
- Reducing the conductivity
- Increasing the length of micro cracks
- Increasing the residual stresses
- Over cutting, and surface crash
- Distortion

3.3 Potential Effects of Failure

The potential effects of failure are the states of errors affecting the final product. It is to underline that the deteriorated pocket milled work part may be obtained if the effect of each potential failure on the final product remain unknown. These effects show the problems that the final product will have. The potential effects of failure in the PFMEA are mentioned by the existing problems in the process. In this project each potential failure mode can have such effect as “Scrap the work piece after milling and/or in application” for the final part.

3.4 Severity

Severity indicates how serious the effect of a potential failure is. There is a direct relationship between the effect and the severity of potential failure. Severity is defined through the design system, products, and client or government regulations. The severity is determined using a prepared table as criterion (see table 3.1). The ranks of the potential failures are presented in table 3.2.

Table 3.1 Severity process and/or service guidelines [78]

rank	Explanation
1	Minor: Unreasonable to expect that the minor nature of this failure would cause any real effect on the product and/or service. Customer will probably not even notice the failure.
2-3	Low: Low severity ranking due to nature of failure causing only a slight customer annoyance. Customer probably will notice a slight deterioration of the product and/or service, a slight inconvenience in the next process, or minor rework action.
4-6	Moderate: Moderate ranking because failure cause some dissatisfaction. Customer is made uncomfortable or is annoyed by the failure. May cause the use of unscheduled repairs and/or damage to equipment.
7-8	High: High degree of customer dissatisfaction due to the nature of the failure such as an inoperable product or inoperative convenience. Does not involve safety issues or government regulations. May cause disruptions to subsequent process and/or services.
9-10	Very high: Very high severity is when the failure affects safety and involves noncompliance with government regulations.

In this project the rank of the potential failure were suggested and the result are shown in the table 3.2.

Table 3.2 The severity ranking proposed for pocket milling of Al-Li skin

No.	Potential effects of failure	Severity rank
1	Thinning of the thickness	7
2	Stretch of pocket	5
3	Roughing the surface of pocket	5
4	Reducing the conductivity	7
5	Increasing the length of micro cracks	7
6	Increasing the residual stresses	7
7	Over cutting, surface crash	5
8	Distortion	6

3.5 Potential Causes of Failure

This section presents the reasons of the potential failure. Potential failure may arise from various reasons with specific impact factor. The potential failure can be directly formulated as a function of potential causes. Each cause may be presented with a specific coefficient. The causes of the potential failures are shown in table 3.3.

Table 3.3 The causes of potential of failures in pocket milling of Al-Li skin

No.	Potential effects of failure	Potential causes of failure
1	Thinning of the thickness	*Fault in milling programming. *Variation of thickness of plate. *Fault in fixturing the plate. *Fault in tool selection.
2	Stretch of pocket	*Fault in milling programming. *Fault in fixturing the plate. *Fault in tool selection.
3	Roughing the surface of pocket	*Fault in cutting parameters. *Wearing the tool. *Machine tool Vibration. *Fault in fixturing the plate.
4	Reducing the conductivity	*Changing the properties because of milling temperature. *Fault in cutting parameters. * Fault in selection of cooling liquid.
5	Increasing the length of micro cracks	*Fault in cutting parameters. * Fault in selection of cooling liquid.
6	Increasing the residual stresses	*Fault in cutting parameters. * Fault in selection of cooling liquid. *Fault in fixturing the plate. *Initial residual stresses. *Fault in geometry of tool. *Fault in selection of pocket milling strategy.
7	Over cutting, surface crash	*Fault in milling programming. *Variation of thickness of plate. *Fault in fixturing the plate.
8	Distortion	*Fault in milling programming. *Variation of thickness of plate. *Fault in fixturing the plate.

3.6 Occurrence

Occurrence is a classification or value that is estimated according to the number of failure with respect to a given case. Similar information could be used for the cases that the frequency of occurrences cannot be estimated. A cumulative number of parts failures per 100 or 1000 parts over the design life could be used to identify the frequencies. A typical example of the estimated occurrence is presented in table 3.4. As presented in table 3.5, the causes and occurrences of the failures were investigated in this work.

Table 3.4 Occurrence of the process and/or service guideline

No.	Frequencies of failure	Rank
1	Remote probability of occurrence. Capability shows at (1/10000).	1
2	Low probability of occurrence. Process in statistical control. Capability shows at (1/5000-1/500).	2-5
3	Moderate probability of occurrence. Process in statistical control with occasional failures, but not in the major proportion. Capability shows at (1/200-1/20).	6-7
4	High probability of occurrence. Process in statistical control with failures often occurring. Capability shows at (1/100-1/20).	8-9
5	Very high probability of occurrence. Failure is almost certain. (1/10+)	10

Table 3.5 Occurrence rank for pocket milling of Al-Li skin

No.	Potential effects of failure	Occurrence rank
1	Thinning of the thickness	4
2	Stretch of pocket	4
3	Roughing the surface of pocket	5
4	Reducing the conductivity	3
5	Increasing the length of micro cracks	3
6	Increasing the residual stresses	4
7	Over cutting, surface crash	2
8	Distortion	4

3.7 Detection Method

These are controls rules used to possibly prevent the failure or to identify the failure mode, should the failure happens. Three types of design controls are:

- Preventing the failure occurrence as well as decreasing the probability of occurrence.
- Identification of failure cause and executing the correction application.
- Tracing and identification of failure

In the process/design, there are two types of controls:

- Preventative: this prevents the cause or mechanism of failure to occur the failure and/or decrease the rate of failure occurrence.
- Identification: this identifies the mode or mechanism of failure and leads to corrective actions.

In the current project, the possible control methods were defined and illustrated in table 3.6.

Table 3.6 Detection methods used to detect the failure in the pocket milling of Al-Li skin

No.	Potential effects of failure	Detection method
1	Thinning of the thickness	C.M.M or Panel Gauge
2	Stretch of pocket	C.M.M or Gauge
3	Roughing the surface of pocket	Surface roughness measuring tester
4	Reducing the conductivity	Ohmmeter
5	Increasing the length of micro cracks	Ultrasonic testing or PT
6	Increasing the residual stresses	X-ray or Drilling or Neutron diffraction
7	Over cutting, surface crash	Visual
8	Distortion	C.M.M or Panel Gauge

3.8 Detection

A specific root cause could be detected by the presented detection control methods. A detection rate is defined according to the capability of detection before a machined part leaves the production line. The typical detection rate guideline is shown in table 3.7. The estimated detection rates used in this project are presented in table 3.8.

Table 3.7 Detection process and/or service guideline

No.	Detection rate	Detection
1	Very high: Controls almost certainly will detect the existence of a defect.	1
2	High: Controls have a good chance of detecting the existence of a failure.	2-5
3	Moderate: Controls may detect the existence of a defect.	6-8
4	Low: Controls more likely will not detect the existence of a detect.	9
5	Very low: Controls very likely will not detect the existence of a detect.	10

Table 3.8 Detection ranks of the control methods for pocket milling of Al-Li skin

No.	Detection method	Detection rank
1	C.M.M or Panel Gauge	4
2	C.M.M or Gauge	4
3	Surface roughness measuring tester	5
4	Ohmmeter	5
5	Ultrasonic testing or PT	5
6	X-ray or Drilling or Neutron diffraction	7
7	Visual	3
8	C.M.M or Panel Gauge	4

3.9 Risk Priority Number (RPN)

The RPN is a function of severity, occurrence, and detection. The failure priority is defined by the RPN. Severity reduction can be achieved by changing the design while improvement in the engineering specifications and/or requirements in the process could reduce the occurrence. The evaluation techniques or adding detection equipment affect the detection. The applied modifications may lead to improvement in the failure detection efficiency. The RPN numbers of the failures are shown in table 3.9.

Table 3.9 RPN number for the potential effects of failure of pocket milling of Al-Li skin

No.	Potential effects of failure	Severity rank	Occurrence rank	Detection rank	RPN
1	Thinning of the thickness	7	4	4	112
2	Stretch of pocket	5	4	4	80
3	Roughing the surface of pocket	5	5	5	125
4	Reducing the conductivity	7	3	5	105
5	Increasing the length of micro cracks	7	3	5	105
6	Increasing the residual stresses	7	4	7	196
7	Over cutting, surface crash	4	2	3	30
8	Distortion	6	4	4	96

According to RPN numbers, the residual stress has the most significant effect on the failure of pocket milling of Al-Li thin skin parts. The next significant effects are surface roughness, thickness, conductivity and micro crack.

CHAPTER 4 TEST SAMPLE PLATE

Thin sheet pocket milled components are widely used for many applications and they are available in very large sizes. Consequently, it is not possible to perform the cutting tests on the real size components currently used in industry. Therefore, at the first phase of this work, the dimension of pocket and the test samples were defined. In order to generate the final curved shape of the component, two pocketing methods were proposed.

The first stage of the first method includes machining the pockets on the flat skin and then stretching the skin on the curved fixture to produce the final part. The second method is to conduct milling on the curved skin surface. As the first phase of the current work, the standard thin-skin samples (see fig 4.1) were provided by Bombardier for the pocket milling tests.

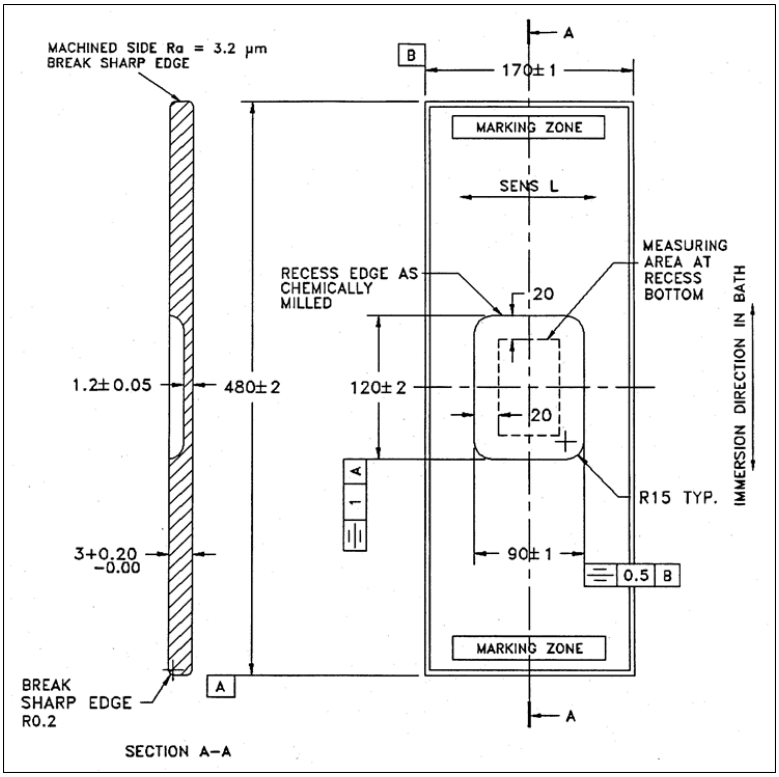

Figure 4.1 Drawing of standard test sample plate

The thickness of testing sample part was 3 mm which has a pocket with the following specifications: pocket size 120× 90× 1.8 mm; corner radius15 mm; radius of the bottom corners of the pocket 4 mm. According to agreement between industrial partner (Bombardier) and research group, the optimal cutting parameters results will be applied on the real parts.

CHAPTER 5 FIXTURE DESIGN [79]

Industrial fixture holds and supports the workpieces in the automated manufacturing, inspection, and assembly operations. The workpieces must be correctly placed and fixed in the fixtures according to the cutting tool or measuring devices used in machining, welding or assembly operations. When a fixture is used, the set-up time in each process is reduced. Other anticipated benefits of using fixtures are better machining accuracy, lower cost of quality control and ability to perform an automated production system. Examples of industrial work holding devices are jaw chucks, machine vises, drill chucks and collets. Each specific work part within a specific manufacturing process needs an individual fixture.

5.1 Fixtures' Elements

The basic elements of fixtures are:

- Locators: parts on the fixtures that localize and maintain the position of a work part.
- Clamps: Used to fix the position of the work part on the fixture.
- Supports: Used to prevent the work parts from deflection and/or deformation under applied operational conditions and clamping forces.
- Fixture body: The major structure of fixture which holds the locators, clamps, supports and work part.

5.2 Fundamentals of Fixture Design

In order to design and manufacture a fixture, certain activities including fixture planning, fixture layout design, fixture element design, and tool body design must be completed by designer. The following lines present a comprehensive overview of abovementioned activities necessary for fixture design.

5.2.1 Fixture planning

The fixture planning is used to identify the available information for the material and geometry of the workpiece, operation required, process equipment etc. The main components in fixture planning are:

- The complexity and type of fixture;

- Number of workpiece per fixture;
- Workpiece orientation;
- Locating datum faces;
- Clamping surfaces;
- Support surfaces.

5.2.2 Fixture Layout

The physical format of fixture can be presented in the fixture layout with following outputs:

- Locators positions and type;
- Clamps positions and type;
- Supports positions and type;
- Clamping forces and sequence.

5.2.3 Fixture Element Design

In this step, the 3D modeling and drawing of each part are prepared, with the following outputs:

- Locators design details;
- Clamps design details;
- Supports design details.

5.2.4 Tool Body Design

The tool box is a rigid structure that carries all the fixture elements.

5.3 Fixture Design Procedure

There are three stages in designing a fixture. At the first stage, the required information about process, equipment, operator safety and the application will be gathered and analyzed.

The clamps and locating schemes could be considered in the second stage. This includes the verification of the cutting tool interference with the clamps and locators. The fixture body frame is designed in the third stage.

5.3.1 Positioning Principles

The main aim of using a fixture during machining operations is to provide a rigid and stable work part surface positioning. The common work parts surfaces are:

- Active surface: this is a machining surface.
- Supporting and locating surfaces: the workpiece is placed and held using these surfaces.
- Clamping surfaces: The clamping forces are applied to work parts in order to fix their positions on the clamping surfaces.
- Datum surfaces: the dimensions are measured from these surfaces.
- Free surfaces: these surfaces are not used in the set-up operation.

5.3.2 Degrees of Freedom of a Workpiece (The motions of the workpiece)

The motion of each solid body can be presented in six degrees of freedom. Three degrees are demonstrated as translation displacements in X, Y, and Z directions and others are devoted to rotational displacements, including pitching, yawing and rolling displacement.

The point locating is known as the best method used for positioning a work part in the surface. The general principle of 3-2-1 location is the most commonly used point locating approach. As a basic rule in designing the fixture, those three points that are far away on the surface would be selected. This approach may lead to improvement in the rigidity and stability of workpiece, when placed in the fixture.

5.3.3 Clamping principles

The essential requirement in each machining operation is to use the correct clamping method. A clamp is a loading system which pushes the workpiece in a special position with respect to locators. Clamping systems should have suitable locking systems which can provide sufficient stability and frictional effects, as well as being, cheap and convenient to manipulate manually. The following basic principles of clamping systems should be considered in the fixture design:

- The main function of clamping devices is to prevent the workpiece from displacements and/or deformations when subjected to applied loads. The thin elements should be clamped directly in the locators, enabling the supporters to transmit the forces to the fixture frame.

- The behavior of clamps elements according to the clamp forces to the workpiece. There are two types of actions in type of increasing (of screw force) or constant (hydraulic force) elastic deformation with the clamping forces.

5.4 Designed Fixture for Skin Sample of Al-Li Alloy

A milling fixture was designed according to the design procedure that was described earlier. In the first step the sample drawing (figure (4.1)) was prepared in the CATIA (V5R20). The sample model is shown in the figure (5.1).

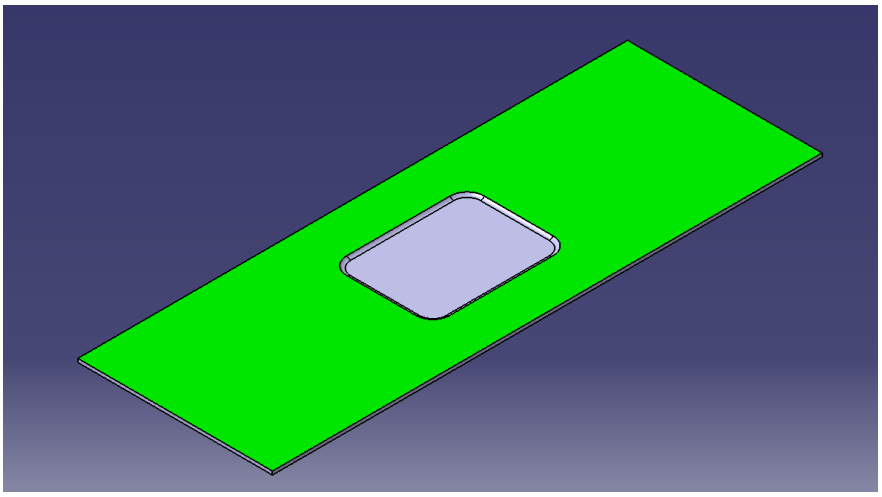

Figure 5.1 Model of standard sample drawing

The locating, supporting and clamping surfaces are presented in figure (5.2).

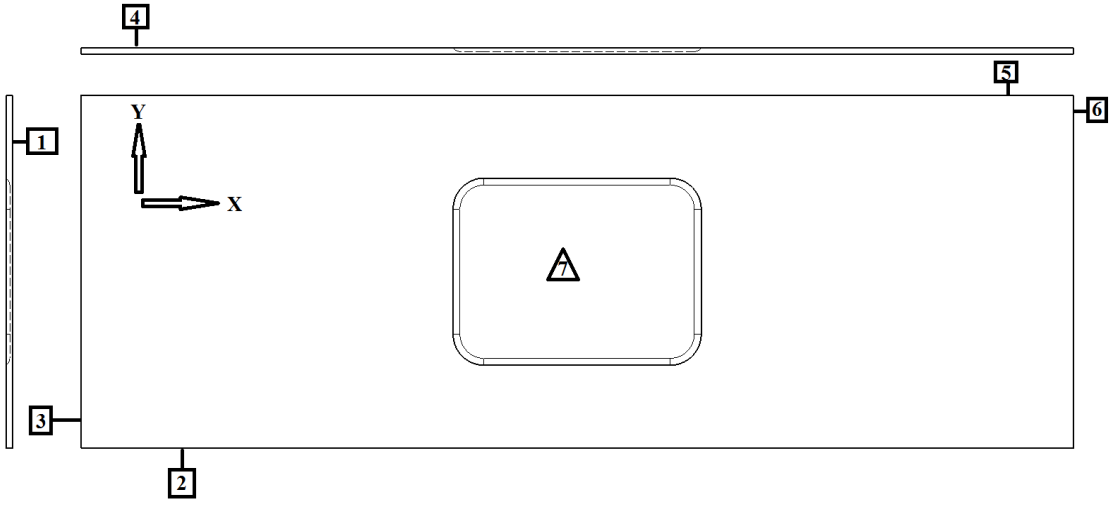

Figure 5.2 Locating, supporting and clamping surfaces

The surfaces No.1, No.2 and No.3 were selected as the locating surfaces to locate the point locators of 3-2-1. The surface No.4 was selected as clamp surface and the surfaces No.5 and No.6 were considered as supporting surfaces. The surface No.7 was an active surface and should be machined.

The surface number one was used as three points to take freedom of sample part in one linear degree (-z axis) and two rotation degree (around X and Y axis). As shown in figures (5.3) and (5.4), three locators were designed and modeled to take other degrees of freedom, which are tangent to the locating surfaces.

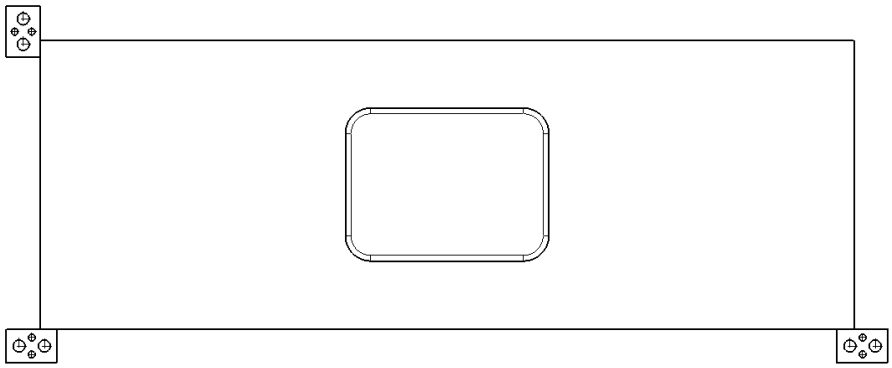

Figure 5.3 Locators (2-1) on the locating surfaces number two and three

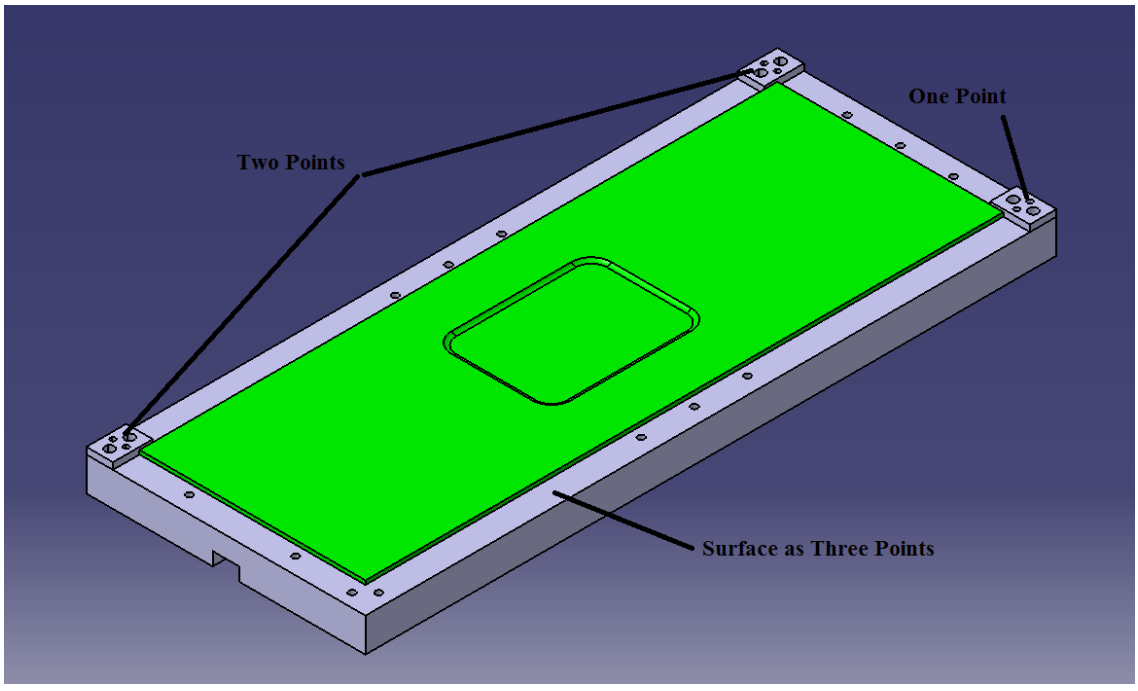

Figure 5.4 Locators (3-2-1) on the locating surfaces

The clamping and supporting systems were designed and added to the model. These clamping and supporting systems are illustrated in the figure (5.5).

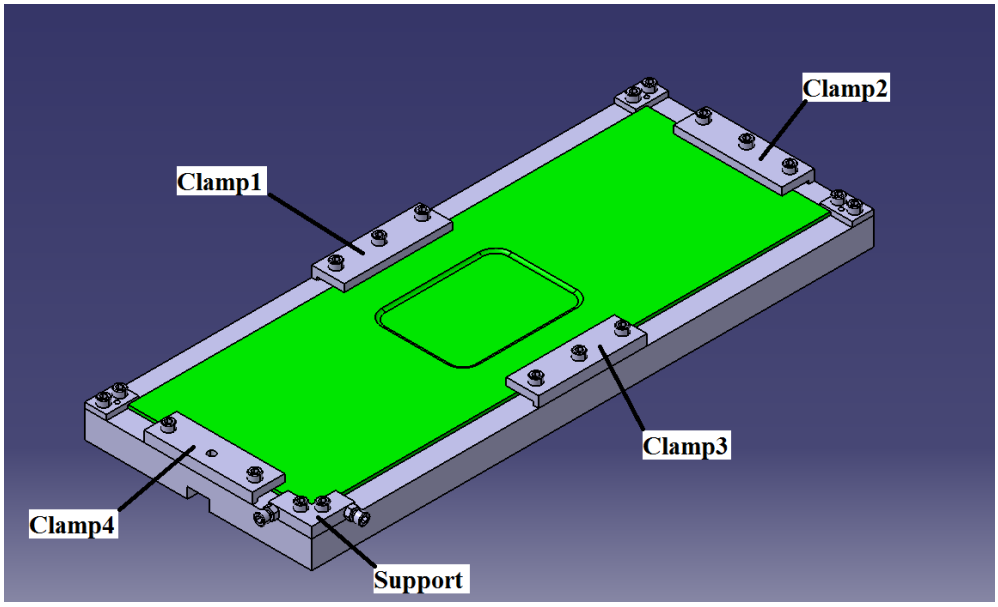

Figure 5.5 Clamping and supporting systems

The main function of the support system is to push the skin part on the locators 2-1 points and help the positioning when the four clamp systems push the skin on the locator 3 points (surface one). The screws apply the force for support and clamp systems to fix the part on the locators. There are nuts in the support system to fix the positions.

This kind of clamp was selected to determine if the pocket milling can be completed with no vibration in the middle of skin. This method could be useful during milling of the real parts. The new clamp design as shown in figure (5.6) can be used when there is a vibration or skin ruptured in pocket milling operation.

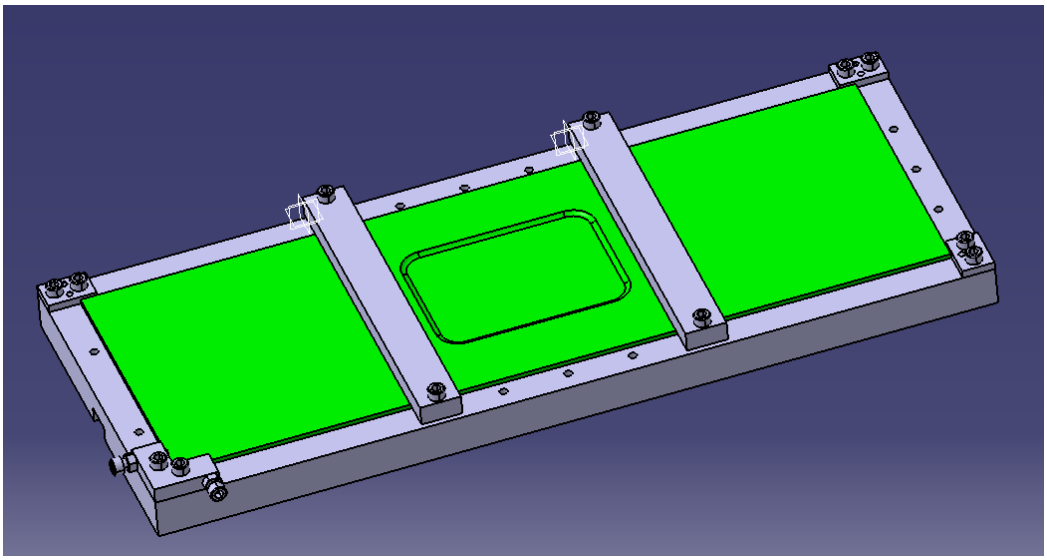

Figure 5.6 New clamping system

As mentioned earlier, High Speed Milling (HSM) operations will be performed in this work. There are three milling machines available at École Polytechnique. The specification of each machine is presented in the table 5.1, 2, and 3.

Table 5.1 Specification of Mitsui Seiki Hu 40-T

Mitsui Seiki Hu 40-T (5axies)	
Spindle (Électro broche)	15000rpm, 30kw, 420Nm
Linear axis (Axes Linéaires)	20m/min, 3.3 m/s^2, (vis à billes)
Rotational axis (Axes rotatifs)	20rpm, (engrenage et pignons)
Table	400mm, 400mm, 100kg, 4 palets
Controler (Contrôleur)	Fanuc 15iMA

Table 5.2 Specification of Matsuura MC-760UX

Matsuura MC-760UX	
Spindle (Électro broche)	4500rpm, 7.5kw, 275Nm
Linear axis (Axes Linéaires)	5m/min, (vis à billes)
Rotational axis (Axes rotatifs)	5.5rpm, (engrenage et pignons)
Table	320mm, 320mm, 80kg
Controler (Contrôleur)	Yasnac MX3

Table 5.3 Specification of Huron KX8

Huron KX8- (5axies)	
Spindle (Électro broche)	24000rpm, 24kw, 38Nm
Linear axis (Axes Linéaires)	50m/min, 5 m/s^2
Rotational axis (Axes rotatifs)	50rpm, 20rad/s^2
Table	500mm, 250kg
Controler (Contrôleur)	Siemens 840D

The Huron KX8 CNC machine was used for experimental tests as it allows machining relatively larger parts at higher rotational speed. Furthermore, the minimum quantity lubricant (MQL) system was installed on this machine. A circular table was used in this machine. In order to make alignment between the table and fixture, a slot with two key were designed in the fixture. The machine table and the fixture are presented in figure (5.7).

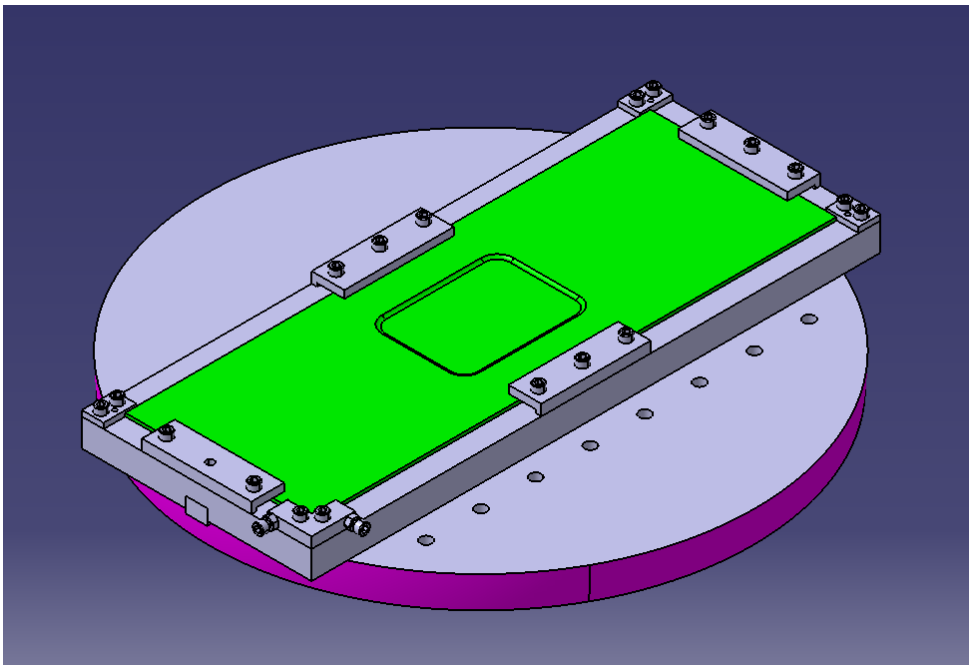

Figure 5.7 Fixture and machine tool table

The base plate depicted in figure (5.8) is made of aluminium alloy that was provided by Bombardier. The raw material was machined according to the drawing specification in figure (5.9).

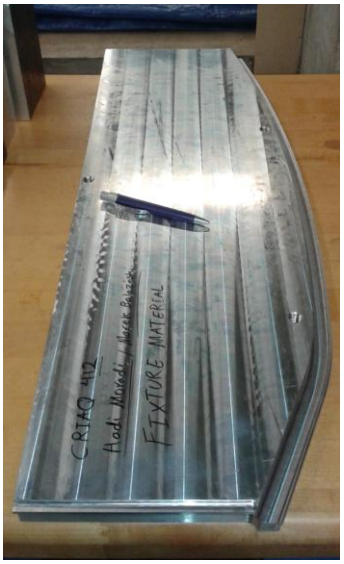

Figure 5.8 The raw material provided by Bombardier

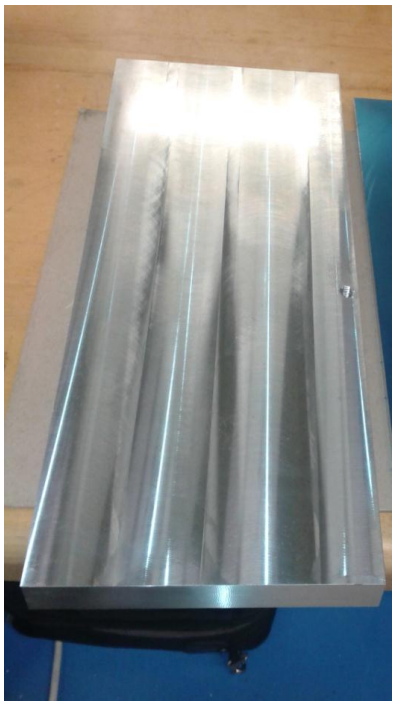

Figure 5.9 The base plate made from aluminum

Using the available commodities in the workshop and by modifying the locators, the milling fixture was manufactured (figure (5.10)).

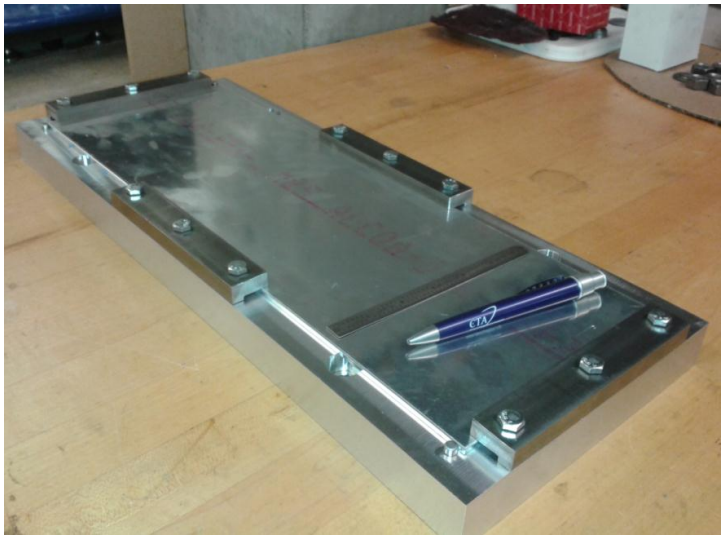

Figure 5.10 Overview of the milling fixture

CHAPTER 6 TOOL SELECTION

In order to have a cost effective and smooth production line, the required cutting tools should be selected accurately through various catalogues and manuals, either manually or by using few recently developed cutting tools, which are still the subject of further investigations.

The most important criterions for appropriate selection of the cutting tools are geometry and dimensions of the machined part, cuts and also the machining costs [80].

As depicted in figure (6.1, 2), the milling cutting tools are available in two different shapes, including solid end mill and indexable mill [81].

Figure 6.1 Different solid end mill tools [81]

Figure 6.2 Different indexable mill tools [81]

The parameters for selecting a milling cutting tool are the diameter, length, number of edges, helix angle, corner radius/chamfer and tool materials/coating [81].

The inserts could be selected from a catalog standard number that consists of few letters and numbers which define the insert geometry. In figure (6.3) an example of catalog standard number is shown.

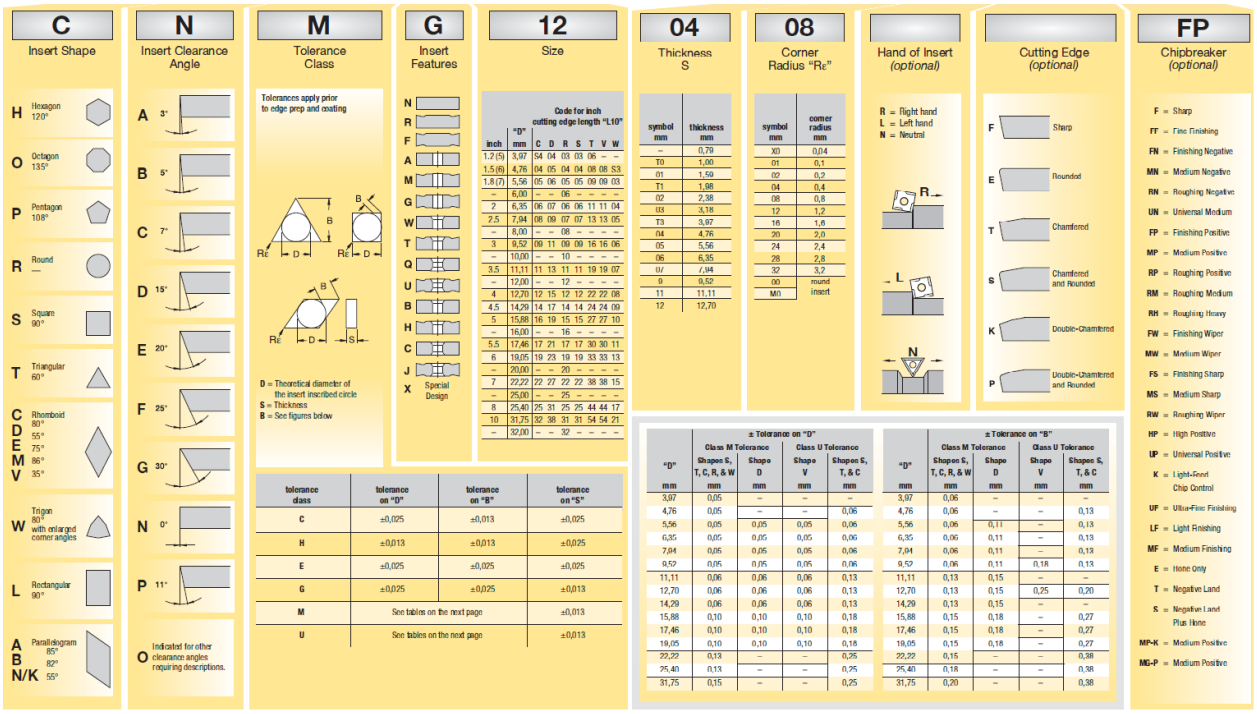

Figure 6.3 Catalog standard number (ISO) [81]

The aluminum alloys can be machine by several cutting tool materials such as tool steel, high speed steel, cemented carbide and diamond. Due to strong chemical affinity between ceramic matrix and aluminum alloys and relatively short tool life, it is not recommended to machine the aluminum alloys by ceramic tool. The similar behavior is visible when machining aluminum alloys with cubic crystalline boron nitride (CBN) tools.

Although coated insert are used to avoid rapid tool wear, this could have negative effect on tool when the coated insert is comprised of titanium. Presence of titanium in the coating may lead to diffusion and rapid tool failure [20].

As shown in figure (4.1), pocket milling operations with dimensions 120×90×3mm, corner radius 15mm and the bottom fillet radius of 4mm were conducted on flat sheet parts. Based on the cutting radius used, the cutting tool radius is smaller than 15mm. Furthermore, for finishing the bottom fillet radius, the cutting tool should have 4mm tip radius.

A solid carbide end mill (see figure (6.4)) with the tip radius 4mm was selected. Various levels of tool diameters including 10, 12, 16, 20, and 25mm could be used in this work.

Figure 6.4 Kennametal standard solid carbide end mill

As an alternative cutting tool, if the tool wear must be measured, an index tool with inserts was selected. As shown in figure (6.5), the insert number was EDCT140440PDERLDJ and index number was 20A02R050A20SED14-170 or 25A03R050A25SED14-170.

Figure 6.5 Kennametal standard insert and index

The industrial partner (Bombardier) proposed using the solid carbide tool (see figure (6.6)) that is currently applied in their production line.

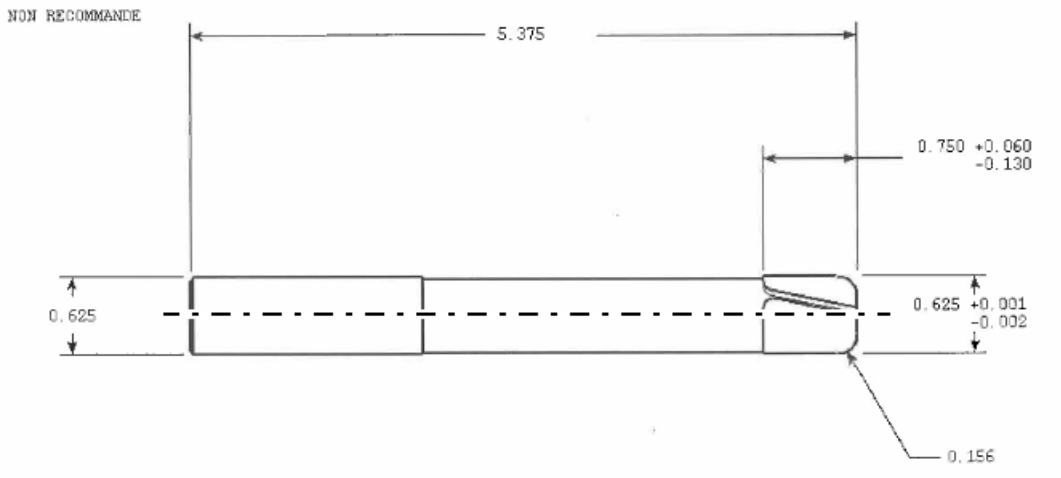

Figure 6.6 Bombardier proposed solid carbide tool

As illustrated in figure (6.7), the tool was assembled to a shrink-fit holder to improve the tool performance.

Figure 6.7 Overview of the shrink-fit holder and cutting tool

CHAPTER 7 DESIGN OF EXPERIMENT (DOE)

An experimental study may consist of one test or multiple tests. Within experimental studies, the inputs are transformed into outputs by means of the process that consists of operations, machines, people and other resources. The general model of a process is shown in figure (7.1). The experimental variables in the process are grouped to controlled variables (x1, x2, …, xp) and uncontrolled variables (z1, z2, …, zq). Appropriate results could be achieved from a well-designed experiment. The accuracy of results has a direct relationship with the number of experimental test [82].

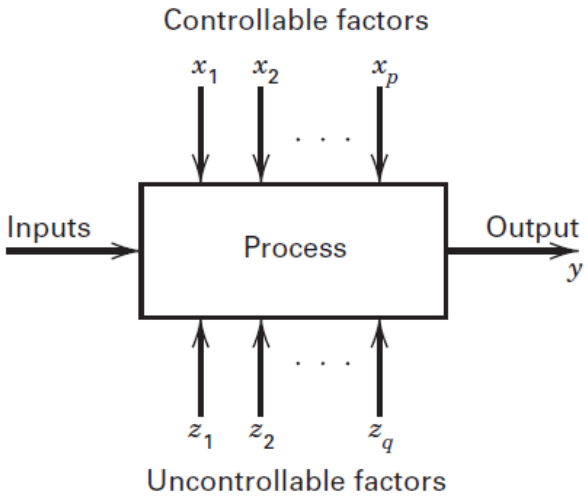

Figure 7.1 General model of a process [82]

The experiments are conducted to determine the effects of input factors on the outputs. There are two kinds of experiments: investigative experiment and demonstrative experiment. Running a large number of experiments to determine the effect of experimental factors on the products and processes is costly. Therefore, conducting a smaller number of experiments with the highest possible accuracy is desirable [82].

To that end, an extensive knowledge is required to better select the design of experiment model. Design of experiment (DOE) is used for many purposes including variable screening, transfer function exploration, system optimization, and system robustness.

The experimental studies are generally arranged in various models, such as full factorial level, fractional factorial levels, 2 levels factorial design, Taguchi orthogonal array, and Placket-Burman design for variable screening; central composite design, and Box-Behnken design for

transfer function identification and optimization; and Taguchi robust design for system robustness [83]. Prior to starting any experiment, it is necessary to select the correct DOE and analysis methods.

Randomization, replication and blocking are the three basic principles of experimental design. The variables must be distributed independently random. In other words, the experimental materials and number of tests must be chosen randomly. Each factor combination could be repeated independently by replication [82].

7.1 Procedure of Design of Experiments

Generally, the main aim and objective of each work, as well as the data collection and data analysis methods should be carefully defined before running experimental works. The main steps involved in a design of experiment procedure are as follows:

1. **Problem statement definition**. define what the main problem is in the system or in the process investigated.
2. **Response variable selection**. The response variable should give useful information about the system and could be also measurable.
3. **Factors and levels selection**. The factors that may have influence on the performance of the process and response variables should be considered. In the next step, the level of each individual experimental factor is defined.
4. **Experimental design selection**. The number of samples and replicates with respect to the optimum way of running the tests are selected. In addition, the decisions for randomization and blocking are taken.
5. **Implementation of the experimental tests**. The design and plan should be clearly defined and controlled. It is recommended to perform a few preliminary tests before conducting the main experiments.
6. **Statistical analysis of the data.** The experimental results are analyzed by using the statistical methods. For instance, simple graphical methods can be used for a better interpretation and analysis of experimental results.

7. **Conclusion and recommendations.** The practical conclusion should be drawn from the statistical analysis, followed by running few verification tests, in order to confirm the conclusion.

7.2 Problem Statement Definition and Response Variable Selection

As it was explained in chapter 3, a PFMEA method was used to define major failure factor in pocket milling of the aluminum skin sheets. These sheets are used in the body of airplane and because of safety mode; during producing and manufacturing process several parameters must be considered as engineering requirements. In this project the machining parameters for pocket milling should be defined to cover the safety results. In table 7.1 some of these parameters that have influence on the safety application are shown.

Table 7.1 Engineering requirements for aluminum skin sheets with pockets

No.	Factor	Comment
1	Tolerance of thickness of pockets	±0.0508 to 0.127 mm
2	Periphery of the pocket	±1.524 mm
3	Surface finish	Ra 1.6 µm
4	Conductivity	Must be verified
5	Micro-Cracks	Inspection
6	Visual effect	Inspection
7	Geometries tolerances	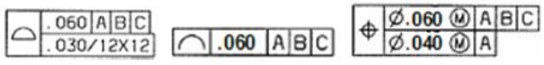

According to FMEA results, the residual stress, surface roughness and bottom thickness of pocket are considered as the main failure modes. Experimental studies are arranged in this work to observe the effects of cutting parameters on the surface roughness. Other responses will be studied by other contributed students in this industrial research project.

7.3 Factors and levels selection

Each parameter that influences the performance of product or process such as time, temperature, pressure, thickness, and type of material is called factors. There are two kinds of factors: continuous factors and discrete factors. The continuous factors are quantitative and the discrete factors are not quantitative. Each factor may have two or more values or status, called level. The experimental factors and their levels used for pocket milling of aluminum thin sheets are presented in the table 7.2.

Table 7.2 Experimental factors and levels used for the pocket milling of aluminum sheets

No.	RPM	Chip Thickness (Max.)	Depth of Cut max1.8mm	Lubrication
1	10000	0.0508 mm	two pass (2x0.9mm)	MQL
2	12000	0.1016 mm	three pass (3x0.6mm)	Wet
3	14000	0.1524 mm	four pass (4x0.45mm)	Dry

Knowing that the tool diameter is Ø15.875 mm (0.625in) and the RPM of spindle 10000, 12000, and 14000 rpm, the corresponding values of cutting speed were calculated. Moreover, as shown in table 7.3, the feed rates were also calculated according to maximum chip thickness values.

Table 7.3 Calculated feed rates

Maximum Chip Thickness (mm) ϕ=45°	Maximum Chip Thickness (mm) ϕ=90°	RPM	Teeth No.	Step Over 25% Feed Rate (m/min)
0.071882	0.0508	10000	3	2,15646
		12000		2,587752
		14000		3,019044
0.143764	0.1016	10000	3	4,31292
		12000		5,175504
		14000		6,038088
0.215646	0.1524	10000	3	6,46938
		12000		7,763256
		14000		9,057132

According to the percentage of cutting tool diameter engagement, the maximum chip thickness can be calculated by using Eqn. (2.3) on page 31. The maximum chip thickness is equal to feed rate per tooth of cutting tool when at least half of cutting tool diameter is in engagement with the machined part. In these tests the engagement is 25% of cutting tool diameter. It means that the maximum chip thickness should be calculated with the angle (ϕ) as 45 degree.

As requested by industry, the one way strategy was selected. The spiral strategy for pocket milling on the flat sample sheet is the best method but on the actual sheet with double curvature, it is very difficult to use.

The depth of cut can be selected according to depth of pocket. The complete depth of cut (1.8mm) as one pass was not recommended by industry, as this method would pass more heat into the part, which is not however favorable in high performance machining. Therefore, two, three and four passes were selected as depth of cut, respectively.

The other experimental parameters such as step over (25%), cutting tool specification (geometry (ball nose), cutting tool material (carbide), shape (solid carbide), number of teeth (3), and diameter (Ø15.875mm)), as well as machining strategy (one way and profile contouring) were treated as constant parameters.

7.4 Experimental design selection

The Design of experiments (DOE) was initially used by Sir R. A. Fisher in England in 1920 [83]. This method was primary used in agriculture, but after a while, it has been also applied in academic research institution and few chemical and fertilizer industries. In order to attain the best quality of products with less number of tests, Dr. Genechi Taguchi proposed a new application of DOE methods, so called signal-to-Nose ratio (S/R) which significantly improved the quality of manufactured products in Japan during 1960s and 1970s.

Several DOE methods have been proposed until now. The correct selection of DOE method depends on many factors, including the desired number of factors and responses. It is a very simple task to design experimental study to observe the effect of one factor on the responses. However in reality, the design of experiments are planned to study the effect of several experimental factors on multiple responses.

The possible combination of all factors in experiment is known as full factorial combinations of experimental parameters. Full factorial design of experiment is often costly, when large number of variables and levels are studied. The full combinations of factors can be calculated by Eqn. 7.1:

$$\text{Total number of combinations} = (\text{number of levels})^{\text{number of factors}} \qquad (7.1)$$

As it was mentioned in the previous section, the number of factors and levels are four and three, respectively. Then full possible combinations of factors of an experiment are 3^4= 81 tests. Many approaches such as fractional factorial design are used to reduce the number of tests while identifying the major effects. Moreover, orthogonal arrays design of experiment (see table 7.4) using Taguchi method is proposed to reduce the number of tests. In the table 7.4 this orthogonal arrays is shown.

Table 7.4 Orthogonal arrays of Taguchi method

Number of Levels	Number of Parameters (P)																										
	2	3	4	5	6	7	8	9	10	11	12	13	14	15	16	17	18	19	20	21	22	23	24	25	26	27
2	L4	L4	L8	L8	L8	L8	L12	L12	L12	L12	L16	L16	L16	L16	L32	L32	L32	L32	L32	L32	L32	L32	L32	L32	L32	L32
3	L9	L9	L9	L18	L18	L18	L18	L27	L27	L27	L27	L27	L36	L36	L36	L36	L36	L36	L36	L36	L36	L36				
4	L'16	L'16	L'16	L'16	L'32	L'32	L'32	L'32	L'32																	
5	L25	L25	L25	L25	L25	L50	L50	L50	L50	L50	L50															

In the current work, the orthogonal array L9 is used to construct the experimental plan (see table 7.5) [83].

Table 7.5 Orthogonal array L9 of Taguchi method [83]

Experiment	P1	P2	P3	P4
1	1	1	1	1
2	1	2	2	2
3	1	3	3	3
4	2	1	2	3
5	2	2	3	1
6	2	3	1	2
7	3	1	3	2
8	3	2	1	3
9	3	3	2	1

The constructed experimental plan using orthogonal array is shown in the table 7.6.

Table 7.6 Orthogonal array for pocket milling on the thin skin

No.	RPM	Feed rate	D.O.C (mm)	Lubrication
1	10000	2,156 m/min	0.9	MQL
2	10000	4,313 m/min	0.6	Wet
3	10000	6,469 m/min	0.45	Dry
4	12000	2,588 m/min	0.6	Dry
5	12000	5,176 m/min	0.45	MQL
6	12000	7,763 m/min	0.9	Wet
7	14000	3,019 m/min	0.45	Wet
8	14000	6,038 m/min	0.6	Dry
9	14000	9,057 m/min	0.45	MQL

7.5 Experimentation

As discussed earlier, the experiment plan must be drawn accurately. In order to determine the stability of system, it is recommended to perform few preliminary tests before conducting the main experimental tests.

7.5.1 First Test

Preliminary tests were conducted to define the accuracy of the CNC program, machine tool, cutting tool, lubrication and cutting condition during pocket milling operations. Since the designed fixture was not available during preliminary test, a small sheet of aluminum was

clamped on the CNC table. The machining specification for the preliminary test is shown in table 7.7.

Table 7.7 Machining specification for the preliminary test

Material	Al2024-T3
Sheet Size	170 X 127 X 2.54 mm
Cutting Tool	Solid Carbide, 3 Flutes, Tip Radius 1.6mm, Diameter 19.05mm
Machining Strategy	Spiral Internal with the corner radius 1mm
Feed Rate	2000 (mm/min)
RPM	10000 (rpm)
Lubrication	MQL, 40 (ml/min) and Air pressure 20 psi
Step-over	50% of cutting tool diameter

The sheet for the preliminary test is shown in figure (7.2).

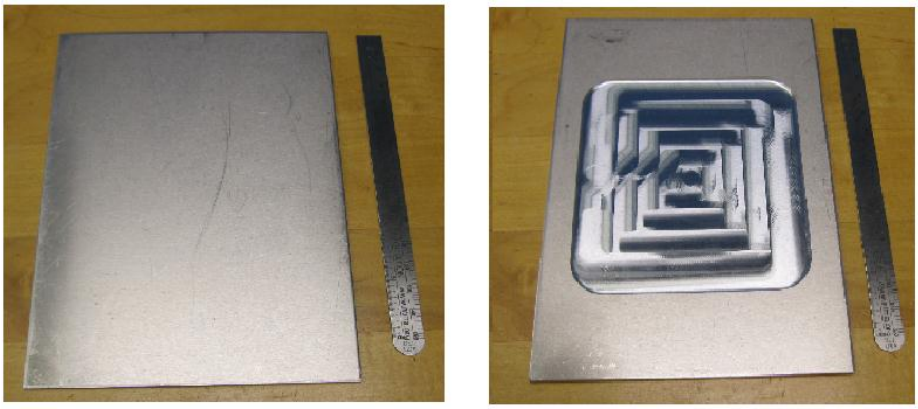

Figure 7.2 The machined sheet metal before and after preliminary test

The program was generated with the CATIA V5R20 and posted to the Huron KX8. The test sheet was clamped on a dynamometer. The experimental setup, including the sheet metal, CNC table and dynamometer are shown in figure (7.3).

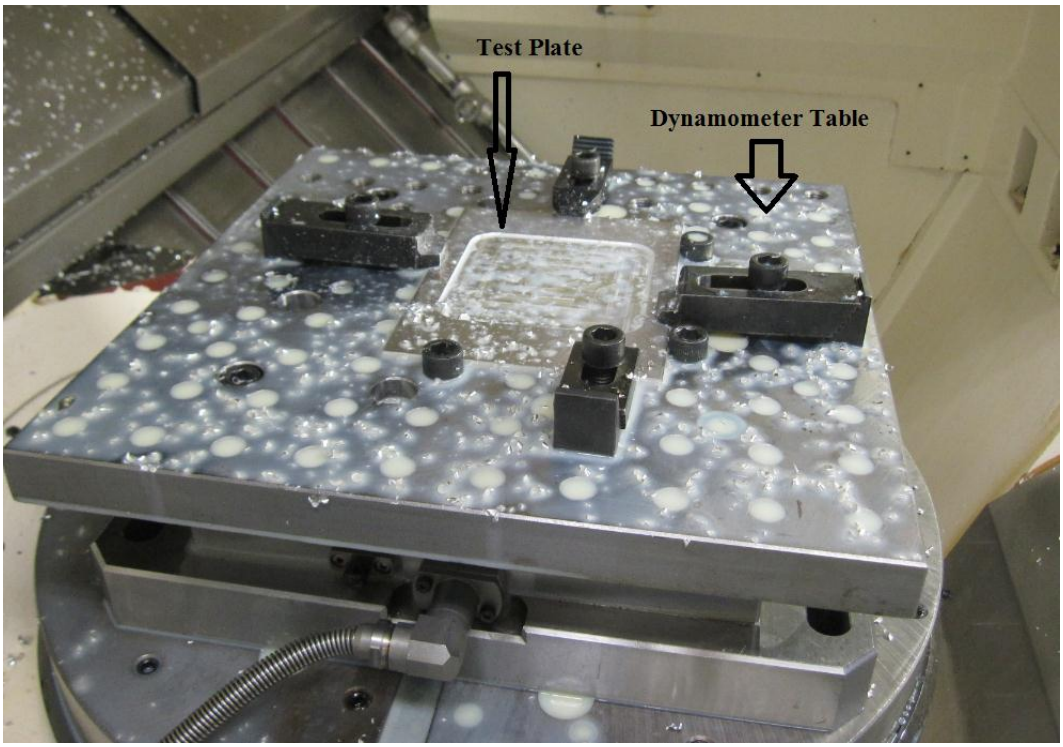

Figure 7.3 Test sheet after pocket milling on the machine and dynamometer table

The cutting forces were recorded using a dynamometer. A profile of the experimental cutting forces is shown in figure (7.4).

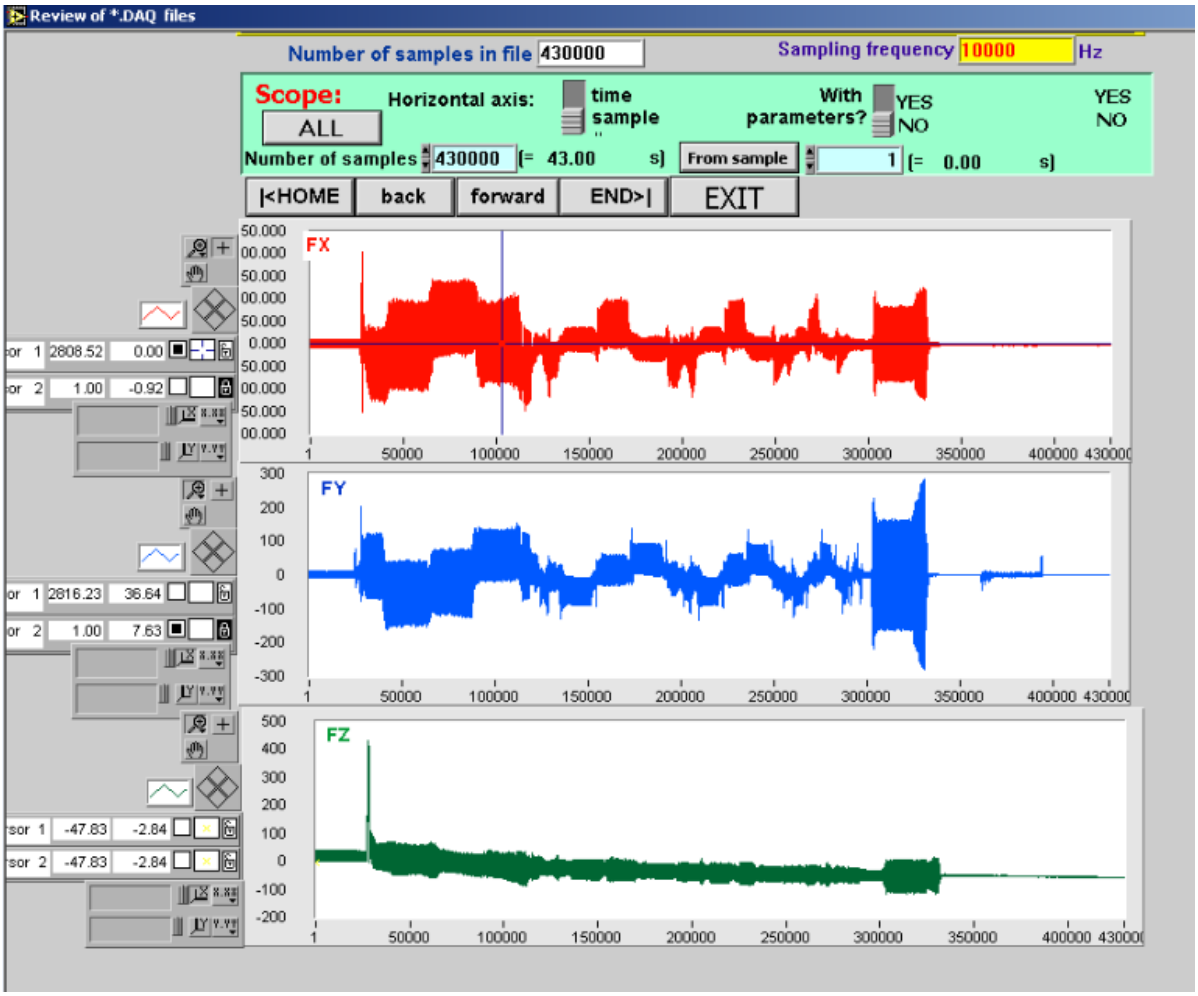

Figure 7.4 Cutting force results recorded during the preliminary pocket milling of test

The resultant cutting force could be calculated using Eqn. 7.2:

$$F = \sqrt{F_X^2 + F_Y^2 + F_Z^2} \qquad (7.2)$$

Where, F_X is cutting force, F_Y is feed force and F_Z is thrust force.

According to Eqn. 7.2 the maximum resultant cutting forces is about 212 N for this pocket dimension and spiral internal machining. The maximum cutting force result could be seen in the first rotation of the boundary of pocket because of maximum engagement of tool and material and at the end of machining in the middle of pocket. The cutting forces results could be distributed on the pocket strategy according to the step over to omit the maximum cutting forces in the middle of pocket.

7.5.2 Second Test

The second test was performed on the real size sheets. The test setup was then modified by installing a bigger table on the dynamometer (figure (7.5)). The machining parameters used as well as supporting information for this test are shown in table 7.8.

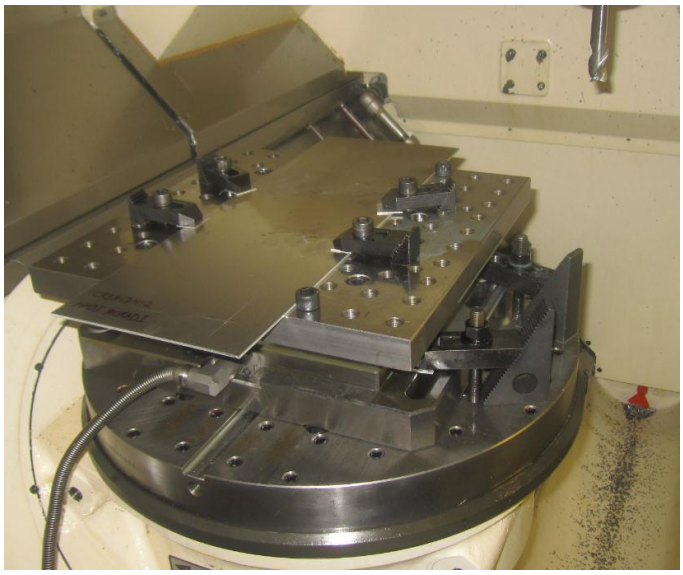

Figure 7.5 The real size sheet and the modified test set up

Table 7.8 Machining specification for the second test

Material	Al2024-T3
Sheet Size	480 X 190 X 2.54 mm^3
Cutting Tool	Solid Carbide, 3 Flutes, Tip Radius 1.6mm, Diameter 19.05mm
Machining Strategy	Spiral Internal with the corner radius 1mm
Feed Rate	2000 (mm/min)
RPM	10000 (rpm)
Lubrication	MQL, 40 (ml/min) and Air pressure 20 psi
Step-over	25% of cutting tool diameter

The pocket milled sheet is shown in figure (7.6).

Figure 7.6 The pocket milled sheet

Changing the sheet size and step over allow to observe the effects of these parameters on the recorded cutting forces. According to experimental results, the relatively similar cutting forces were observed as that in the first test. However different cutting force profiles are observed from these in the first test. The results are shown in figure (7.7).

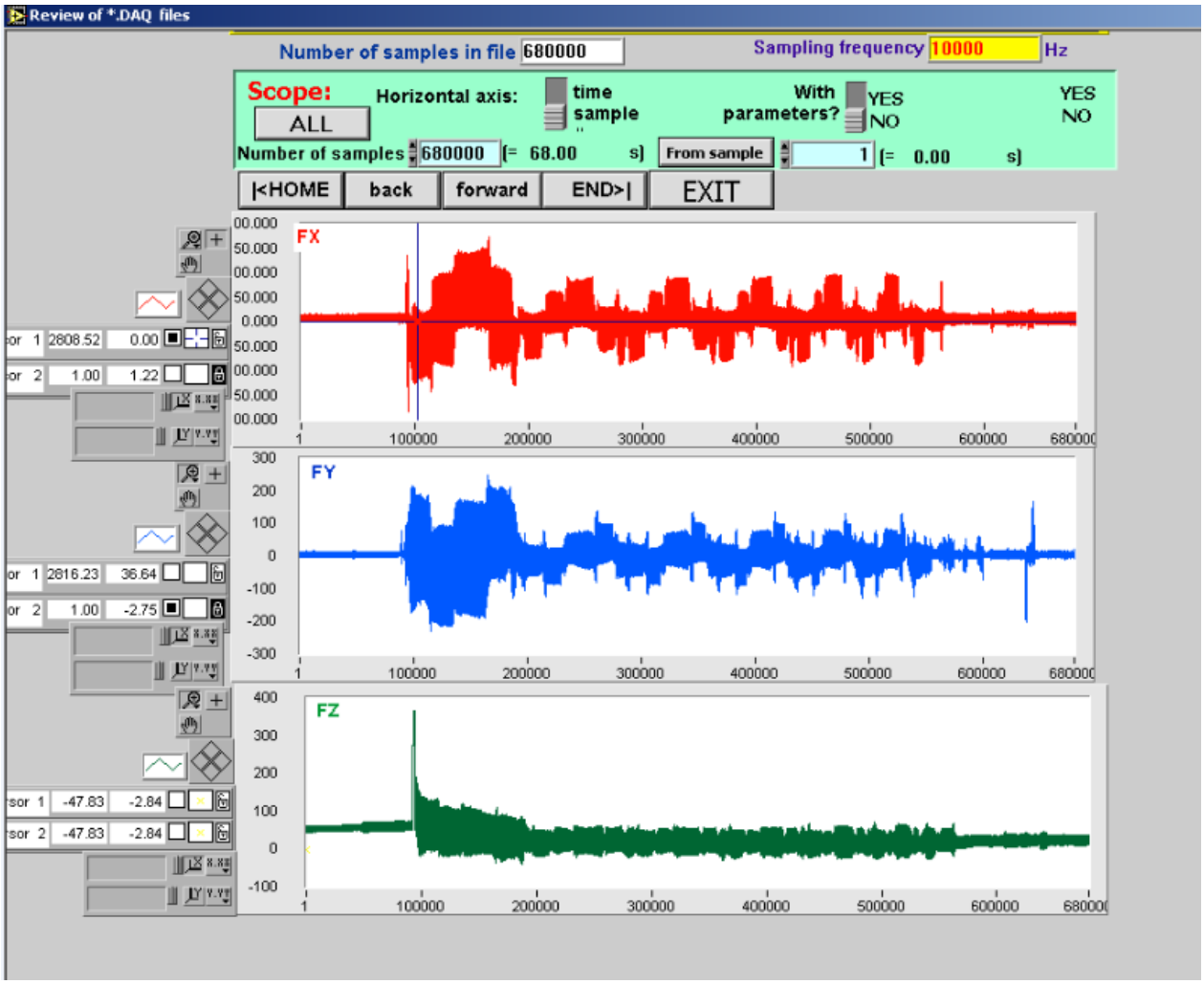

Figure 7.7 The recorded cutting forces of second test sheet

Using Eqn. 7.2, the maximum cutting force is calculated. A similar value of the maximum force is obtained. According to experimental tests, by changing the step-over of pocket machining from 50% to 25%, the maximum force decreases at the beginning of the cut and also when the cutting tool is in engagement at the middle of cutting operation. The maximum cutting force for this test was repeated but the distribution of force was different. Moreover, the cutting forces can be minimal in the middle of pockets, when the step-over is decreased to 25%. The deflection of the aluminum sheet was measured by the machine tool probe. In the long side of sheet 20 points and in the short side 8 points were located in the cad model. The program was performed before and after the pocket milling. The surface of the sheet was touched by the probe system. The probing system and sheet metal placed on the table are illustrated in the figure (7.8).

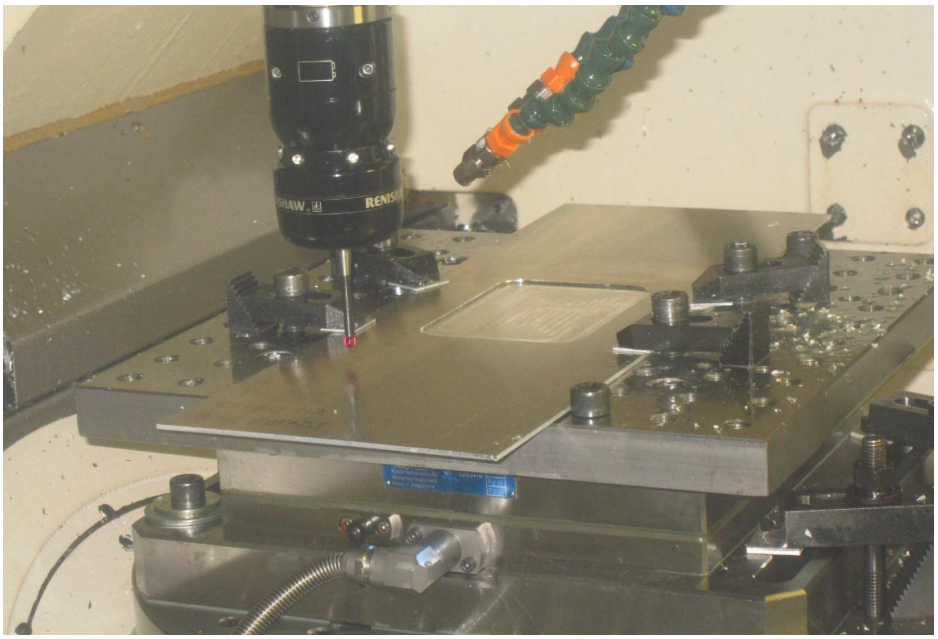

Figure 7.8 Probing system and sheet on the table

The deflection measurements were analyzed and corresponding graphs are shown in figure (7.9). Considering that the probing forces would displace the sheet part when the probe touched the surface, it is understood that the recorded deflection results are not accurate.

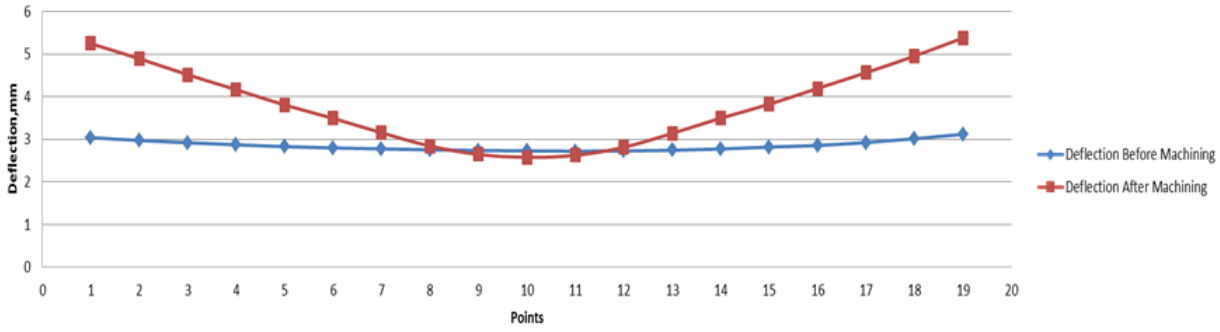

Figure 7.9 Deflection profile obtained during pocket milling of the aluminum sheet

As depicted in the figure (7.10), the real deflection of the work part could be monitored after machining test 2.

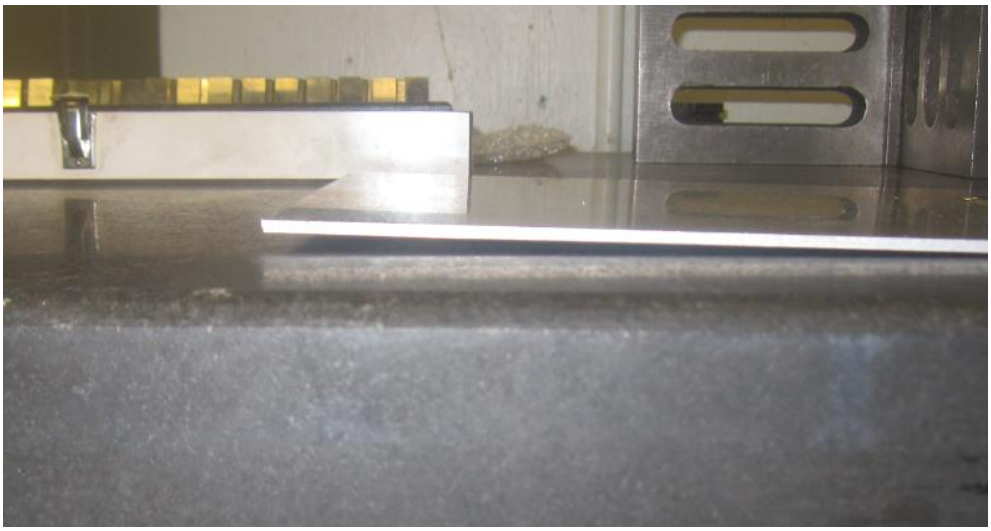

Figure 7.10 Real deflection of aluminum sheet after pocket milling

The profilometer Mitutoyo (SV-C4000) was used for surface roughness measurement. The procedure used for surface roughness measurement is shown in the figure (7.11).

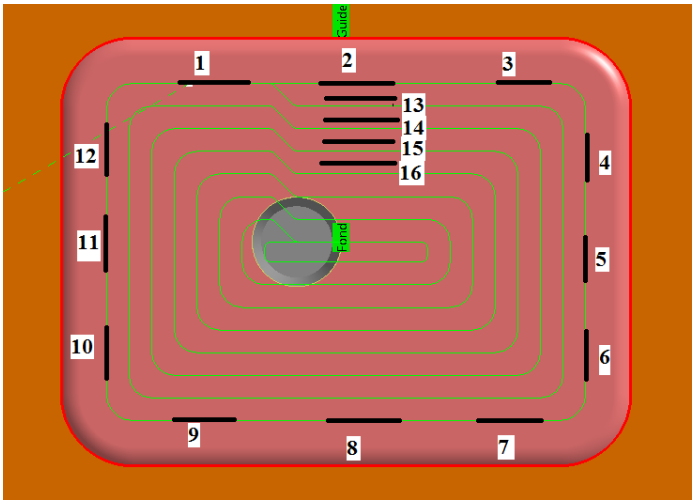

Figure 7.11 The procedure used for surface roughness measurement

According to experimental results (figure (7.12)), the maximum value of average surface roughness Ra is 1.02µm.

	0.92		0.89		0.51	
0.74			0.32			0.05
			0.41			
			0.51			
0.68			0.51			0.56
0.11						0.66
	0.75		0.98		1.02	

Figure 7.12 Surface roughness Ra (μm) measurement results in different pocket positions

7.5.3 Third Test

As shown in figure (4.1), the similar work part geometry as that in tests 2 was used, except the thickness of sheet was changed to 3.18m.

The machining parameters used are presented in the table 7.9. Except the machined part thickness, different tool diameter, machining strategy and lubrication mode are used in the third test. This test was performed to check the capability of the machining operation.

Table 7.9 Machining specification for the third test

Material	Al2024-T3
Sheet Size	480 X 190 X 3.180 mm
Cutting Tool	Solid Carbide,3 Flutes, Tip Radius 1.6mm, Diameter 15.875mm
Machining Strategy	One way with the counter milling to finish the boundary.
Feed Rate	6000 (mm/min)
RPM	14000 (rpm)
Depth of Cut	1.8 mm
Lubrication	dry
Step-over	50% of cutting tool diameter

In the figure (7.13) the machining part for the Third Test is shown.

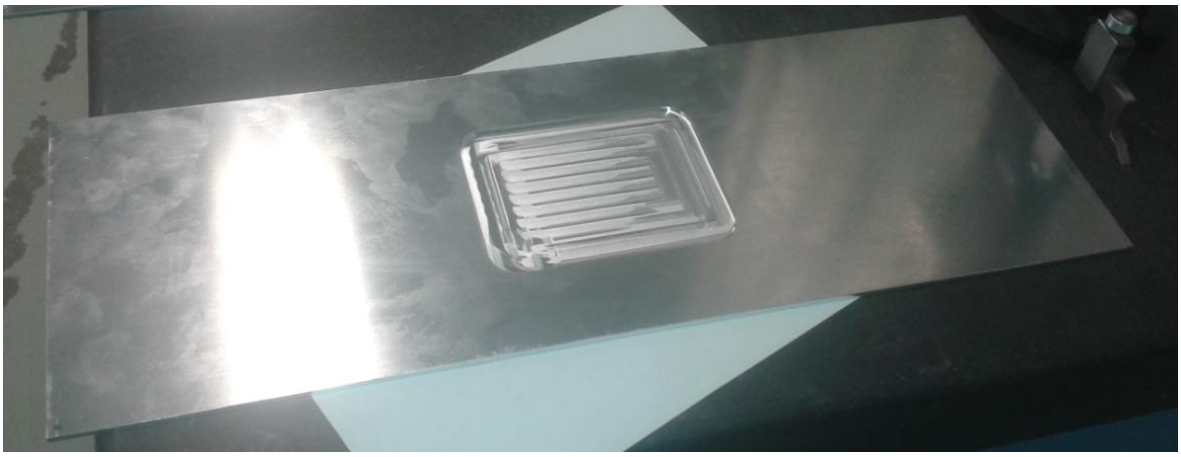

Figure 7.13 Machining test part for the third test

7.5.4 Main Tests

The list of the tests completed after the randomization are shown in the table 7.10.

Table 7.10 List of tests after randomization

Random Test N.	No.	RPM	Feed rate	D.O.C (in)	Coolant
TEST 4	4	12000	2,588 m/min	0.6	DRY
TEST 7	7	14000	3,019 m/min	0.45	WET
TEST 5	5	12000	5,176 m/min	0.45	MQL
TEST 3	3	10000	6,469 m/min	0.45	DRY
TEST 9	9	14000	9,057 m/min	0.6	MQL
TEST 6	6	12000	7,763 m/min	0.9	WET
TEST 1	1	10000	2,156 m/min	0.9	MQL
TEST 8	8	14000	6,038 m/min	0.9	DRY
TEST 2	2	10000	4,313 m/min	0.6	WET

7.6 Measurement and Test Results

The experimental tests were conducted according to the setting levels of process parameters listed in table 7.10. The surface quality, deformation, bottom thickness, position and dimension tolerances were measured in each test.

7.6.1 Surface Quality

In order to reduce the work-part temperature, the one way strategy with ramping angle 7° was used in this work. In this condition, the cutting tool enters the material from the nearest position of a side of pocket. In the second step, the cutting tool proceeds in the work part up to the nearest distance of other side of pocket. At this point, cutting tool leaves the work part perpendicularly. The described strategy for pocket machining with four passes is shown in figure (7.14).

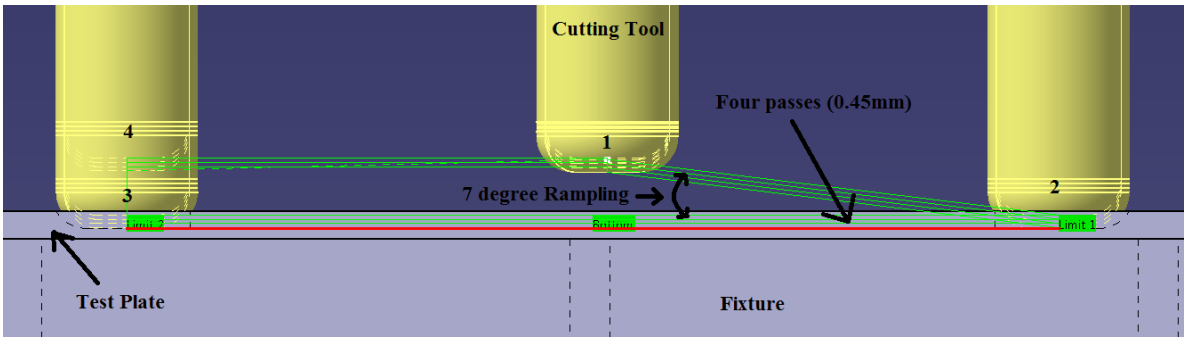

Figure 7.14 One way strategy with depth of cut (four passes)

As shown in the figure (7.14), the cutting tool from point one with the ramping angle as 7° enters to the part. The cutting tool stops at point two in the first depth of cut. The moving direction of tool will be changed along point three. Even though, there is a 0.66mm remain material from edge of cutting tool at point two and the border of pocket. The cutting tool removes the whole remained materials from point two to point three. It will stop at point three. The same stock material will be in this side of pocket to the cutting tool edge. The tool leaves the part from point three to point four and then starts the next pass from point one. At this stage, the tool moves to the second level of depth of cut and this strategy will be repeated to up to completing the one pass. The figure (7.15) shows the one pass of the strategy.

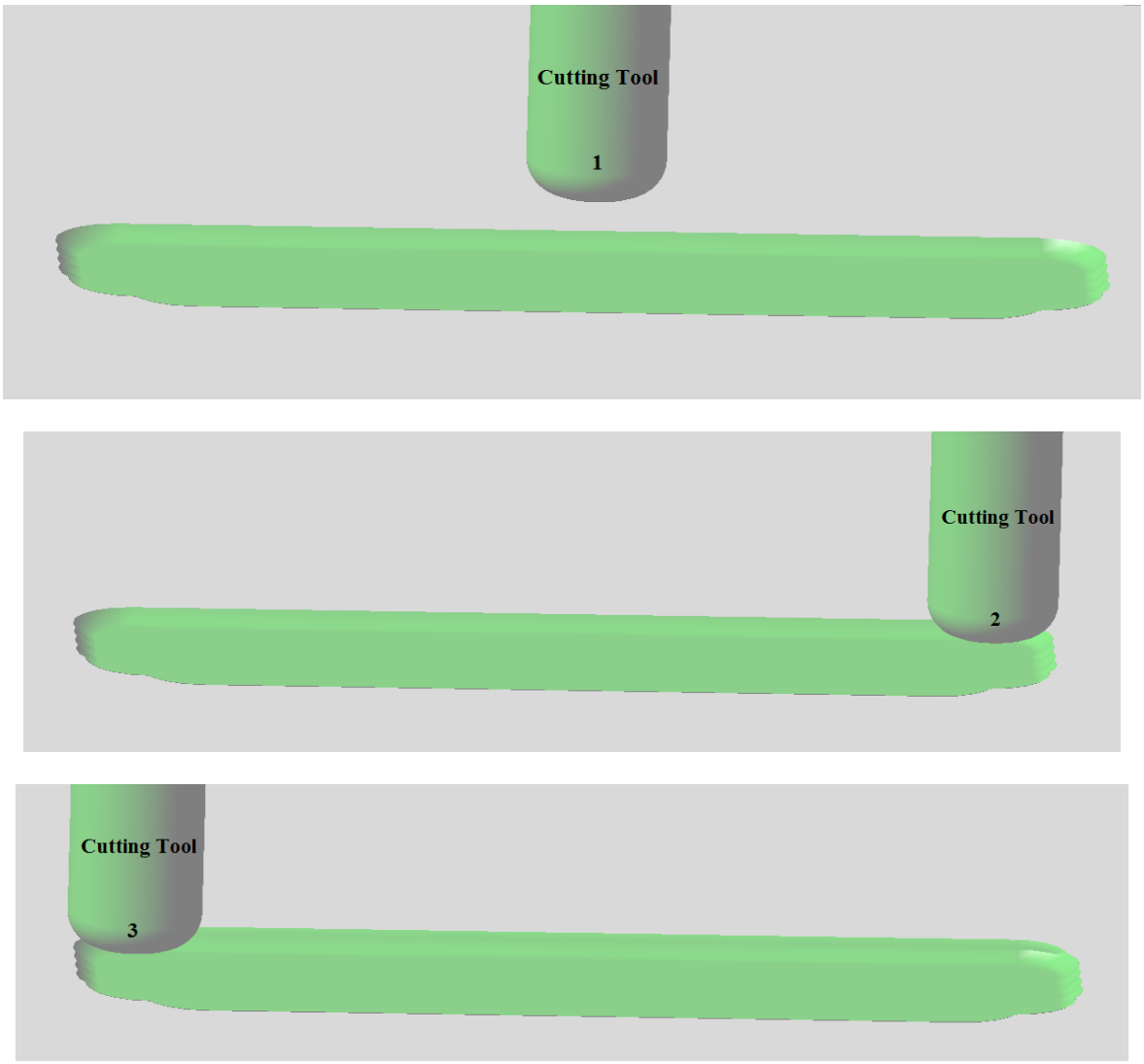

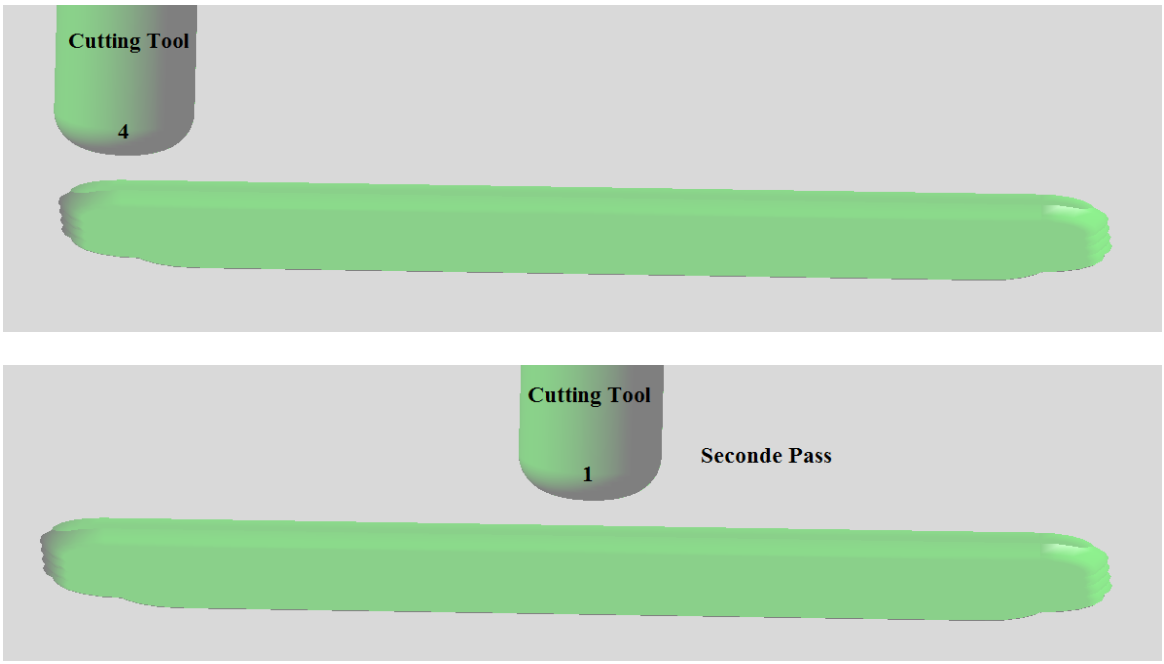

Figure 7.15 One pass of the one way strategy used for pocket milling

This process will be repeated up to completing the pocket milling. In the figure (7.16), the one way strategy used to complete the pocket machining is presented.

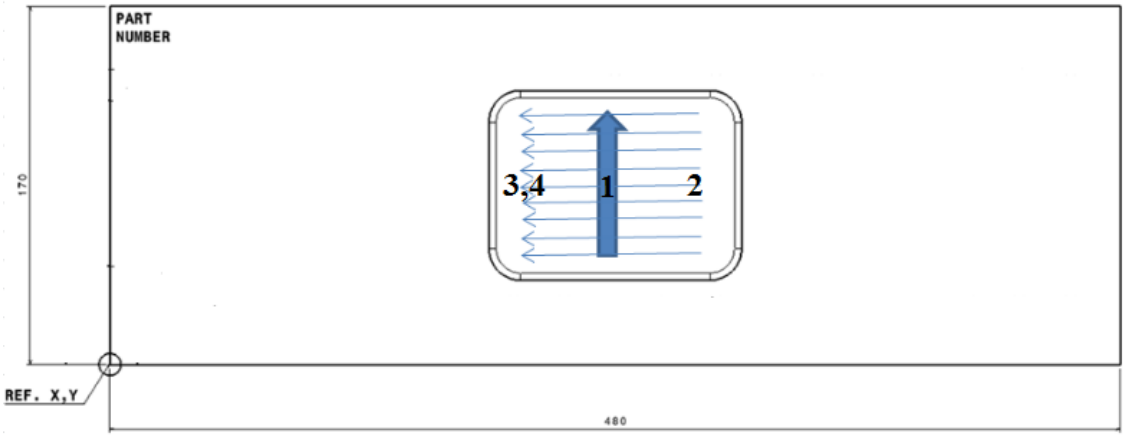

Figure 7.16 One way strategy used for the pocket machining

The typical four positions of cutting tool in one pass as well as machining direction in one way strategy are illustrated in the figure (7.16).

The boundary of the pocket with this strategy cannot be finished. Then, a profile contouring program was added to finish the pocket size. The mode of pocket machining after executing the one way strategy is shown in figure (7.17).

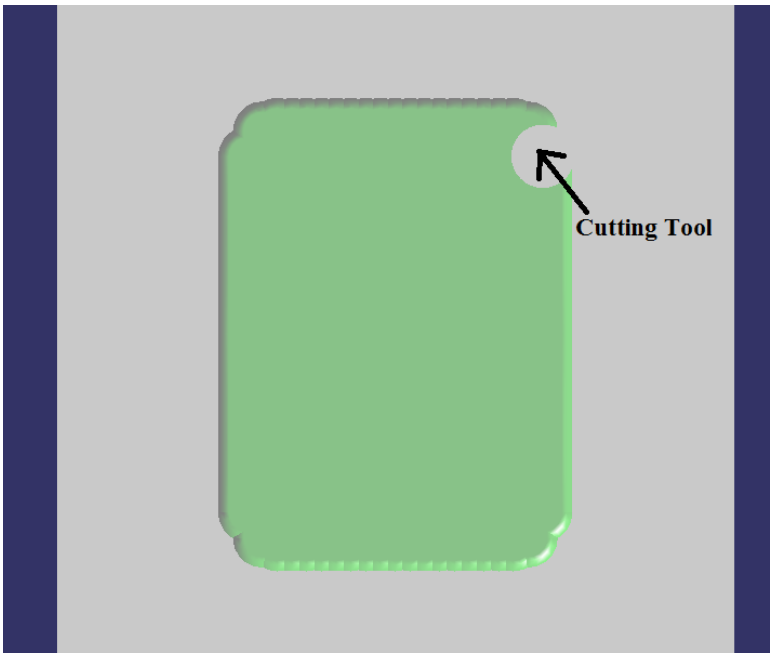

Figure 7.17 Shaped of machined part after implementing the one way strategy

According to figure (7.17), the border sides of pocket are with shape of indentation. The pocket size has not been completed. As it is illustrated in the figure (7.18 and 19), the final size of pocket can be achieved.

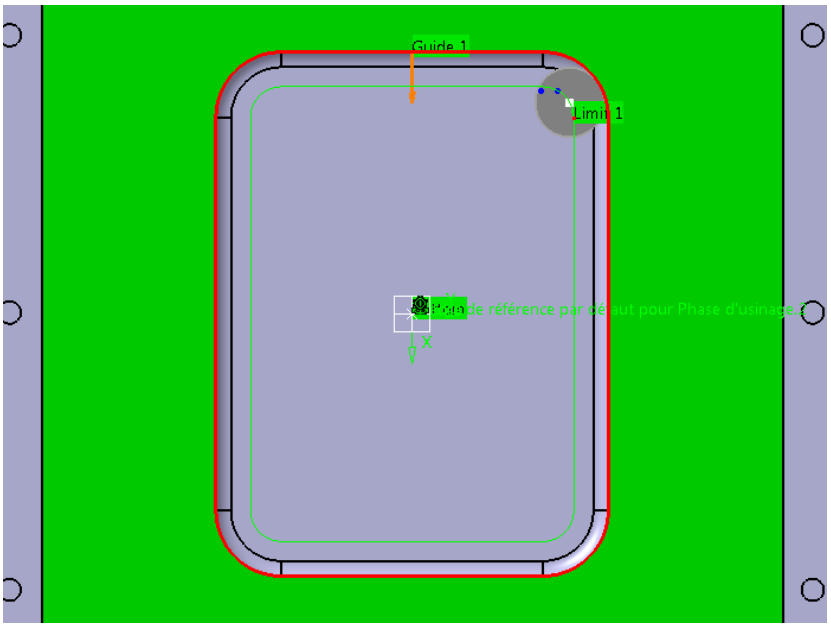

Figure 7.18 Tool path of profile contouring

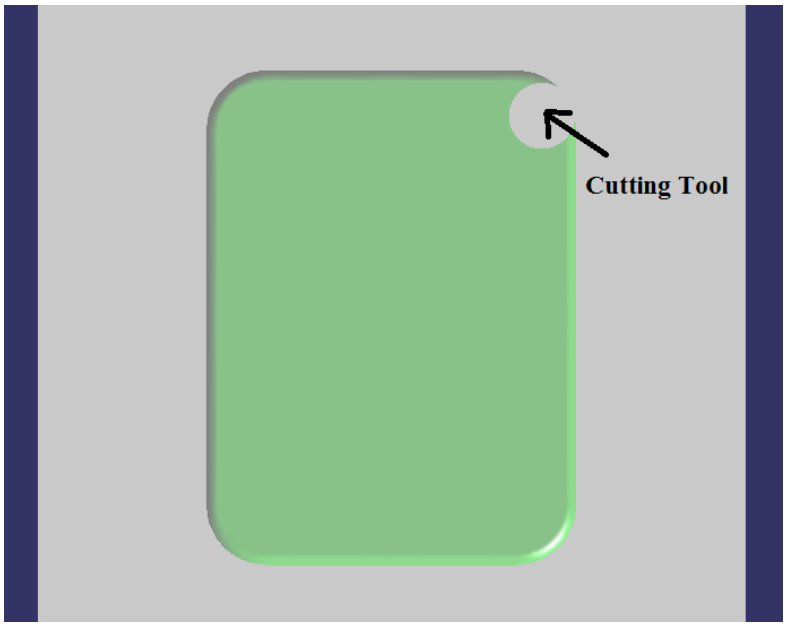

Figure 7.19 Final shape of the work part after pocket machining

The profile contouring machining starts at the last point of one way strategy when the cutting tool is still engaged with the work part. It means that cutting tool in the last pass of one way does not leave the work part. The start and end point as well as moving direction used in profile contouring are shown in the figure (7.20).

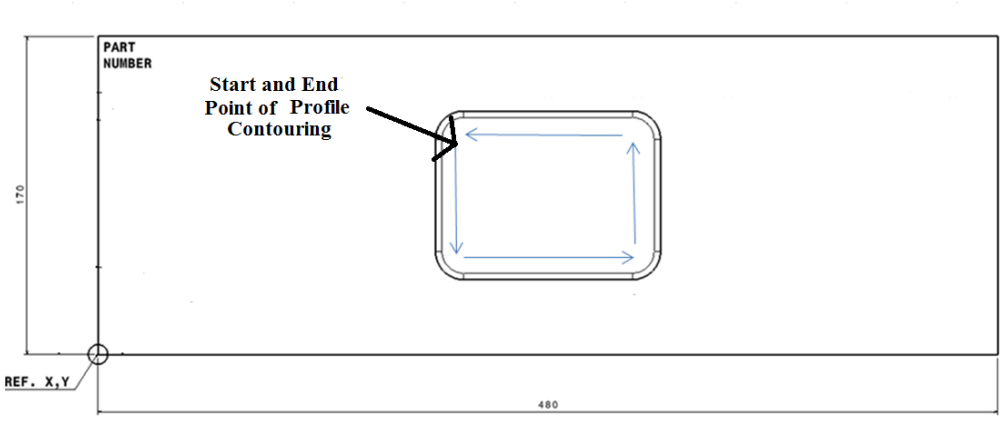

Figure 7.20 Start and end points of profile contouring

During the pocket milling, two different milling strategies generate two different surfaces with different surface quality. The first surface is generated when using the one way strategy and step over of 25%, while the second surface is generated when profile contouring strategy is used. Both generated surfaces in a pocket milling operations are shown in the figure (7.21).

Figure 7.21 Two different surfaces inside the pocket

The surface quality can be evaluated by two different surface attributes; surface roughness (Ra) and mismatch, which both can be measured by Profilometer.

The surface roughness measurement was conducted based on using the procedure presented in the figure (7.22).

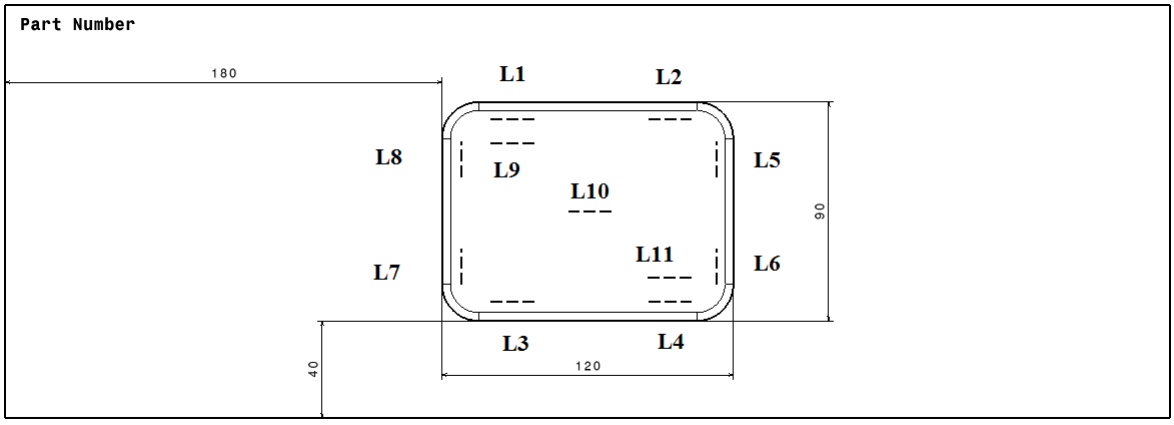

Figure 7.22 Surface roughness measurement positions

The two different surfaces inside the pocket were measured at eleven lines or areas (L1 to L11). The eight lines (L1 to L8) located on the profile contouring surface and the three lines (L9 to L11) located on the one way surface.

Each side of profile contouring surface was measured by two lines. The one way surface was measured by putting the three lines in different positions to cover the surface.

The measurements were completed using a profilometer Mitoyoto Formtracer SV-C4000. The surface roughness tester was adjusted for the Ra 1.6 µm or better. The experimental results are shown in table 7.11.

Table 7.11 Surface roughness results Ra (µm)

Test No.	Profile Contouring, Ra (µm)								One Way, Ra (µm)			Stra. P C (Max.) (µm)	Stra. O W (Max.) (µm)
	L1	L2	L3	L4	L5	L6	L7	L8	L9	L10	L11		
1	0.49	0.5	0.62	0.69	0.52	0.42	0.76	0.59	0.29	0.38	0.57	0.76	0.57
2	0.72	0.68	0.67	0.66	0.78	0.72	0.95	0.97	0.66	0.80	0.75	0.97	0.80
3	0.93	0.55	0.64	1.14	0.78	1.22	1.10	1.18	0.53	0.75	0.85	1.22	0.84
4	0.55	0.51	0.55	0.56	0.56	0.55	0.39	0.71	0.69	0.39	0.72	0.71	0.72
5	0.6	0.71	0.64	1.93	0.74	0.65	0.78	0.96	0.48	0.69	0.61	1.93	0.69
6	0.76	0.9	1.65	2.07	0.88	1.11	0.95	0.73	0.90	1.09	1.04	2.07	1.09
7	0.45	0.45	0.50	0.48	0.40	0.52	0.38	0.60	0.37	0.40	0.61	0.60	0.61
8	0.63	0.62	1.13	0.75	0.71	0.73	0.66	0.75	0.82	0.66	0.46	1.13	0.82
9	0.51	0.72	1.99	2.02	0.88	0.99	0.80	1.04	0.85	1.20	0.91	2.02	1.20

*Stra. P C: Strategy Profile Contouring

*Stra. O W: Strategy One Way

The surface roughness values (Ra) of each line are listed under L1 to L11 in the columns. The test parts numbers are defined in the rows. The maximum value of surface roughness for each test part is located in the two last columns.

The auto-correlation functions were used during the surface roughness measurements. The analyses of the work part indicate that the recorded surface roughness values are within the same range. This exhibits that except for line (L4) of work parts six and nine, the cutting operations were not influenced by vibrations. An example of auto-correlation functions is shown in the figure (7.23).

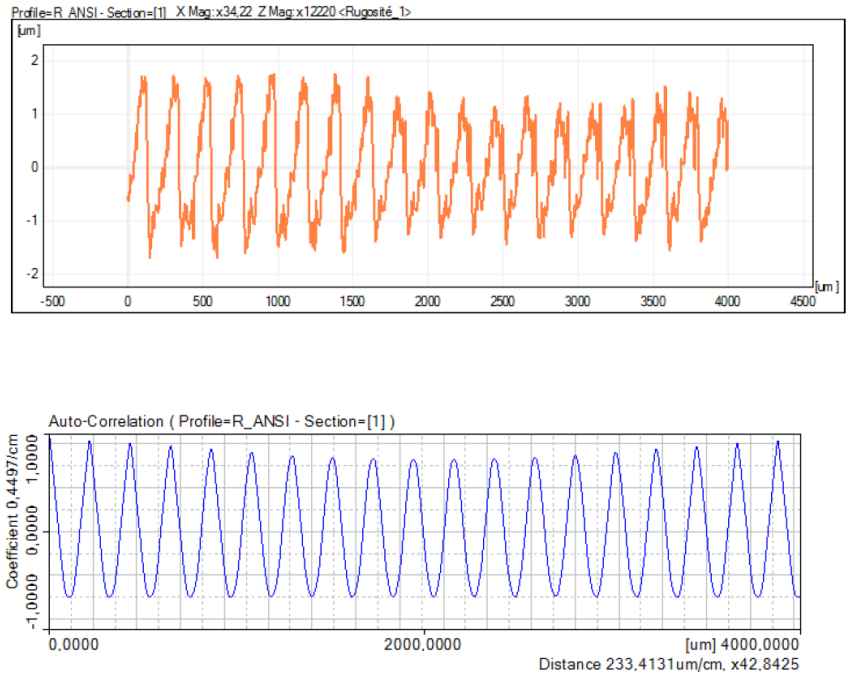

Figure 7.23 Auto-correlation function for test part one and line seven

The parts six and nine were machined with at least two maximum value for cutting parameters. The cutting parameters for test part six were such as RPM (12000rpm), feed rate (7763m/min) and depth of cut (0.0354mm); and the cutting parameters for test part nine were such as RPM (14000rpm), feed rate (9057m/min) and depth of cut (0.0236mm). The auto-correlation functions for this line (L4) of test part six and nine are shown in the figures (7.24, 25)

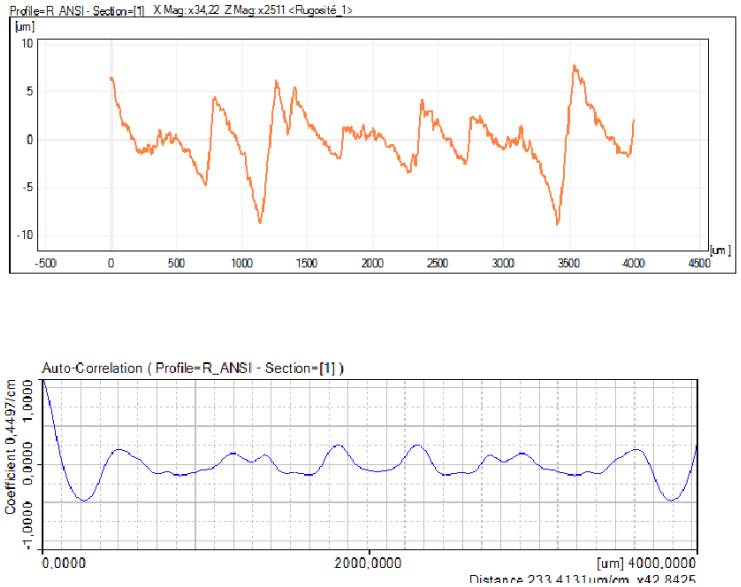

Figure 7.24 Auto-correlation function for test part six and line four

Inappropriate surface roughness in this position indicates that the cutting operation was influenced by vibration.

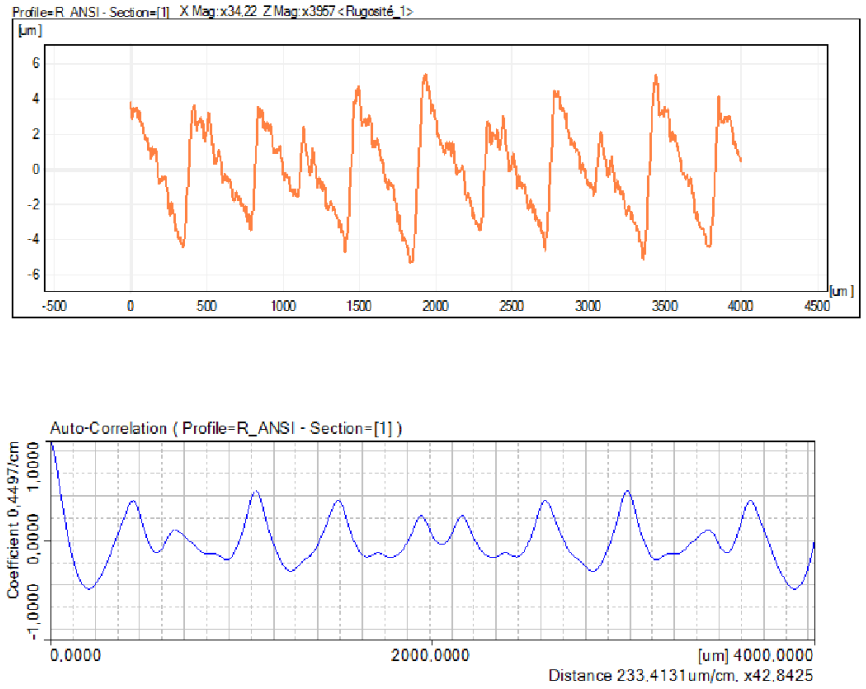

Figure 7.25 Auto-correlation function for test part nine and line four

The smooth surfaces roughness in this position exhibits that the cutting process was less likely affected by vibration.

The inappropriate surface quality of machined parts six and nine in the line (L4) can be clearly distinguished by naked eyes. The line four (L4) of test parts six and nine are shown in the figure (7.26).

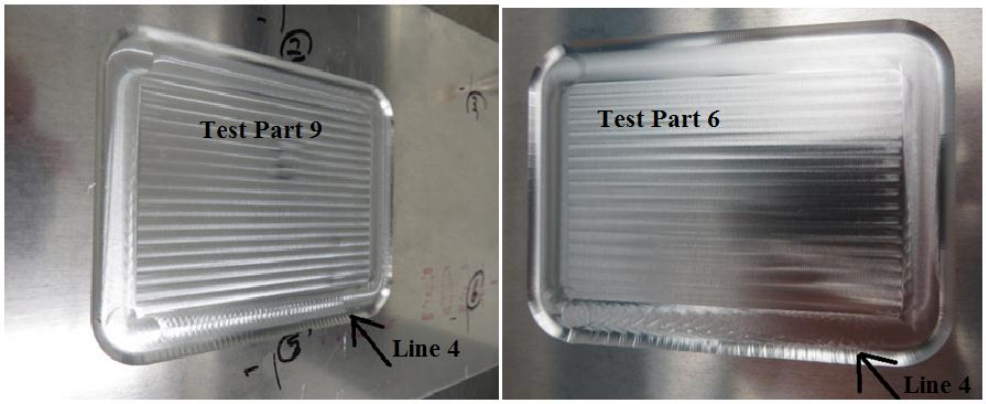

Figure 7.26 Line four (L4) of test part six and nine

The results of surface roughness were investigated. The position of the worst surface roughness for each test parts was defined. In the figure (7.27) these locations are illustrated.

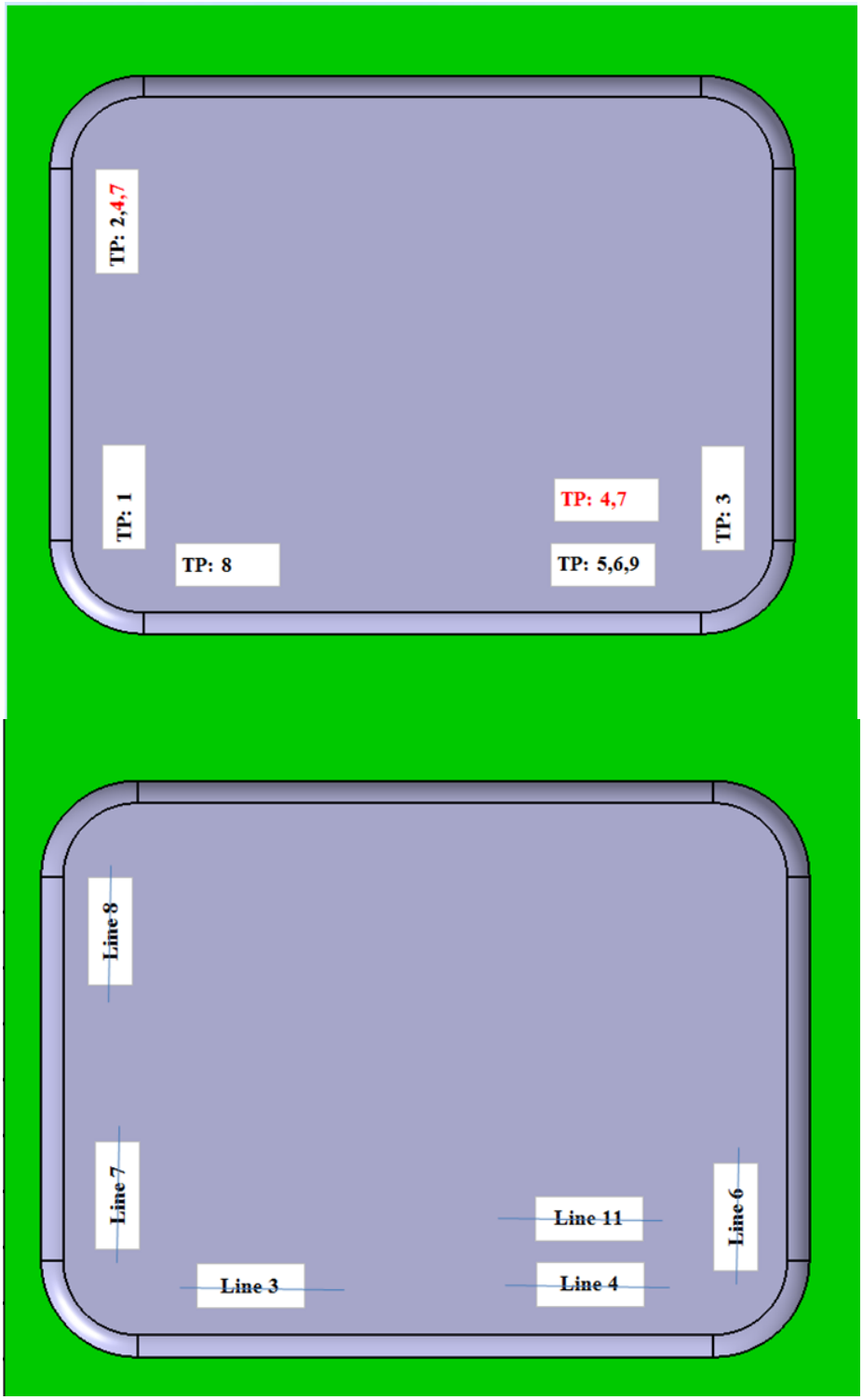

Figure 7.27 Locations of the worst surface roughness on nine test parts

The locations show that seven test parts have the worst surface roughness on the profile contouring surface. The location of the worst surface roughness for other two parts (test parts four and seven) is in the line eleven. By comparison the value of the worst surface roughness, these are very close for one way surface and profile contouring surfaces of these two parts (test parts 4 and 7).

It could be concluded that in all nine test, the worst surface roughness were observed in the profile contouring surfaces.

Upon changing the probing system, the surface roughness instrument could be used as a Profilometer. In the figure (7.28) a view of this measurement instrument is shown.

Figure 7.28 The Profilometer used

The procedure used to measure the mismatch areas is shown in the figure (7.29).

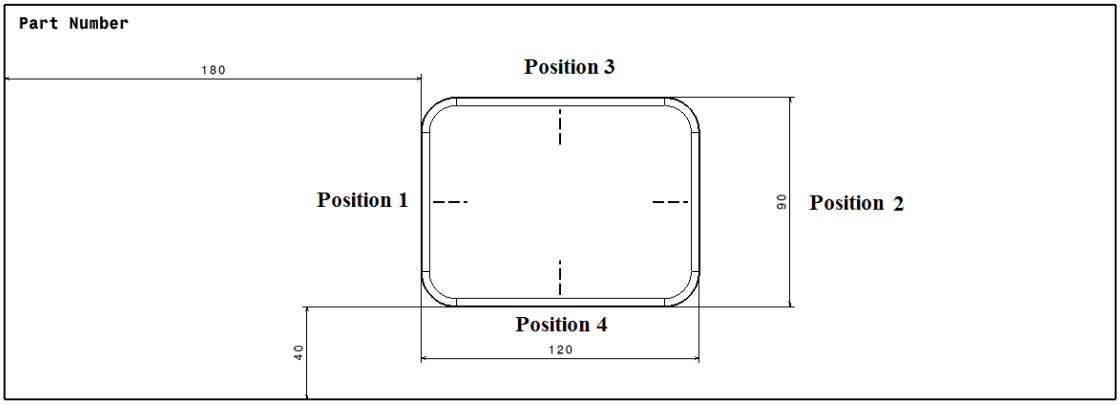

Figure 7.29 Positions of mismatch measurement

The mismatch measurement was conducted inside the machined pockets. Four positions are in the four sides of the bottom surfaces pockets that should be checked (see figure (7.29)). In order to conduct the mismatch measurement, the probe was moved from profile contouring surface to the one way surface.

The template of measurement was adjusted to give the distance between two surfaces. In the figure (7.30) a layout results for the mismatch measurement is shown. The obtained results of mismatch measurement are shown in table 7.12.

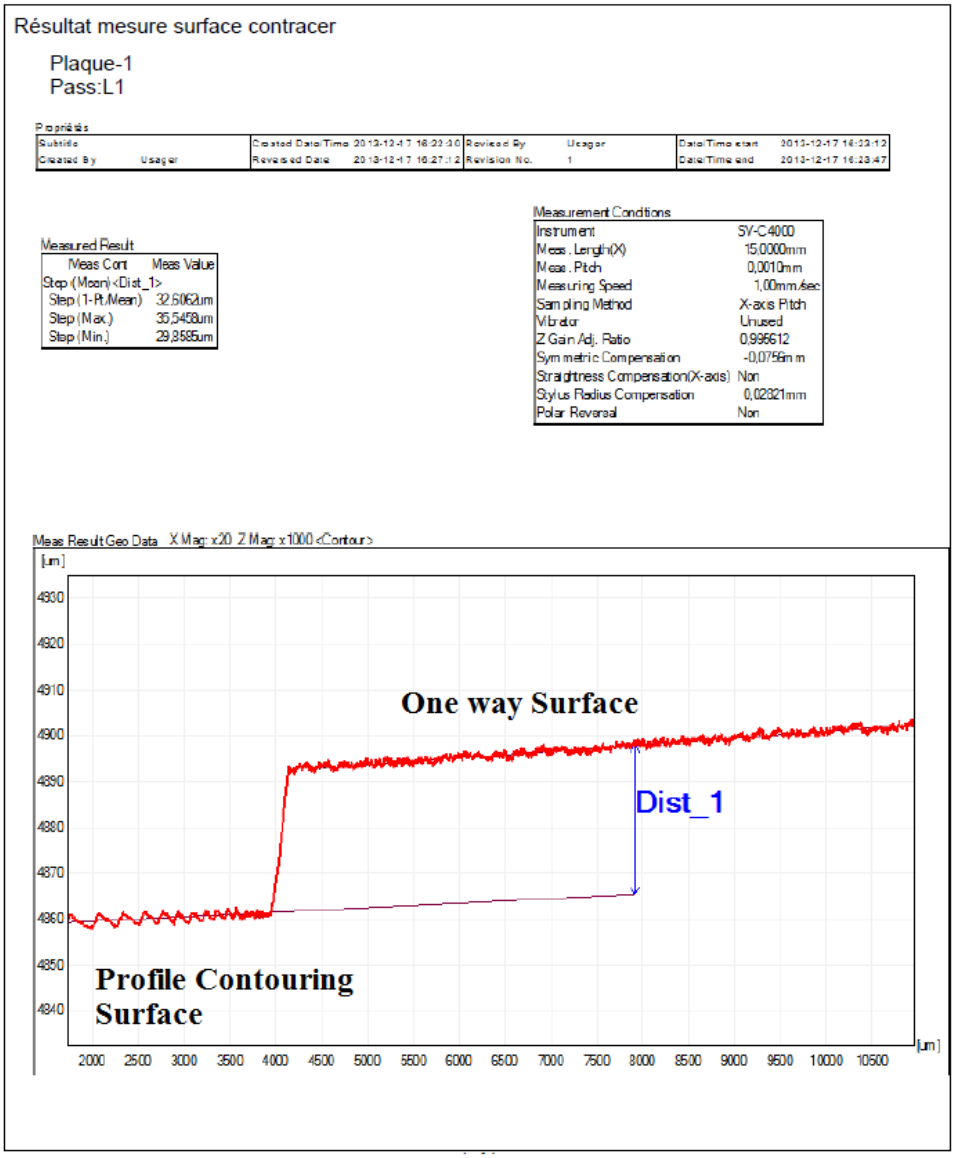

Figure 7.30 A layout result of mismatch for the first test part and position one

Table 7.12 Mismatch measurement results for nine test parts

Test No.	Position 1 (µm)	Position 2 (µm)	Position 3 (µm)	Position 4 (µm)	Max (µm)
1	32.61	22.35	15.97	26.97	32.61
2	22.86	17.67	14.20	16.34	22.86
3	7.45	6.40	1.92	11.63	11.63
4	20.88	15.43	15.20	13.77	20.88
5	24.29	14.20	14.66	9.37	24.29
6	17.42	16.82	15.16	24.71	24.71
7	18.32	21.19	14.91	10.12	21.19
8	8.35	14.96	1.22	10.16	14.96
9	13.36	18.02	11.74	9.77	18.02

The values of mismatch for the four positions were listed in the columns. The test part numbers are shown in the rows. In the last column the maximum value of mismatch for each test part was written. The results of mismatch show that the profile contouring surface is placed lower than one way surface. The average of this displacement was calculated as 21.24 (µm).

The mismatch indicates that the bottom surface of the pocket has been displaced during the machining operations. This displacement is intensified during the profile contouring. The results show that the bottom of pocket is being separated of the fixture surface while the cutting tool is removing the material. The phenomena of metal cutting and cutting forces cause this problem.

It can be noted that work part rigidity was gradually reduced during the pocket milling. The reduction is increasing while the material is removed pass by pass from the pocket. The minimum rigidity was recorded during the last pass of one way strategy.

The schematic overview of displacement when cutting tool moves inside the pocket is illustrated in the figure (7.31).

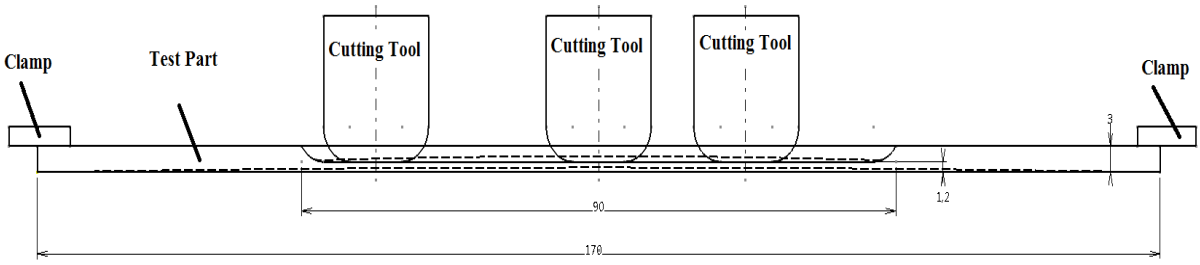

Figure 7.31 Displacement of test plate during the machining

The hidden lines in the figure (7.31) show how the test plate is deformed or displaced during the machining operation. The major part of the work part was removed when using one way strategy. Upon completing one way strategy, the thickness of the plate inside the pocket shows 63% reduction. Therefore, the maximum deformation occurs in the profile contouring because of the lowest rigidity of bottom pocket.

7.6.2 Pocket Deformation

Those real size metal sheets that need pocket milling are large. This poses severe difficulties in assembly process, owing to possible deviation and deformation of these sheets. In this project, a deformation measurement procedure was proposed (see figure (7.32)) and was respectively applied for deformation measurements of the sample sheets. The deformation of test plates was evaluated through nineteen points (p1 to p19).

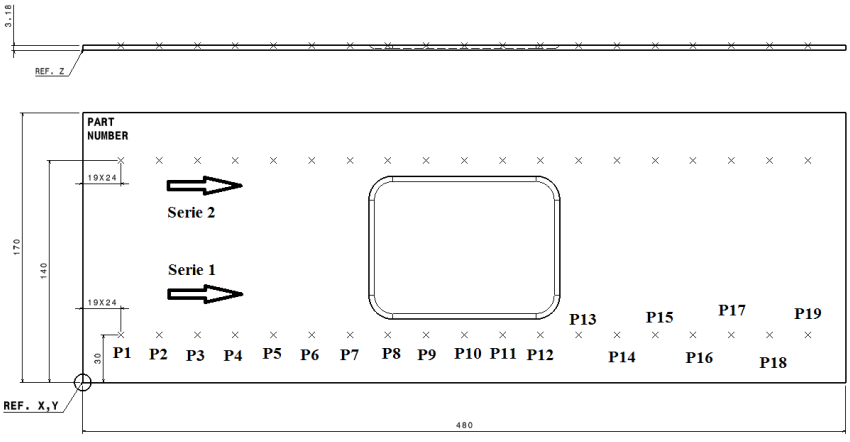

Figure 7.32 Deformation measurement procedure

These points were put in both side of pocket on the long side of test plate. An example of the deformation measurement results is presented in the figure (7.33). The measurement was performed by a CMM (Mitutoyo LEGEX 9106).

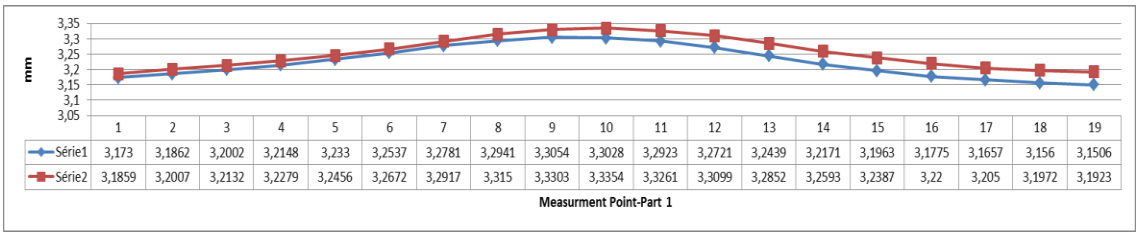

	1	2	3	4	5	6	7	8	9	10	11	12	13	14	15	16	17	18	19
Série1	3,173	3,1862	3,2002	3,2148	3,233	3,2537	3,2781	3,2941	3,3054	3,3028	3,2923	3,2721	3,2439	3,2171	3,1963	3,1775	3,1657	3,156	3,1506
Série2	3,1859	3,2007	3,2132	3,2279	3,2456	3,2672	3,2917	3,315	3,3303	3,3354	3,3261	3,3099	3,2852	3,2593	3,2387	3,22	3,205	3,1972	3,1923

Figure 7.33 Deformation profile of the work part

According to experimental results, the deformation is increased in both sides of the work part pocket. Moreover, the maximum deformation is in the middle of the work part (P10). As depicted in figure (7.33), larger deformation is resulted in the in the second row (serie 2), owing to lower rigidity of this side of pocket. The maximum value of deformation for all nine tested parts is listed in table 7.13.

Table 7.13 Deformation results

Test No.	Max. Deformation (mm)	Deviation (mm)
1	3.3354	0.1554
2	3.3486	0.1686
3	3.2228	0.0428
4	3.2629	0.0829
5	3.2500	0.0700
6	3.2979	0.1179
7	3.3872	0.2072
8	3.2569	0.0769
9	3.3266	0.1466

Subtracting the maximum deformation from the thickness of test plate (3.18mm), the deviation was calculated.

7.6.3 Bottom Thickness of the Pocket Milled part

The bottom thickness of pocket milled part is generally requested by industry. This parameter was measured after each machining test. The procedure used for bottom thickness measurement is shown in the figure (7.34).

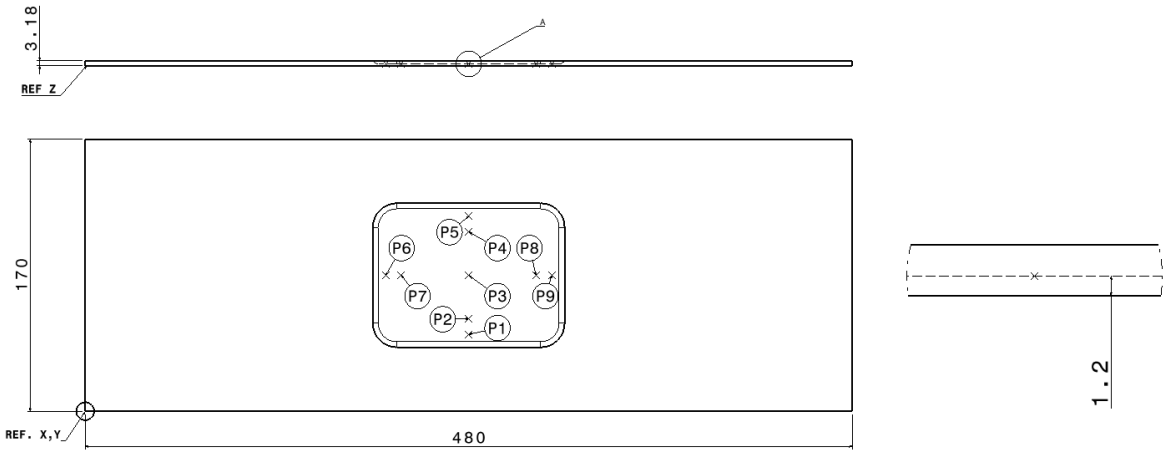

Figure 7.34 The procedure used for bottom thickness measurement

The bottom thickness as should have a dimension of 1.2 ± 0.05mm. This was measuring through positions (P1 to P9) at the bottom surface of pocket. The recorded experimental results are presented in the table 7.14.

Table 7.14 Bottom thickness measurement results

Test No.	P 1 mm	P 2 mm	P3 mm	P4 mm	P5 mm	P6 mm	P7 mm	P8 mm	P9 mm	Ave. mm	Dev. mm
1	1.1	1.12	1.12	1.11	1.1	1.11	1.14	1.13	1.11	1.11	-0.087
2	1.09	1.11	1.12	1.12	1.10	1.11	1.13	1.13	1.11	1.11	-0.088
3	1.10	1.12	1.12	1.11	1.11	1.11	1.12	1.12	1.11	1.11	-0.087
4	1.09	1.10	1.10	1.10	1.09	1.10	1.13	1.12	1.1	1.10	-0.096
5	1.11	1.12	1.13	1.12	1.10	1.01	1.12	1.14	1.12	1.12	-0.083
6	1.06	1.06	1.06	1.03	1.01	1.03	1.05	1.10	1.1	1.06	-0.142
7	1.12	1.13	1.13	1.13	1.11	1.12	1.14	1.14	1.12	1.13	-0.073
8	1.15	1.18	1.18	1.13	1.11	1.13	1.15	1.16	1.14	1.15	-0.053
9	1.1	1.11	1.12	1.13	1.11	1.12	1.14	1.14	1.13	1.12	-0.078

Based on experimental results, the bottom thickness of the pocket is thinner than that presented in drawing dimension. The minimum thickness was detected in P1 and P5, which are located in the middle of the long side of the plate and on the profile contouring surface respectively. It exhibits that this side had the maximum deformation. It proves that the cutting tool removes more material in these positions because of the largest deformation.

The surface of test plate without pocket was checked to be sure that there is no deformation during the bottom thickness measurement. It showed that there is no significant deformation behind the pocket.

7.6.4 Pocket Dimension

As shown in figure (7.35), the same CMM machine was used to measure the length (D1) and width (D2) of pocket

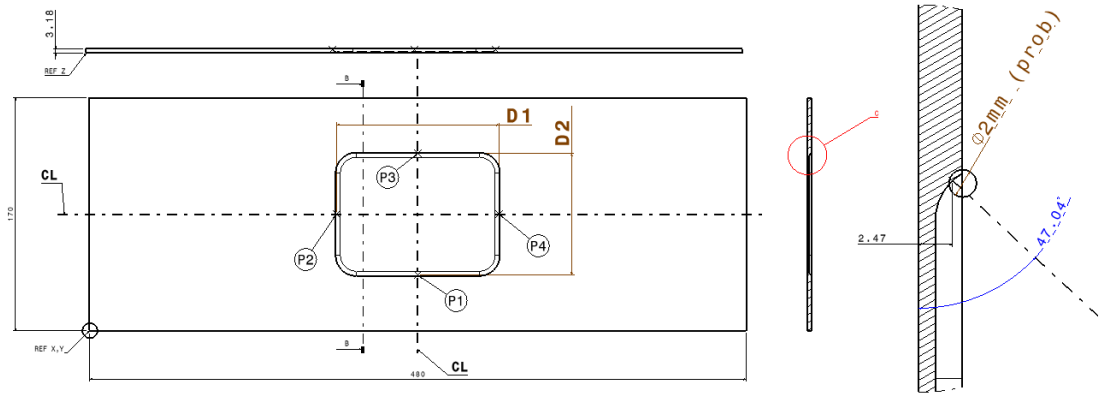

Figure 7.35 Pocket dimension measurement procedure

The bottom corner of pocket has a fillet with a radius of 4 mm. This means that sides of pockets are curved. Four points (P1- P4) are placed on the four curved sides of pocket. The length and width of pocket were measured by CMM. Experimental values of pocket dimension deviation are presented in table 7.15.

The results show that the machining dimensions for length and width of pocket are within tolerances.

Table 7.15 Experimental values of pocket dimension deviations for length and width

Test Number	Deviation of D1 120±2mm	Deviation of D2 90±1mm
1	0,000	-0,031
2	-0,010	-0,038
3	-0,024	-0,022
4	0,010	0,008
5	0,006	-0,017
6	0,047	0,130
7	-0,009	-0,025
8	-0,010	0,002
9	-0,010	-0,007

7.7 Statistical analysis of the data

Taguchi method is a simple and robust technique for optimizing the process parameters. The main aim of this method is to determine how different process parameters affect the mean and variance of the performance characteristics studied. Furthermore the contribution of each parameter on the responses can be determined using Taguchi method.

Robust design is recognized as the most significant contribution of Taguchi method which improves the product quality and system reliability. Taguchi method based on factorial design of experiment divides the independent variables to controllable and noise factors. Controllable factors are those that can be maintained to a desired value, while noise factors are those that may not be controlled. A careless selection of these factors can lead to false conclusions, thus experimentations must be repeated.

The experimental design proposed by Taguchi uses the orthogonal arrays to organize the parameters affecting the responses, while the level of process parameters can also varied. This allows testing only a limited collection of parameters instead of all combinations, such as

factorial design. Such method allows determination factors governing the product quality with number of experiments, which relatively reduced the time and resources.

A robust design drawn by Taguchi method aims to achieve a robust process or product design whose response values are less sensitive to noise factors. Considering signal to noise ratio (S/N), the goal can be achieved by reducing the variability around a target value through the use of the quality loss function. Upon adequately applying the S/N to experimental responses, it is then possible to reduce the mean of responses while also minimizing their variances.

The main aim of this work is to define the cutting parameters that may lead to generate the machined part with the best surface finish. To that end, the observed values of surface roughness was set to minimum and the objective function, is defined as the calculated based on the smaller signal to noise (S/N) ratio, the better response characteristic [84] as Eq.7.3.

$$S/N = -10 * log \frac{1}{n} \sum y^2 \qquad (7.3)$$

Where y is the observed data an n is the number of observations.

7.7.1 Surface Roughness Analysis

Table 7.16 shows the S/N values of surface roughness corresponding to each strategy, consist of the results of profile contouring (8 results) and one way strategy (3 results).

Table 7.16 S/N ratio of the surface roughness values measured in each strategy

Test No.	P1	P2	P3	P4	S/N One Way	S/N Profile Contouring
1	1	1	1	1	7.302	4.65
2	1	2	2	2	2.605	2.193
3	1	3	3	3	2.870	0.240
4	2	1	2	3	4.113	5.145
5	2	2	3	1	4.418	0.300
6	2	3	1	2	-0.096	-1.702
7	3	1	3	2	6.480	6.395
8	3	2	1	3	3.543	2.259
9	3	3	2	1	0.01	-1.881

As shown in tables 7.17 and 7.18, the S/N values of both strategies with respect to each factor and level are calculated. The larger the range R (R = high S/N - low S/N), the larger the effect the process variable has on the response (e.g. surface roughness).

Table 7.17 S/N values for each factor and level for one way strategy

Level	RPM	Chip Thickness (mm)	Depth of Cut (mm)	Lubricant
1	4.259	5.965	3.583	3.903
2	2.812	4.522	2.236	2.996
3	3.338	0.921	4.589	3.509
R	2.447	5.044	2.353	0.907
Rank	3	1	2	4

Table 7.18 S/N values for each factor and level for profile contouring strategy

Level	RPM	Max. Chip Thickness	Depth of Cut	Lubricant
1	2.361	5.397	1.736	1.023
2	1.248	1.584	1.819	2.295
3	2.258	-1.114	2.312	2.548
R	1.113	6.511	0.576	1.525
Rank	3	1	4	2

The maximum chip thickness seems to have the most significant influence of the surface roughness values recorded when using both strategies. Since the chip thickness is a function of feed rate, it could be inferred that the feed rate is the most effective parameter on the surface quality of pocket milled work parts. The next influential cutting parameters for one way strategy are as depth of cut, RPM and lubrication mode, while lubrication mode, RPM and depth of cut are known as the next effective cutting parameters on surface roughness recorded during profile contouring strategy. These optimal cutting parameters for one way strategy and profile contouring are shown in figures (7.36 and 37).

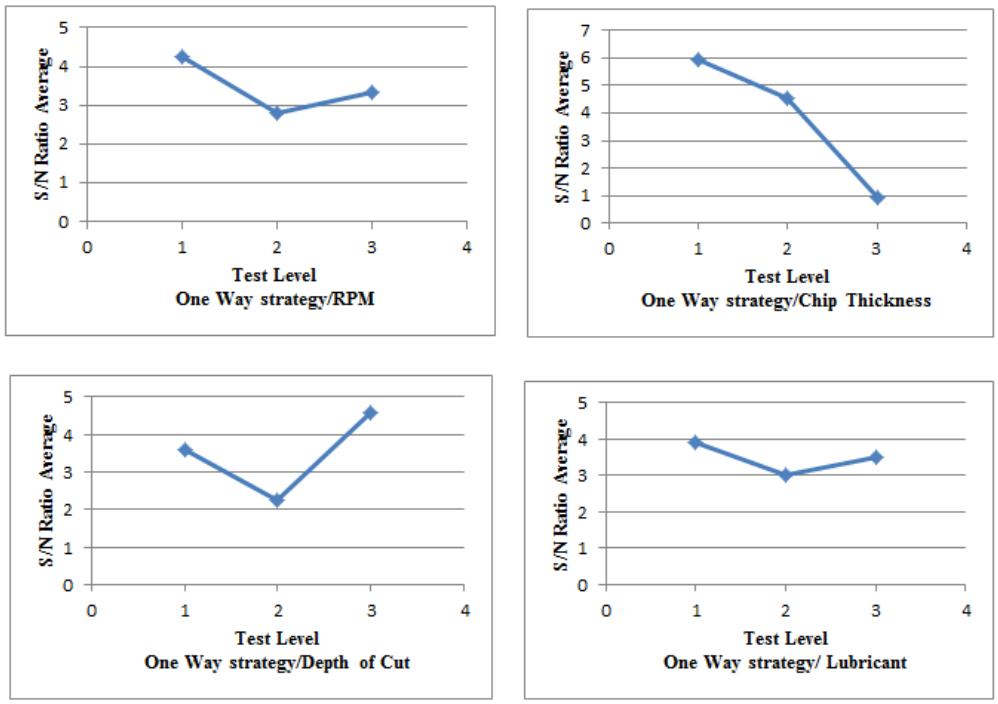

Figure 7.36 S/N ratio average for each level of one way strategy

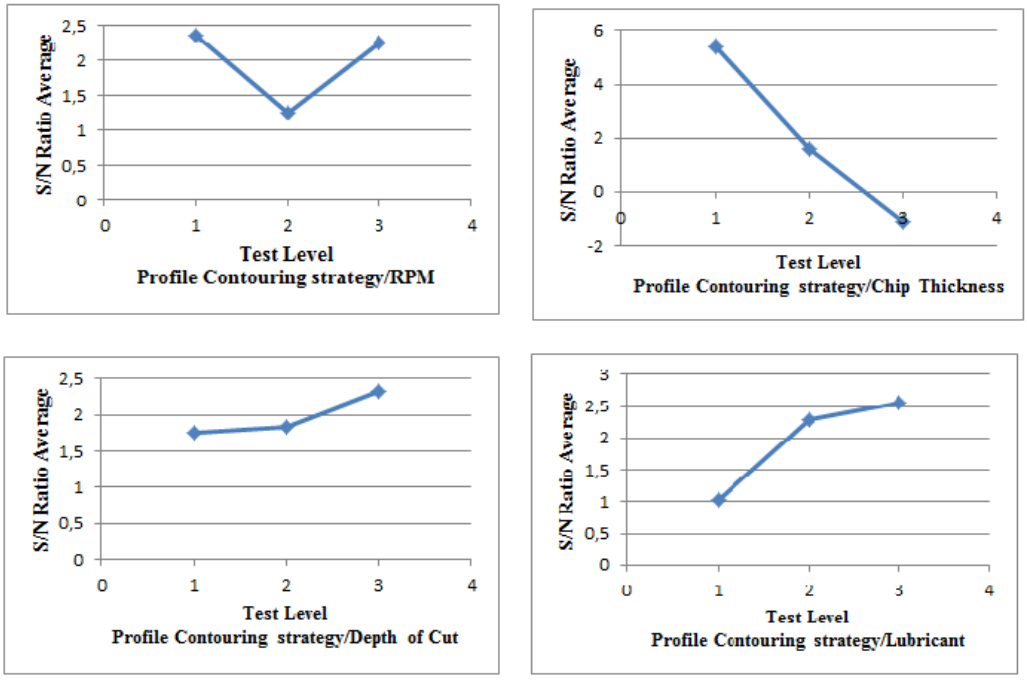

Figure 7.37 S/N ratio average for each level of profile contouring strategy

The similar optimal cutting parameters were obtained for both cases as follows: RPM (10000 rpm), chip thickness (0.0508 mm) and depth of cut (0.45 mm), However dry and MQL are preferred lubrication conditions in one way strategy and profile contouring.

7.8 Verification Tests

In this section, the verification tests will be conducted to confirm the validation of the proposed optimum process parameters proposed in the last section. As presented earlier, the bottom thickness is generally 0.037mm lower than the tolerance (1.2mm±0.05) and there is about 0.02mm under cut as mismatch for the profile contouring strategy according to the one way surface.

This shows that if the optimal condition is used by changing the references in z direction during machining, the results could be acceptable. So, with this procedure strategy, two cutting tests were performed to confirm the results.

The tests parts were deformed during machining tests. This could be due to mechanical and thermal stresses and may not be considered as an important issue. Furthermore, the verification of whether or not the optimal cutting parameters may lead to lowest residual stress is not within the scope of this work. Based on experimental results, the pocket dimensions are acceptable and are aligned with tolerance.

The verification tests were conducted on two work part using the optimal cutting parameters (see table 7.19). The work parts used for verification tests are shown in figure (7. 38).

Table 7.19 Optimal cutting parameters used

RPM (rpm)	Max. Chip Thickness (mm)	Depth of Cut(mm)	Lubricant
10000	0.0508	0.45	MQL

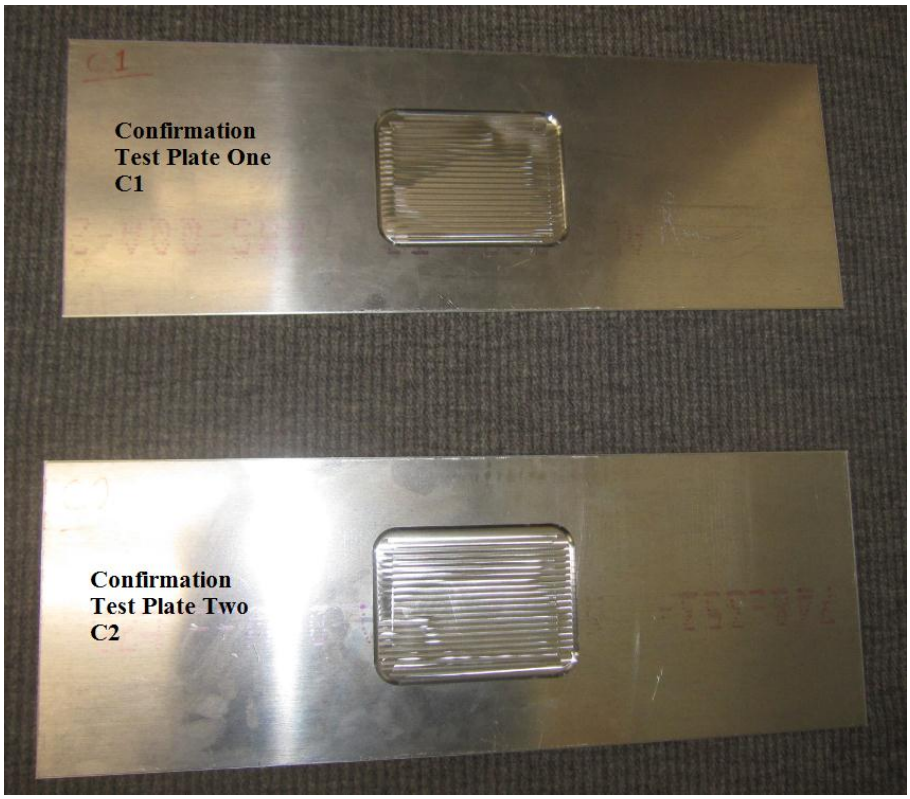

Figure 7.38 The work parts used for verification tests

The recorded values of surface roughness for the two strategies are shown in table 7.20. It can be inferred that the surface quality of pocket milled parts is improved when using the optimal setting levels of process parameters.

Table 7.20 Surface roughness Ra (µm) results for two verification tests

Test	Profile Contouring Strategy								One Way Strategy			Stra. Profile Contour (Max.)	Stra. One Way (Max.)
	L1	L2	L3	L4	L5	L6	L7	L8	L9	L10	L11		
C1	0.37	0.25	0.27	0.44	0.42	0.46	0.27	0.29	0.28	0.45	0.39	0.46	0.45
C2	0.34	0.43	0.47	0.46	0.61.	0.57	0.32	0.37	0.37	0.58	0.40	0.61	0.58

The maximum surface roughness occurred in the same area of pocket for each strategy in two tests and the point to point comparison of the deviation is not more than 0.200 (µm).

The second measurement was conducted to verify the mismatch and step between the two strategies using the same profilometer. The results are given in the table 7.21 and in figure (7.39) the layout results for the mismatch measurement of two verification test parts are shown.

Table 7.21 Mismatch and step measurement results for two verification tests

Test No.	Position 1 (µm)	Position 2 (µm)	Position 3 (µm)	Position 4 (µm)	Max
C1	4.35	3.61	2.53	6.13	6.13
C2	5.97	4.34	2.52	7.47	7.47

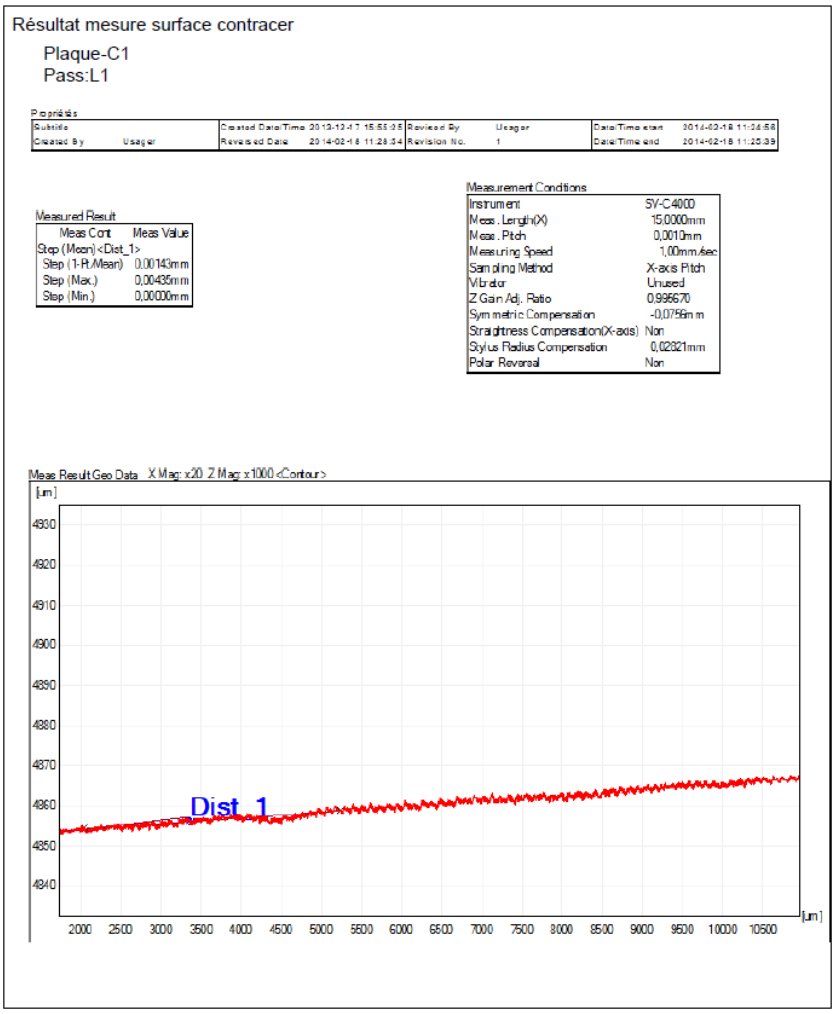

Figure 7.39 A layout result of mismatch for the two verification test parts

According to experimental results, no significant mismatch and step were observed between two surfaces when using both strategies. Moreover, as shown in table 7.22, the reduction in the bottom thickness of the pocket milled components is resolved when using the proposed process parameters.

Table 7.22 The bottom thickness results for both verification tests

Test No.	Point 2	Point 3	Point 4	Point 5	Point 6	Point 9	Point 10	Point 11	Point 12	Average (mm)	Dev. (mm)
1	1.22	1.23	1.23	1.22	1.21	1.25	1.26	1.20	1.20	1.22	+0.025
2	1.22	1.23	1.23	1.22	1.21	1.26	1.26	1.21	1.21	1.23	+0.029

The deformation of verification test parts were measured with the procedure was used for the nine test parts of DOE and the results are shown in the table 7.23.

Table 7.23 Deformation results for two verification tests

Test No.	Max. Deformation (mm)	Deviation (mm)
C1	3.2245	0.0545
2	3.2231	0.0731

In the figure (7.29) one of these results for deformation of parts is shown according to the points of measuring.

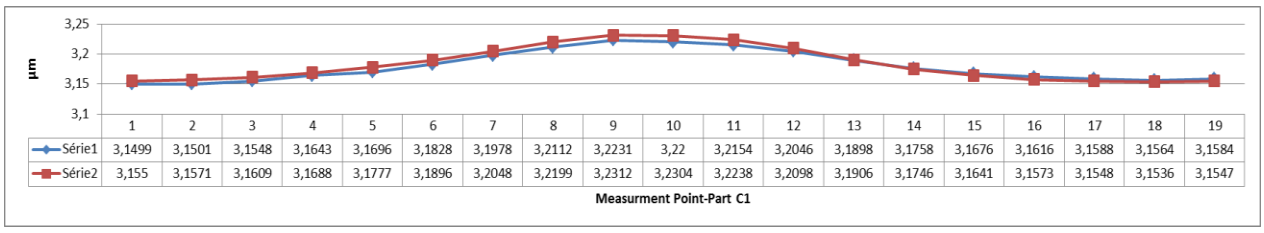

Fig 7.24 Deformation shape of two verification test parts

The deformation results show that the deformations are in the range of minimum according to the results of nine tests. It can be said that the result for deformation was not improved with these optimal cutting parameters.

CONCLUSION AND RECOMMENDATIONS

In this project the pocket milling strategy on the aluminum alloy skin plates was investigated. The engineering requirements for the machined pockets were investigated. A Process Failure Mode and Effect Analysis (PFMEA) was performed. The main criteria for optimization were defined and statistically analyzed. Based on Taguchi orthogonal array design of experiment, the optimum setting levels of cutting parameters were defined and then implemented.

The main failure modes in this work are residual stresses, surface roughness and bottom thickness variation. The optimum setting levels of cutting parameters to generate the best quality surface were introduced.

Surface roughness measured after pocket machining is defined as the main performance criteria. As described earlier, similar setting levels of experimental factors as found in the literature were used and experimental tests were conducted under three different lubrication modes.

The optimum setting levels of experimental factors that led to the best surface roughness of pocket surface are designed. The lowest machining time, the less thermal effects and reducing the production the harmful material for the environment as lubrication liquids were considered to set the levels.

A standard sample plate was proposed by industry to be used and a milling fixture was designed and manufactured.

Pocket milling has been conducted using two milling strategies; one way strategy and profile contouring strategy. The bottom of pocket has been machined with one way strategy. The one way strategy could reduce the heat generation during machining operation. The profile contouring strategy was used to machine the length and width of pocket.

Preliminary and main experimental tests were conducted according to Taguchi method design of experiment. Next, the tests were performed with a five axis milling machine tool, which could be used to machine the pockets on the curved plate.

The surface roughness and mismatch on the bottom surface of pockets were measured after each test. The deformation, pocket dimension and bottom thickness of the each pocket were measured with a CMM.

According to experimental result, the deteriorated surface finish was observed when the profile contouring strategy was used. This strategy is generally used after using the one way strategy. The main portion of material can be removed when using the one way strategy. The profile contouring is then used to remove a small portion of material left around the border. Using auto-correlation functions, the irregularities in the recorded surface roughness in two test plates were detected. A similar irregularity pattern was observed on the surfaces generated by on profile contouring.

The cutting parameters have significant influence on the surface roughness in pocket milling of thin aluminum plates. The optimal cutting parameters that produce the best surface quality in the pocket milling of the thin aluminum plates were defined.

The first point of machining on the test plate has the highest rigidity and minimal deformation. The bottom thickness in the primary one way tool pass should be close to the nominal size (1.2mm). Gradually, the deformation increases when material removal is advanced in one way strategy. Therefore, the bottom thickness at the last position of the one way strategy should have the minimal size. At this time, the profile contouring must complete the size while there is the deformation and variation in the bottom thickness of pocket.

The test plate in the bottom of the pocket experiences around 63% of reduction in the thickness (3.18mm to 1.2mm). Consequently, the rigidity of test plate in the pocket area is reduced and the deformation can be intensified during material removal process. According to experimental measurements, test plate was deformed during the machining operation. Generally, the cutting tool should remove more materials. Therefore, the bottom thickness of pocket seems to be thinner than that presented in the drawings.

Finally, the profile contouring is located lower than one way surface as average value of 21.24 μm. And, the bottom thickness is thinner as the average value of 37.40 μm.

Based on experimental results, the chip thickness (feed rate) has the most significant influence on the surface quality. The optimum setting levels of cutting parameters were reconfirmed through verifications tests.

The optimal cutting parameters are: RPM (10000 rpm), maximum chip thickness (0.0508 mm) and depth of cut (0.45 mm). Two verifications tests were performed by modifying the NC program in Z direction, which led to better control of the mismatch size and bottom thickness.

The following recommendation could be used to improve the pocket milling when the optimal setting levels of cutting parameters are used:

- Using the vacuum table to eliminate the deformation of test plate and variation in the bottom thickness of pocket.

- Determining an accurate position for the MQL nozzle during lubrication process.

- In order to decrease the machining time, the feed rates of approach and retract paths could be modified.

According to literature, a similar machining specification could be applied for conventional aluminium alloys and the Al-Li alloys. Consequently in order to reduce the experimental cost and time, the proposed optimum setting levels of process parameters in this work could be similarly used in future machining tests on Al-Li work parts with similar dimensions as used in this work.

BIBLIOGRAPHIE

1. http://kids.britannica.com/elementary/art-88070.
2. B. Han, C.Z.R., X. Y. Yang, G. Chen, *Experiment study on deflection of aluminum alloy thin-wall workpiece in milling process.* Materials Scienece Forum, 2012. **697-698**: p. 129-132.
3. Committee, A.S.M.I.H., *ASM Handbook, Volume 02 - Properties and Selection: Nonferrous Alloys and Special-Purpose Materials*, ASM International. p. 178.
4. Garza Elizondo, G.H., *Machinability of aluminum-(7-11%) silicon casting alloys: Role of free-cutting elements*, 2010, Universite du Quebec a Chicoutimi (Canada): Canada.
5. Jong, H.F.d., *Aluminium-Lithium Alloys: The answer of the aluminium industry to the threat of advanced fibre-reinforced materials.* January 1984.
6. N.E.Prasad, A.A.G., P.R.Rao, *Mechanical behaviour of aluminium-lithium alloys.* Sadhana, April,2003. **28**: p. 209-246.
7. R.J.Mcdonald, *Characterization of delamination in 2099-T861 Aluminum-Lithium.* Thesis of Doctor of Philosophy in Mechanical Engineering, University of Illinois at Urbana-Champaign, 2009.
8. A.JOSHI, *Lithium Aluminium alloys- the new generation aerospace alloys.* Junior Research Fellow, Mechanical Engineering Department, Indian Institute of Technology, I.I.T - Bombay.
9. Standardations(ECSS), E.C.f.S., *Structural materials handbook -Part 5: New advanced materials,advanced metallic materials, general design aspects and load transfer and design of joints.* 2011. **Part 5**.
10. C. Fu, C.W., T. Li, W. Wang, *Simulation of end milling for weak-rigidity structural parts of aluminum alloy in aviation.* Advanced Materials Research, 2011. **201-203**: p. 332-336.
11. O.Çakir, A.Y., T. Özben *Chemical machining.* Materials Science and Engineering, 2007. **28**(8): p. 499-502.
12. O.Çakir, H.T., M. Kiyak *Chemical etching of Cu-ETP copper.* Materials Processing Technology, 2005. **162-163**: p. 275-279.

13. O.Çakir, *Chemical etching of Aluminum.* Materials Processing Technology, 2008. **199**: p. 337-340.

14. A. Fadaei Tehrani, E.I., *A new etchant for the chemical machining of St304.* Materials Processing Technology, 2004. **149**: p. 404-408.

15. C. Y. Liao, J.K.W., *Chemical machining of nickel in ferric chloride solution.* Materials Science Letters 1992. **11**: p. 689-691.

16. H. B. Synder, L.R., *Chemical milling process and composition.* U.S. Patent (2981610), 1961.

17. Vijayaram, T.R., *Application of chemical milling, chemical blanking and photochemical blanking in metal working industries.* Department of Manufacturing Process and System, Faculty of Manufacturing Engineering, UTeM, Universiti Teknikal Malaysia Melaka, Ayer Keroh, 75450 Melaka, Malaysia.(E-mail: thoguluva@utem.edu.my).

18. http://coromant.sandvik.com/pdf/metalworking_products_061/tech_d_1.pdf.

19. L. Huzeng, W.Y., Z. Naixiong, H. Raobo, Z. Chong, *Measurment and analysis of cutting forces and optimization of cutting parameters by high speed milling.* Applied Mechanics and Materials, 2012. **141**: p. 344-349.

20. P.Johne, A.-Z., *TALANT (Training in Alumnium Application Technologies) Lecture 3100, Machining of Products, EAA-European Aluminium Association.* 1994: p. 38.

21. B. Denkena, L.d.L., *Milling induced residual stresses in structural parts out of forged aluminium alloys.* Int. J. Machining and Machinability of Materials, 2008. **4**(4): p. 335-344.

22. Y. Wang, B.L., J. Song, X. Yan, K. Wu, *Study on the wear mechanism of PCD tools in high-speed milling of Al-Si alloy.* Advanced Materials Research, 2012. **381**: p. 16-19.

23. Rahman, A.K.M.A. and H.-Y. Feng, *Effective corner machining via a constant feed rate looping tool path.* International Journal of Production Research, 2012. **51**(6): p. 1836-1851.

24. Aggarwal, S. and P. Xirouchakis, *Selection of optimal cutting conditions for pocket milling using genetic algorithm.* The International Journal of Advanced Manufacturing Technology, 2013. **66**(9-12): p. 1943-1958.

25. G. Zhao, Y.Z., S. Wang, *The acceleration/deceleration control algorithm based on trapezoid-curve jerk in CNC machining.* Research Journal of Applied Sciences, Engineering and Technology, 2013. **5**: p. 1639-1645.

26. Altintas, Y., *Manufacturing Automation Metal Cutting Mechanics, Machine Tool Vibration, and CNC dESIGN.* Cambridge University Press, 2000.

27. Tonnessen, k.S.K., *Methodology for selection of cutting tool and machining data for High Speed Flank Milling.* Dept. of Production and Quality Engineering, Norwegian University of Science and Technology, 1996.

28. R. Komanduri, D.G.F., *CRC Handbook of Lubrication and Tribology.* 1994. **3, Monitoring, Materials, Synthetic Lubricants, and Applications**: p. 438-439.

29. L. N. Lopez de Lacalle, A.L., J. A. Sanchez, I. Cabanes, *Cutting conditions and tool optimization in the high-speed milling of aluminium alloys.* Proceeding of the Institution of Mechanical Engineers, 2001. **215-part B**.

30. Kishawy, H.A., et al., *Effect of coolant strategy on tool performance, chip morphology and surface quality during high-speed machining of A356 aluminum alloy.* International Journal of Machine Tools and Manufacture, 2005. **45**(2): p. 219-227.

31. Tsao, C., *An experiment study of hard coating and cutting fluid effect in milling aluminum alloy.* The International Journal of Advanced Manufacturing Technology, 2007. **32**(9): p. 885-891.

32. López de Lacalle, L.N., et al., *Experimental and numerical investigation of the effect of spray cutting fluids in high speed milling.* Journal of Materials Processing Technology, 2006. **172**(1): p. 11-15.

33. M. Hiroki, I.I., *Cutting with minimal quantity lubrication.* proceeding of the International Symposiium Improving Machine Tool Performance, 1998. **2, Michelena, San Sebastian**: p. 655-665.

34. I. Zaghbani, V.S., R. Khettabi, *Fine and Ultrafine Particle Charactrization and Modeling in Hugh Speed Milling of 6061-T3 Aluminum Alloy.* Journal of Materials Engineering and Performance, 2009. **18**: p. 38-48.

35. Hwang, Y.-K., C.-M. Lee, and S.-H. Park, *Evaluation of machinability according to the changes in machine tools and cooling lubrication environments and optimization of cutting conditions using Taguchi method.* International Journal of Precision Engineering and Manufacturing, 2009. **10**(3): p. 65-73.

36. N. Tosun, M.H., *Effect of MQL on surface roughness in milling of AA7075-T6.* Materials and Manufacturing Processes, 2010. **25**: p. 793-798.

37. S. Tangjitsitcharoen, C.R., *Investigation of dry cutting and applications of cutting fluid in ball-end milling process.* Advanced Materials Research, 2011. **291-294**: p. 3013-3023.

38. B. Boswell, M.N.I., *Feasibility Study of Adopting Minimal Quantities of Lubrication for End Milling Aluminium.* Proceeding of the World Congress on Engineering, 2012. **3**.

39. J. Y. Xu, Q.L.A., M. Chen, *Analysis on milling performance of 2024-T351 aluminum alloy using TiAlN coated carbide cutting tools.* Advances in Materials Manufacturing Science and Tchnology XIV, 2012. **697-698**: p. 218-222.

40. Msaddek, E., et al., *Optimization of pocket machining strategy in HSM.* The International Journal of Advanced Manufacturing Technology: p. 1-13.

41. Heo, E.-Y., et al., *High speed pocket milling planning by feature-based machining area partitioning.* Robotics and Computer-Integrated Manufacturing, 2011. **27**(4): p. 706-713.

42. J. F. Chatelain, J.F.L., A. S. Tahan, *Effect of Residual Stresses Embedded within Workpieces on the Distortion of Parts after Machining.* International Journal of Mechanics, 2012. **6**(1): p. 41-51.

43. S. Smith, D.D., *Tool path strategies for high speed milling aluminum workpieces with thin webs.* Mechatronics, 1998. **8**(4): p. 291-300.

44. M. Balazinski, S.G., F. Trochu, *Évaluation de la distance entre les passes d'usinage pour les outils à bout torique.* 2e conférence internationale sur la conception et la fabrication intégrées en mécanique, IDMME'98, 1998: p. p. 569-575.

45. Lee, C.M., et al., *Evaluation of cutter orientations in high-speed ball end milling of cantilever-shaped thin plate.* Journal of Materials Processing Technology, 2003. **140**(1–3): p. 231-236.

46. D. Vakondios, P.K., S. Yaldiz, A. Antoniadis, *Influence of milling strategy on the surface roughness in ball end milling of the aluminum alloy Al7075-T6.* Measurment, 2012.

47. Y. M. Liu, Z.L.J., Z. Li, *A surface residual-stress model of optimizaing milling parameters for millining aluminum alloy 6061.* Advanced Material Research, 2012. **426**(2012): p. 7-10.

48. KH. Guo, D.W.Z., S. H. Wang, L. L. Xu, M. Wang, J. Hu, *The application of FEM technology on the deformation analysis of the aero thin-walled frame shape workpiece.* Key Engineering Materials, 2006. **315-316**: p. 174-179.

49. J. M. Lee, D.L., S. J. Kim, D. S. Lim, *The deflection of airframe thin plate part after milling.* Proceeding of the 9th International Symposium on Aerospace Technology, KARI, Sacheon, Korea, Oct. 22-24, , 2008.

50. T. Aijun, L.Z., *Deformations of thin-walled plate due to static end milling force.* Journal of Materials Processing Technology, 2008. **206**: p. 345-351.

51. Y. Cao, Y.B., Y. He,Y. Li, *NC milling deformation analysis of aluminum alloy thin-walled component based on orthogonal cutting experiments on a vertical machining center.* 2th International Conference on Industrial Mechatronics and Automation, 2010.

52. C. K. Wang, G.H.Q., D. Lu, S. Q. Xin, *Simulation and experimental investigation for the end milling process of 7075-T7451 aluminum alloy.* Advanced Materials Research, 2010. **97-101**: p. 3014-3019.

53. S. Lin, X.H., F. Y. Ma, L. Jinguo, W. Weiwei, L. Wei, C. Lijun, *Evaluation method for milling machining deformation of thin-walled structures.* CSEE 2011, PARTIII,CCIS, 2011. **216**: p. 468-473.

54. D. Dudzinski, A.M., H. Schulz, *Metal cutting and high speed machining.* Kluwer Academic/ Plenum Publishers, 2002: p. 201-211.

55. Yuanwei, L., *Numerical simulation of the machining distortion of aircraft aluminum part caused by redistribution of residual stress.* Advanced Material Research, 2011. **142**: p. 122-125.

56. X. J. Cai, W.W.M., M. Chen, *Surface integrity analysis on high speed end milling of 7075 aluminum alloy.* Advanced Materials Research, 2012. **426**: p. 321-324.

57. Y. Liu, L.Z., Z. Xu, *Experimental investigation on high-speed milling of aluminum alloys.* Advanced Materials Research, 2012. **418-420**: p. 1141-1147.

58. C. Li, Y.W., R. R. Zhang, Z. Q. Liu, *Effect of milling speed and feed on the surface residual stress of 7075-T7451 aluminum alloy.* Key Engineering Materials, 2012. **499**: p. 217-222.

59. K. Kadirgama, M.M.N., N. M. Zuki, M. M. Rahman, M. R. M. Rejab, R. Daud, K. A. Abou-El-Hossein, *Optimization of surface roughness in end milling on mould aluminium alloys (AA6061-T6) using surface method and radian basis function network.* Jordan Journal of Mechanical and Industrial Engineering, 2008. **2**: p. 209-214.

60. Patel, K., A. Batish, and A. Bhattacharya, *Optimization of surface roughness in an end-milling operation using nested experimental design.* Production Engineering, 2009. **3**(4): p. 361-373.

61. F. Xiuli, P.Y., W. Yi, A. Xing, *Research on predictive model surface roughness in high speed milling for alumium alloy 7075-T7451*. International Conference on Computing, Control and Industrial Engineering, 2010: p. 186-189.

62. V. H. Mould, F.I.P., *Fabrication Characteristics of 8090 Alloy.* AGARD CONFERENCE PROCEEDINGS No.444, 1989.

63. Lequeu, P., K. Smith, and A. Daniélou, *Aluminum-Copper-Lithium Alloy 2050 Developed for Medium to Thick Plate.* Journal of Materials Engineering and Performance, 2010. **19**(6): p. 841-847.

64. Wilson, W.R. and D.J. Allan, *Aluminium-lithium aerospace alloys: a new challenge for recycling.* Transactions of the Institution of Mining and Metallurgy, Section C: Mineral Processing and Extractive Metallurgy, 1993. **102**(Compendex): p. C44-C56.

65. W.R. WILSON, J.W., E.P. SHORT and C.F. PYGALL, *RECYCLING OF ALUMINIUM-LITHIUM PROCESS SCRAP*. PHYSIQUE, 1987. **48**.

66. R. P. Reed, N.J.S., J. D. McColskey, J. R. Berger, C. N. McCowen, J. W. Bransford, E.S.Drexler, R. P. Walsh, *Aluminum Alloys for Cryogenic Tanks:Oxygen Compatibility.* Astronautics Laboratory (AFSC) report, 1990. **Volume 1.**

67. H. Babel, C.P., *Manufacturing Considerations for Aluminum-Lithium Alloys.* Society of Manufacturing Engineers, Technical Paper, 2004. **Conference WESTEC, Losangles, California**.

68. Tournier, C., *Usinage à grande vitesse.* Édition Dunod, Paris, ISBN 978-2-10-051810-4, 2010.

69. Kazban, R.V., *Effect of tool parameters on residual stress and temperature generation in high-speed machining of aluminium alloys.* PhD thesis, Aerospace and Mechanical Engineering Notre Dame, Indiana, 2005.

70. J. R. Davis et al., e., *High-speed machining.* ASM Handbooks online, Volume 16, ninth edition,1989.

71. Pompa, M., *Computer aided processplanningfor high speed millingof thin walled parts* Ph.D Thesis, Department of Engineering Technology (CTW) of the University of Twente, Enschede, Netherlands., 2010.

72. Ishee, D., *A comprasion of the distortion of thin aluminum ribs in high speed machining and low speed machining.* Master's thesis, Department of mechanical engineering, Mississippi state university, 1998.

73. A. B. Mhenni, M.B., *Agility in High Speed Machining: Optimization between Tool and Holder Advances in Integrated Design and Manufacturing in Mechanical Engineering II*, P. Ray, Editor 2007, Springer Netherlands. p. 475-488.

74. R. Field, T.B., *High speed machining of dies and molds.* Modern Machine Shop, 1996: p. 76-83.

75. Schulz, H. and S. Hock, *High-Speed Milling of Dies and Moulds — Cutting Conditions and Technology.* CIRP Annals - Manufacturing Technology, 1995. **44**(1): p. 35-38.

76. S. Smith, J.T., *Current trends in high speed machining.* Journal of Manufacturing Science and Engineering, 1996. **119**(4B): p. 664-666.

77. F. Xu, J.Z., X. Zang, X. Wu, *Rapid parameter optimization of high speed milling aluminum alloy thin-walled workpiece.* Key engineering materials, 2010. **431-432**: p. 41-44.

78. D.H.Stamatis, *Failure Mode and Effect Analysis FMEA from Theory to Execution* ASQC, 1995.

79. A. Y. C. Nee, N.J.T., A. S. Kumar, *An advanced treatise on fixture design and planning.* World Scientific Publishing Co., Series on Manufacturing Systems and Technology-Vol.1, 2004.

80. Arezoo, B., K. Ridgway, and A.M.A. Al-Ahmari, *Selection of cutting tools and conditions of machining operations using an expert system.* Computers in Industry, 2000. **42**(1): p. 43-58.

81. www.kennametal.com/content/dam/kennametal/kennametal/common.

82. Montgomery, D.C., *Design and Analysis of Experiments.* Seven Edition, John Wiley & Sons, 2008.

83. H. Guo, A.M., *Design of Experiments and Data Analysis*. Annual RELIABILITY and MAINTAINABILITY Symposium, 2012.

84. D. Fratila, C.C., *Application of Taguchi method to selection of optimal lubrication and cutting conditions in face milling of $AlMg_3$.* Journal of Cleaner Production, 2011. **19**: p. 640-645.